



UNIVERSIDAD AUTÓNOMA DE MADRID

DEPARTMENT OF BIOCHEMISTRY

PhD Thesis

**Control of DNA replication *in vivo*: study of mouse
models for Cdc6 and Cdt1 overexpression**

Sabela Búa Agúin
Madrid, 2013



**DEPARTMENT OF BIOCHEMISTRY
FACULTY OF MEDICINE
UNIVERSIDAD AUTÓNOMA DE MADRID**

**Control of DNA replication *in vivo*: study of mouse
models for Cdc6 and Cdt1 overexpression**

SABELA BÚA AGUÍN

Graduate in Biology

Thesis Director: **Dr. Juan Méndez Zunzunegui**
Centro Nacional de Investigaciones Oncológicas (CNIO)

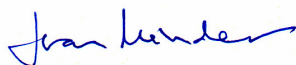
Madrid, June 2013

Madrid, 30 Mayo 2013

El Dr. **Juan Méndez Zunzunegui**, Investigador principal del Grupo de Replicación de DNA, Programa de Oncología Molecular, Centro Nacional de Investigaciones Oncológicas (CNIO),

CERTIFICA

Que Doña **Sabela Búa Aguiñ**, Licenciada en Biología por la Universidad de Vigo, ha llevado a cabo bajo mi dirección el trabajo experimental contenido en la Tesis Doctoral "**Control of DNA replication *in vivo*: study of mouse models for Cdc6 and Cdt1 overexpression**" y reúne los requisitos necesarios para optar al título de Doctor en Ciencias. El trabajo realizado cuenta con el visto bueno de la Dra. **Carmela Calés Bourdet**, Investigadora del Grupo de "Células madre hematopoyéticas y leucémicas de ratón", Instituto de Investigaciones Biológicas "Alberto Sols", que ejerce como Tutora Académica. La Tesis será defendida próximamente en la Universidad Autónoma de Madrid ante el tribunal designado a tal efecto.



Fdo. **Juan Méndez Zunzunegui**
Director de la Tesis



Fdo. **Carmela Calés Bourdet**
Tutor Académico



ACKNOWLEDGMENTS

I want to thank in the first place Dr. Juan Méndez Zunzunegui for giving me the great opportunity to carry out my PhD in his group, as well as for his scientific guidance, discussion of my project and support throughout these years. I also want to thank my lab colleagues for scientific input, for being excellent people, for making me feeling like home. Big thanks go to my family and friends who have always been there for me every day, no matter the time of the day.

ABSTRACT

DNA replication is a biological process that leads to the transmission of genetic information to the next cell generation. Failure to maintain a tight control on DNA replication may result in genome underreplication or overreplication, which have been linked to a variety of human diseases, including cancer. Origins are licensed for replication from late mitosis to G1 by the coordinated action of the Origin Recognition Complex (ORC), Cdc6 and Cdt1, which promote the loading of the MCM2-7 helicase onto DNA. Previous studies in yeast, human and mouse cells have shown that insufficient origin licensing through MCM downregulation leads to genomic instability and oncogenesis *in vivo*. Nevertheless much less is known about the effects of overexpressing 'licensing factors' such as Cdc6 and Cdt1 *in vivo*, although both factors have been reported to have oncogenic activity in culture. In order to characterize *in vivo* the effects of Cdc6 and Cdt1 deregulated expression we have generated inducible mouse models for Cdc6 and Cdt1 proteins. High Cdc6 levels enhance MCM chromatin association both *in vivo* and *in vitro*. In contrast, Cdt1 overexpression did not increase MCM chromatin loading, suggesting that Cdc6 is the limiting factor for this reaction. At the molecular level, Cdc6 overexpression changes the dynamics of DNA replication by increasing the frequency of origin firing and decreasing the fork progression rate to an extent that cannot be significantly enhanced under conditions of replicative stress, suggesting that upon Cdc6 overexpression most of the potential origins are fired. Although no defects on cell proliferation were observed in short-term cultured cells, Tet^{ON}-CDC6 mice are prone to developing histiocytic sarcomas and B-cell lymphomas and have a shorter lifespan. In contrast, a tissue-specific transgenic model generated in parallel, K5-CDC6^{tg}, showed a normal lifespan but mice were hypersensitive to chemically-induced skin tumorigenesis. Interestingly, K5-CDC6^{tg} mice display a skin-specific anti-ageing phenotype that might be related to a delayed progression of the hair growth cycle. When Cdc6 and Cdt1 overexpression were combined by crossbreeding Tet^{ON}-CDC6/CDT1 mice, MEFs undergo partial DNA re-replication, activating the DNA damage response and apoptotic programs. Strikingly, mice overexpressing Cdc6 and Cdt1 displayed morbidity signs in few days. Proliferative tissues showed severe cytoarchitectural abnormalities, increased mitotic activity, DNA damage response activation and increased apoptosis. This Thesis provides evidence that aberrant expression of Cdc6 and Cdc6/Cdt1 threatens genomic stability and promotes cell transformation *in vivo*.

RESUMEN

La replicación del ADN es el proceso por el cual el material genético se duplica para su transmisión a la siguiente generación. Los errores en la regulación de este proceso están asociados a múltiples enfermedades, incluidos varios tipos de cáncer. Los orígenes se preparan para la replicación mediante la acción de las proteínas ORC, Cdc6 y Cdt1, que actúan coordinadamente para atraer a la helicasa MCM2-7 al ADN. Estudios previos han mostrado que la reducción de la concentración de MCM produce inestabilidad genómica y facilita la tumorigénesis *in vivo*. Sin embargo, se ha estudiado menos el posible efecto de la sobre-expresión de proteínas iniciadoras como Cdc6 o Cdt1 *in vivo*. En este trabajo, hemos generado modelos de ratón modificados genéticamente que permiten la sobre-expresión inducible de ambos factores. La sobre-expresión de Cdc6 incrementa los niveles de MCM en cromatina *in vivo* e *in vitro*. A nivel molecular, hace aumentar la eficiencia de activación de orígenes y disminuye la velocidad de progresión de las horquillas. En condiciones de estrés replicativo, las células que sobre-expresan Cdc6 disponen de menos orígenes latentes para contribuir a completar la replicación. *In vivo*, los ratones Tet^{ON}-CDC6 son más propensos a desarrollar sarcomas histiocíticos y linfomas de tipo B y tienen menor esperanza de vida. En otro modelo que hemos desarrollado para la sobre-expresión de Cdc6 en epitelios estratificados (K5-CDC6^{tg}) la esperanza de vida es normal, pero los animales son más susceptibles a la inducción de carcinogénesis química en la piel. La expresión de Cdc6 en la capa basal de la epidermis también ralentiza el ciclo del crecimiento del pelo. Por otro lado, la sobre-expresión simultánea de Cdc6 y Cdt1 produce re-replicación parcial en fibroblastos primarios y es letal *in vivo*. A nivel histológico, los ratones presentan importantes defectos en la organización de los tejidos más proliferativos acompañados de la activación de la respuesta de daño al ADN y de elevada actividad mitótica y apoptótica. Esta tesis ofrece nuevas evidencias de que la sobre-expresión de Cdc6, y especialmente la sobre-expresión simultánea de Cdc6 y Cdt1, constituyen una amenaza para la estabilidad genómica y favorecen la tumorigénesis *in vivo*.

TABLE OF CONTENTS

ABBREVIATIONS	3
INTRODUCTION	4
1. CONTROL OF DNA REPLICATION IN THE CELL DIVISION CYCLE	4
2. CDC6 GENE IS ESSENTIAL FOR INITIATION OF DNA REPLICATION	6
2.1. <i>Cdc6</i> protein participates directly in pre-RC complex assembly	6
2.2. <i>Cdc6</i> protein uses ATPase activity during origin licensing	7
2.3. <i>Cdc6</i> influences origin specificity	9
3. CDC6 REGULATION IN THE CELL CYCLE	10
4. CDC6 AND THE CELLULAR CHECKPOINTS	11
5. TRANSCRIPTIONAL ROLE OF CDC6	13
6. IDENTIFICATION OF CDT1 AS AN ESSENTIAL INITIATION GENE	13
7. CELL CYCLE REGULATION OF CDT1 FUNCTION	14
8. PREVENTION OF DNA RE-REPLICATION	17
9. DEREGULATED DNA REPLICATION ACTIVATES THE DDR AND MAY PROMOTE SENESENCE	18
10. ORIGIN LICENSING MACHINERY IS DEREGULATED IN CANCER	19
OBJECTIVES.....	23
MATERIALS AND METHODS	24
1. GENERATION OF GENETICALLY-MODIFIED MOUSE STRAINS	24
1.1. <i>Ethical statement</i>	24
1.2. <i>K5-CDC6^{tg} mouse generation</i>	24
1.2. <i>Gene walking by unpredictably primed (UP) PCR</i>	24
1.3. <i>Generation of Lox-CDH1; K5-Cre^{tg}; K5-CDC6^{tg} mice</i>	25
1.4. <i>Generation of K5-CDC6^{tg} mice in a p53-null background</i>	25
1.5. <i>Tet^{ON}-CDC6 and Tet^{ON}-CDT1 mouse generation</i>	25
1.6. <i>Tet^{ON}-CDC6/CDT1 mouse generation</i>	26
2. MICE GENOTYPING	26
3. MOUSE PROCEDURES	27
3.1. <i>TPA-induced skin hyperplasia</i>	27
3.2. <i>DMBA-TPA skin chemical carcinogenesis assay</i>	27
3.3. <i>Wound-healing</i>	27
4. CELL CULTURE EXPERIMENTS.....	27
4.1. <i>Primary keratinocyte isolation from adult mice</i>	27
4.2. <i>Isolation and culture of keratinocytes from newborn mice</i>	28
4.3. <i>Primary Mouse Embryonic Fibroblasts (MEFs) isolation</i>	28
4.4. <i>Proliferation curves with MEFs</i>	29
4.5. <i>Serum starvation and cell cycle re-entry</i>	29
4.6. <i>MTT survival assay</i>	29
4.7. <i>Single-molecule analysis of DNA replication in stretched fibers</i>	29
4.8. <i>Oncogenic transformation assay</i>	30
4.9. <i>Chromatid breaks and Sister Chromatid Exchange (SCE) analyses</i>	30
4.10. <i>Flow cytometry analyses</i>	31
5. RNA EXPRESSION ANALYSES	32
5.1. <i>RNA isolation, retrotranscription and quantitative PCR (RT-qPCR)</i>	32
6. PROTEIN ANALYSIS	32
6.1. <i>Whole cell extracts</i>	32
6.2. <i>Biochemical fractionation</i>	32
6.3. <i>Antibody generation</i>	33
6.4. <i>Immunoblots</i>	33

6.5. Immunofluorescence	33
7. HISTOLOGICAL ANALYSIS	34
RESULTS.....	37
CHAPTER 1. K5-CDC6 TRANSGENIC MOUSE	37
1.1. Generation of a K5-CDC6 transgenic mouse.....	37
1.2. Overexpression levels of CDC6 transgene in the skin and other organs	39
1.3. Cdc6 overexpression leads to increased chromatin association of MCM proteins ..	40
1.4. Cdc6 overexpression does not confer a cell proliferation advantage in vitro	41
1.5. Histopathological characterization of the skin of K5-CDC6 ^{tg} mice.....	42
1.6. Further increase of Cdc6 overexpression does not increase MCM loading.....	43
1.7. Susceptibility of K5-CDC6 ^{tg} mice to skin carcinogenesis	46
1.8. K5-CDC6 ^{tg} mice have a normal lifespan	49
1.9. Cdc6 overexpression in a p53-null background	50
1.10. Old K5-CDC6 ^{tg} mice show better skin/hair fitness	51
1.11. Normal wound healing in K5-CDC6 ^{tg} skin	54
CHAPTER 2. TET ^{ON} -CDC6 MOUSE MODEL	59
2.1. Generation of a mouse model for inducible Cdc6 overexpression	59
2.2. Cdc6 overexpression increases MCM-chromatin loading in MEFs.....	60
2.3. Overexpressed Cdc6 protein is regulated in the cell cycle	61
2.4. Cdc6 overexpression increases origin activity during S-phase	65
2.5. Spatio-temporal regulation of DNA replication is not affected by Cdc6 overexpression.....	68
2.6. Cdc6 overexpressing-cells do not show signs of replicative stress.....	69
2.7. Cdc6 overexpression does not affect homologous recombination rate.....	71
2.8. No effect of Cdc6 overexpression on cell growth or viability	72
2.9. Cdc6 overexpression does not facilitate transformation in MEFs.....	73
2.10. Cdc6 overexpression increases MCM-content in proliferative tissues	74
2.11. Increased tumor susceptibility in Cdc6-overexpressing mice.....	75
CHAPTER 3. TET ^{ON} -CDC6/CDT1 MOUSE MODEL	79
3.1. Cdt1 overexpression by itself does not enhance MCM chromatin association	79
3.2. Cdc6 and Cdt1 overexpression increases MCM chromatin-association to a similar extent than Cdc6 overexpression alone.....	81
3.3. Cdc6 and Cdt1 overexpression leads to a slight increase in cells with >G2 DNA content	82
3.4. Cdc6 and Cdt1 overexpression activates the DNA-damage response.....	83
3.5. Cdc6 and Cdt1 overexpression promotes re-replication in primary MEFs.	86
3.6. Cdc6 and Cdt1 overexpressing- cells undergo apoptosis but not senescence.....	88
3.7. Overexpression of Cdc6 and Cdt1 is lethal in vivo.....	90
DISCUSSION	95
1. CDC6 INCREASES MCM LOADING EFFICIENCY	95
2. CDC6 OVEREXPRESSION INCREASES ORIGIN FIRING EFFICIENCY	97
3. CDC6 AND ORIGIN SELECTION	99
4. CDC6 OVEREXPRESSION <i>IN VIVO</i>	102
5. CDC6 AND CDT1 OVEREXPRESSION INDUCES PARTIAL RE-REPLICATION IN PRIMARY MEFs	104
6. RE-REPLICATION IN CDC6/CDT1-OVEREXPRESSING CELLS INDUCES ACTIVATION OF THE DDR.....	105
7. CDC6 AND CDT1 OVEREXPRESSION IS LETHAL <i>IN VIVO</i>	107
CONCLUSIONS	108
CONCLUSIONES.....	109
BIBLIOGRAPHY.....	110

ABBREVIATIONS

CldU	5-Chloro-2'-deoxyuridine
CPT	Camptothecin
DDR	DNA damage response
DMBA	7,12-dimethylbenz[α]anthracene
Dox	Doxycycline
DSB	Double strand break
EdU	5-Ethynyl-2'-deoxyuridine
ESC	Epidermal Stem cell
FLPe	Flipase
FR	Fork rate
HF	Hair follicle
HR	Homologous recombination
HTM	High-throughput microscopy
HU	HU
IdU	5-Iodo-2'-deoxyuridine
IF	Immunofluorescence
IFE	Interfollicular epidermis
IHC	Immunohistochemistry
IOD	Inter-origin distance
MEF	Mouse embryonic fibroblast
MMS	Methyl methanesulfonate
MTT	1-(4,5-Dimethylthiazol-2-yl)-3,5-diphenylformazan
OCT	Optimal cutting temperature compound
PC	Progenitor cell
PFA	Paraformaldehyde
SA-β-gal	Senescence-associated β -galactosidase
SCC	Squamous Cell Carcinoma
SCE	Sister chromatid exchange
TMRE	Tetramethylrhodamine ethyl ester
TPA	12-O- tetradecanoylphorbol 13-acetate
Ts	Temperature-sensitive

INTRODUCTION

1. Control of DNA replication in the cell division cycle

DNA replication is an essential step process that leads to the transmission of the genetic information to the next cell generation. The regions of the genome where replication starts are called replication origins. The activity of these origins must be carefully regulated to ensure complete and accurate replication. Errors that result in DNA underreplication or overreplication produce a variety of human genetic diseases, including developmental abnormalities and several types of cancer (DePamphilis, 2006).

In contrast to viral and prokaryotic organisms and with the exception of *Saccharomyces cerevisiae*, in eukaryotes the identity of replication origins is not defined by a specific DNA sequence. Instead, a combination of genetic and epigenetic features might determine the accessibility of specific proteins, called initiators, to permissive sites in the chromatin. AT-rich elements, CpG islands, nucleosome-free regions, histone acetylation and active transcription have been found at several metazoan replication origins, although they are not present in all of them (reviewed by Méchali, 2010).

From late mitosis and throughout the G1 phase, origins undergo a process called 'licensing'. This process consists on the loading of the MCM2-7 (Mini-Chromosome Maintenance) complex that upon subsequent activation will become the core of the replicative DNA helicase in S-phase. The loading of MCM2-7 at replication origins is mediated by the concerted action of the initiator proteins ORC (Origin Recognition Complex), Cdc6 (Cell Division Cycle-6) and Cdt1 (Cdc10-Dependent Transcrip-1). The protein structure resulting after MCM2-7 loading constitutes the pre-Replicative Complex (pre-RC). At the G1/S transition, CDKs (Cyclin-dependent kinases) and DDK (Dbf4-dependent kinase), phosphorylate different members of the pre-RC allowing the recruitment of additional initiation factors such as Mcm10, Cdc45, GINS, Sld2/RecQ4L, Sld3/Treslin and TOPBP1 that activate the helicase and facilitate the loading of the replisome components (DNA polymerases and their accessory factors).

The temporal separation between helicase loading (late mitosis-G1) and helicase activation (G1/S) is regulated by the CDK activity and constitutes an important mechanism to

control that replication takes place only once in the same cell cycle (**Fig. 1**; reviewed by Diffley, 2011; Boos et al., 2012; Remus and Diffley, 2009; Sclafani and Holzen, 2007; Méndez and Stillman, 2003). This Thesis is focused on the effects of overexpressing CDC6 and CDT1; therefore, the rest of the introduction describes these two proteins, their known functions and regulation.

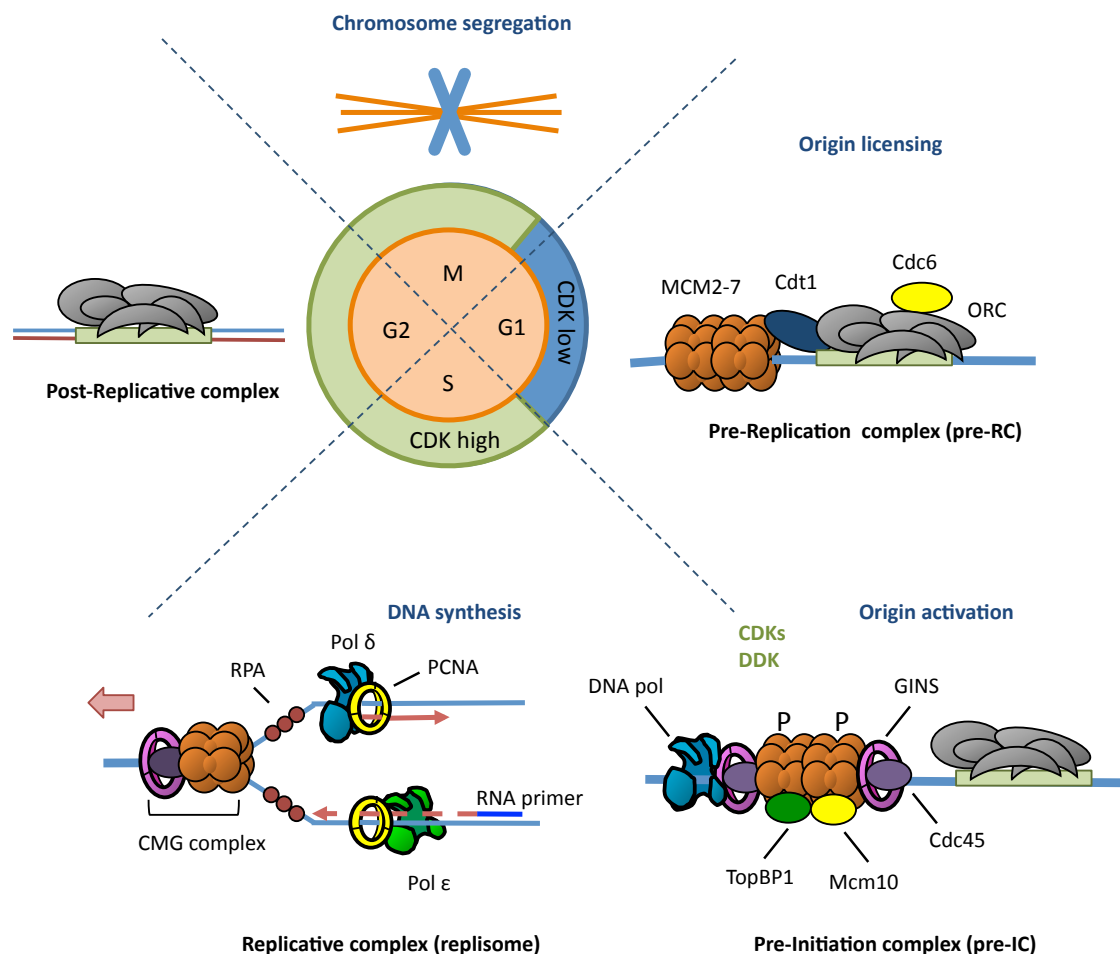


Figure 1. DNA replication in the cell cycle. Origin licensing is restricted to late mitosis and G1. The concerted action of ORC, Cdc6 and Cdt1 loads the MCM2-7 complex as a double hexamer leading to the pre-replication complex (pre-RC). At the G1/S transition the CDKs and DDK allow the loading of Mcm10, Cdc45, GINS, Sld2/RecQ4L, Sld3/Treslin, TOPBP1 and the DNA polymerases. Cdc45 and the GINS complex associate with MCM and give rise to an active helicase known as CMG (Cdc45-Mcm2-7-GINS). Two bidirectional replication forks are established from each origin (only one is depicted here). ORC remains bound to the origins during S and G2 but in an inactive state (post-RC).

2. Cdc6 gene is essential for initiation of DNA replication

Cdc6 was discovered in a genetic screen performed to identify DNA replication factors in the yeast *S. cerevisiae*. In this study, the yeast *cdc6* mutant grown at the restrictive temperature completed one round of DNA replication but failed to reinitiate the next one. Therefore, it was suggested that Cdc6 is necessary for the initiation of DNA replication and in the absence of its function the replicated DNA was either faulty or incomplete (Hartwell, 1976). The *S. cerevisiae* CDC6 gene was cloned in 1989 (Zhou et al., 1989) and homologs were subsequently identified in *S. pombe*, where it is called Cdc18 (Kelly et al., 1993), *Xenopus laevis* (Coleman et al., 1996), human (Williams et al., 1997) and mouse (Berger et al., 1999). In fact, Cdc6 is conserved in every eukaryotic organism and Cdc6-related genes are found in *archaea* (reviewed by Barry and Bell, 2006).

Direct evidence for the role of Cdc6 in initiation of DNA replication came from a study in which a Cdc6 temperature-sensitive (*ts*) mutant strain of *S. cerevisiae* arrested at the G1/S transition. Apart from its involvement in DNA replication, this study also showed a role of Cdc6 in the coordination of S-phase and mitosis (S-M checkpoint). In this regard, interfering with the cyclic expression of Cdc6 by inducing Cdc6 expression in G2 prevented the onset of mitosis (Bueno and Russell, 1992). In addition, a different study showed that Cdc18 (Cdc6) deletion in *S. pombe* caused an accumulation of cells with 1C DNA content that still proceeded to mitosis, suggesting that Cdc18 somehow prevents mitosis until S-phase is completed (Kelly et al., 1993). Similar results were obtained later in *S. cerevisiae* regarding the inhibition of DNA replication and the failure in the S-M checkpoint that led cells to undergo a reductional anaphase (Piatti et al., 1995).

In human cells, abrogation of Cdc6 function either by antibody microinjection (Hateboer et al., 1998; Yan et al., 1998) or interference RNA (RNAi) (Feng et al., 2003; Lau et al., 2006; Lau et al., 2009; reviewed by Borlado and Méndez, 2008), also led to inhibition of DNA replication and loss of the S-M checkpoint.

2.1. Cdc6 protein participates directly in pre-RC complex assembly

Two findings contributed to establishing Cdc6 as a key factor during origin licensing: the identification of ORC, an essential 6-subunit protein complex that specifically binds to replication origins in *S. cerevisiae* (Bell and Stillman, 1992) and the existence of two 'chromatin states' at origins in the cell cycle (Diffley et al., 1994). Diffley and colleagues

studied the regulation of ORC binding through the cell cycle by genomic footprinting. The pattern of protection from nuclease digestion was extended in cells in late mitosis and G1 phase (the 'pre-replicative state') compared to the pattern in S or G2 phases (the 'post-replicative state'). They proposed that the ORC complex remains bound to replication origins throughout the cell cycle and additional proteins, responsible for the extended ORC footprints, are recruited in late mitosis and G1.

In the search of proteins that could interact with ORC, a 'multicopy suppression' screening performed with an *orc5-1* strain found that Cdc6 partially suppressed the initiation defects observed in this mutant. Furthermore, it was also found that Cdc6 and ORC interact functionally and physically (Liang et al., 1995). This led to the proposal of Cdc6 being a member of a pre-RC complex together with ORC and possibly the MCM proteins. This hypothesis was further supported by using a conditional Cdc6 knock-out strain in which the pre-replicative footprint was lost upon loss of Cdc6 (Cocker et al., 1996).

In the following years, several studies showed that Cdc6 is essential for MCM loading on chromatin in yeast. In one of these studies, MCMs were recovered in chromatin-isolated fractions from G1-arrested cells only if Cdc6 was present (Donovan et al., 1997). In another one, immunoprecipitation of crosslinked DNA showed that Cdc6 and MCM proteins bound specifically to replication origins in G1. It also showed the importance of S- and M-CDKs in preventing re-association of MCM proteins to origins outside G1 (Tanaka et al., 1997). In addition, a Cdc6 gain-of-function mutant showed constant MCM protein association to chromatin throughout the cell cycle and promiscuous initiation of DNA replication (Liang and Stillman, 1997). In quiescent mammalian cells, where Cdc6 is normally absent, expression of Cdc6 was sufficient to induce MCM loading on chromatin (Cook et al., 2002).

2.2. Cdc6 protein uses ATPase activity during origin licensing

Cdc6 belongs to the AAA⁺ family (*ATPases associated with a variety of cellular activities*), a class of chaperone-like ATPases associated with the assembly, operation and disassembly of protein complexes (Neuwald et al., 1999). To date, the only Cdc6 high-resolution structure available is that of an archeal ortholog, which has revealed at the atomic detail the characteristics of the ATP-binding domain and the existence of the winged-

helix domain (WHD), a common DNA binding motif (Liu et al., 2000). The main domains and conserved motifs of Cdc6 are shown in **figure 2A**.

Different studies have shown that the ATPase domain of Cdc6 is indispensable for MCM loading onto DNA. In particular, *in vitro* studies using *S.cerevisiae* extracts and purified proteins have contributed to unravel the biochemical mechanism underlying the licensing reaction. First, ORC binds to origin DNA in an ATP-bound state. Cdc6 associates with ORC and then binds ATP, inducing a conformational change in the ORC complex that might trigger the recruitment of the MCM complex along with Cdt1. Cdc6 ATP hydrolysis might be responsible for the topological engagement of the MCM2-7 complex with the DNA, whereas the ORC ATPase activity only becomes essential for multiple rounds of MCM loading (**Fig. 2B**) (Randell et al., 2006). The biological significance of repetitive MCM loading is unclear but it is likely responsible for the high amount of MCM complexes loaded onto DNA compared to the number of origins activated in a normal S-phase. The 'excess' of MCM complexes plays an important role in the licensing of back-up origins that are activated under situations of stress (Ge et al., 2007; Ibarra et al., 2008).

The combination of *in vitro* assays in yeast with electron microscopy techniques has provided additional insights into the molecular mechanism of pre-RC assembly. Two hexameric MCM complexes bound to Cdt1 are loaded as a double head-to-head dodecamer in an ATP-dependent reaction, with the DNA running through the MCM central channel (Evrin et al., 2009; Remus, et al., 2009). In addition, it has been recently reported that the carboxy-terminal domain of MCM3 is essential for MCM2-7 recruitment to the pre-RC independently of Cdt1. This domain stimulates the ATPase activity of ORC and Cdc6, but only leads to MCM loading if all the components of the pre-RC are present (Frigola et al., 2013).

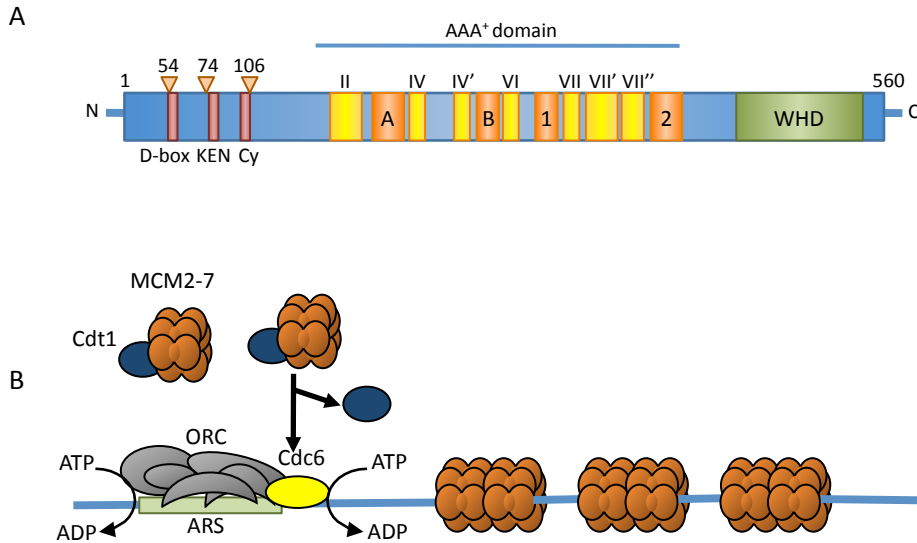


Figure 2. A. Conserved domains of human Cdc6. The cyclin binding domain and protein degradation motifs (KEN box and D-box) are indicated. Cdc6 has three consensus targets for CDK phosphorylation indicated with orange triangles. The Walker A, Walker B, Sensor 1 and Sensor 2 motifs are shown in orange boxes. The rest of conserved AAA⁺ motifs are indicated in yellow. WHD, winged-helix domain for DNA interaction. **B. The licensing reaction.** ATP hydrolysis by Cdc6 leads to the loading of MCM2-7 complexes on DNA and the release of Cdt1 from the origin. ATP hydrolysis by ORC completes the MCM2-7 loading reaction either by catalyzing the dissociation of MCM complexes from other pre-RC components or by resetting the conformation of the complex to allow the subsequent association of additional Cdc6, Cdt1 and MCM proteins (adapted from Borlado and Méndez, 2008).

2.3. Cdc6 influences origin specificity

Apart from its role in MCM loading, one interesting feature of Cdc6 activity in *S. cerevisiae* is its ability to influence the specificity of ORC to bind origin DNA. In the presence of non-origin DNA, Cdc6 hydrolyses ATP and promotes the dissociation of ORC and Cdc6 from chromatin, whereas in the presence of origin DNA the ORC-Cdc6-DNA interaction is stabilized (**Fig. 3**) (Mizushima et al., 2000). As mentioned above, Cdc6 overexpression alleviates the phenotype of an *orc5-1* mutant defective in DNA replication initiation. Higher levels of Cdc6 might cause a better binding of ORC to origin DNA increasing the probability of firing or promoting the efficient recruitment of other replication proteins (Liang et al., 1995). Although metazoan origins may not have specific DNA sequences it is interesting to speculate that Cdc6 could somehow influence the ORC binding sites. At least in one study, expressing GAL4-Cdc6 in human cells was sufficient to recruit endogenous ORC and create an artificial origin of replication in a plasmid containing GAL4-DNA binding sites (Takeda et al., 2005).

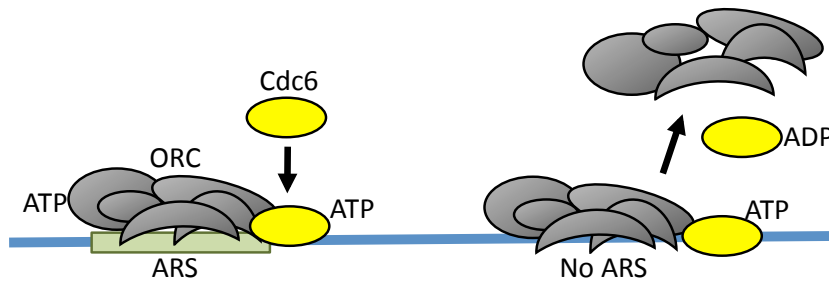


Figure 3. Cdc6 influences origin specificity. In *S. cerevisiae*, where the origins are defined by specific DNA sequences, Cdc6 modulates the DNA binding activity of ORC to functional origin sequences in an ATP-dependent manner (adapted from Borlado and Méndez, 2008).

3. Cdc6 regulation in the cell cycle

Expression of Cdc6 is cell cycle-regulated from *S. cerevisiae* to mammalian cells. In *S. cerevisiae* and *S. pombe*, Cdc6 expression levels peak at the G1/S transition in response to MBF/SBF and Cdc10- transcriptional control respectively (Bueno and Russell, 1992; Kelly et al., 1993; Piatti et al., 1995). In human cells, Cdc6 expression peaks in late G1 and is regulated by the E2F transcription factors which regulate genes involved in DNA replication and cell cycle progression (Hateboer et al., 1998; Ohtani et al., 1998; Yan et al., 1998).

In yeast, Cdc6/Cdc18 phosphorylation by CDKs at the G1/S transition leads to ubiquitin-mediated proteolysis. In *S. pombe* the degradation of Cdc18 is critical to avoid multiple rounds of DNA replication. Overexpression of Cdc18 promotes re-replication that is enhanced by a mutant lacking the CDK consensus sites (Nishitani and Nurse, 1995; Jallepalli et al., 1997). In contrast, overexpression of Cdc6 in *S. cerevisiae* does not cause re-replication, due to different overlapping mechanisms aimed to restrain origin usage (reviewed by Diffley, 2011; Arias and Walter, 2007) (see below).

Mammalian Cdc6 is a substrate of the Anaphase Promoting Complex/Cyclosome (APC/C), an E3 ubiquitin ligase that targets specific substrates for degradation by the 26S proteasome during mitosis and G1 (reviewed by Manchado et al., 2010). Cdc6 recognition is mediated by the APC cofactor Cdh1, which targets Cdc6 for degradation in early G1 and during quiescence (Petersen et al., 2000). When cells re-enter the cell cycle, Cyclin E-CDK phosphorylates Cdc6 and protects it from APC/C-Cdh1-mediated proteolysis. This

mechanism is proposed to provide a window of opportunity for Cdc6 accumulation and origin licensing in the presence of APC/C-Cdh1 activity (Mailand and Diffley, 2005).

In proliferating cells, Cdc6 is also degraded in G1 by the same complex, but it rapidly re-accumulates during S-phase and a population remains chromatin-bound throughout the cell cycle (Méndez and Stillman, 2000; Alexandrow and Hamlin, 2004). Different studies also show that Cdc6 might be relocalized to the cytoplasm during S-phase in a Cyclin A-CDK-dependent manner especially if the protein is ectopically expressed (Saha et al., 1998; Petersen et al., 1999; Cook et al., 2002; Alexandrow and Hamlin, 2004; Paolinelli et al., 2009) although the biological meaning of this relocalization is still unclear. It is possible that specific posttranslational modifications determine the subcellular localization of at least part of Cdc6 and its participation in cellular functions different from MCM loading. For example, the phosphorylated form of Cdc6 on serine 54 is strongly bound to chromatin in S-phase (Alexandrow and Hamlin, 2004; Duursma and Agami, 2005) whereas previous acetylation of Cdc6 by the acetyltransferase GCN5 in early S-phase promotes Cyclin A-CDK2-mediated phosphorylation of Cdc6 at serine 106 and subsequent translocation to the cytosol (Paolinelli et al., 2009). In any case, non-phosphorylatable versions of Cdc6 fully support DNA replication without causing re-replication (Petersen et al., 1999; Pelizon et al., 2000; Cook et al., 2002)

Cdc6 protein levels are also regulated upon DNA damage. In a context where the activation of the checkpoints decreases CDK activity to slow down or arrest the cell cycle, *de novo* assembly of pre-RCs would be facilitated and possibly induce re-replication. Upon ionizing radiation, p53 is activated and inhibits Cyclin A-CDK2 activity through p21 protein. As a result Cdc6 is targeted for degradation by the APC/C complex (Duursma and Agami, 2005). In addition, exposure to UV light or MMS-induced DNA damage leads to release of Cdc6 from chromatin and its targeting for proteolysis by the Huwe1 ubiquitin ligase (Hall et al., 2007).

4. Cdc6 and the cellular checkpoints

Checkpoints are molecular signalling cascades activated in response to DNA damage that delay or arrest the cell cycle to allow DNA repair or otherwise promote cell death or senescence if the damage cannot be overcome. The S-M checkpoint ensures that cells do

not divide until the DNA has been fully replicated. Failures in the S-M checkpoint lead to mitotic cell death (reviewed by Bartek et al., 2004).

As previously mentioned, yeast Cdc6 prevents premature entry into mitosis (Bueno and Russell, 1992; Kelly et al., 1993; Piatti et al, 1995) and this effect is mediated by its interaction with the mitotic kinase Cyclin B-Cdk1 (Weinreich et al., 2001). In human cells this role seems conserved in part, as Cdc6 overexpression in G2 cells can restrain mitosis. However, this effect is dependent on Chk1 activity, an effector protein of the checkpoint pathway activated upon DNA damage that arises during DNA replication, and not on direct inhibition of Cyclin B-CDK1 (Clay-Farrace et al., 2003). Further support for a role of Cdc6 in restraining mitosis comes from RNAi-mediated knock-down of Cdc6 in S-phase-synchronized HeLa cells, which enter mitosis while DNA replication is still ongoing. These cells also activate fewer origins in S-phase without ATR-Chk1 activation, suggesting a potential role for Cdc6 in origin firing (Lau et al., 2006).

At least in model systems, Cdc6 might also have a role in the replicative checkpoint, which is activated upon frequent fork stalling. This checkpoint, which can be induced by hydroxyurea (HU), results in the preferential activation of the ATR kinase that phosphorylates different substrates including Chk1 (reviewed by Bartek et al., 2004). In *S. pombe*, Cdc18 is needed for the long-term maintenance of the HU-induced checkpoint as it contributes to anchor the Rad3-Rad26 (ATR/ATRIP) complex to chromatin, which in turn signal to restrain mitosis (Hermand and Nurse, 2007). In *X. laevis*, Cdc6 is needed for the activation of Chk1 upon induction of replicative stress. Cdc6 can activate Chk1 without being bound to chromatin (Oehlmann et al, 2004).

In contrast, human Cdc6 seems to have limited participation in the replicative checkpoint. Although in HeLa cells interaction between ATR and Cdc6 has been reported, the activation of Chk1 was not impaired in the absence of Cdc6 and the interaction of ATR with Cdc6 was not enhanced in conditions of replicative stress (Yoshida et al., 2010). In a different study, Cdc6 was found to interact with ATR after DNA damage induced by ionizing radiation. Chk1 phosphorylation and the G2/M arrest caused by the activation of the checkpoint were reduced in the absence of Cdc6, and these effects were shown to be p53-independent (Chung et al., 2010).

5. Transcriptional role of Cdc6

Some studies have linked Cdc6 with transcriptional repression of specific loci that are important for tumor development and cancer progression. The *INK4/ARF* locus that encodes the tumor suppressor genes p15, p16^{INK4a} and p19^{ARF}, may be transcriptionally repressed upon Cdc6 overexpression in human and mouse cells (González et al., 2006). The mechanism involves the binding of Cdc6 to a conserved motif that contains an origin of replication upstream of the *INK4/ARF* locus and the subsequent recruitment of histone deacetylases that promote the heterochromatinization of the locus. Consequently, high levels of Cdc6 facilitated immortalization and neoplastic transformation in cooperation with oncogenic *Ras* (González et al., 2006). The repressive function of Cdc6 on the *INK4/ARF* locus has been found to be mediated through direct interaction with BMI1, a member of the Polycomb Group genes, which encode for proteins that regulate chromatin structure and gene transcription (Agherbi et al., 2009).

Cdc6 overexpression in epithelial cells has also been found to transcriptionally repress the *CDH1* locus, which encodes the E-Cadherin tumor suppressor (Sideridou et al., 2011). Downregulation of E-Cadherin is one of the key events in EMT (*Epithelial-to-Mesenchymal Transition*), a common feature in tumor progression. In this study, overexpression of Cdc6 in human and murine epithelial cells leads to repression of E-Cadherin transcription and acquisition of a mesenchymal phenotype. Cdc6 binds to the E-boxes of the *CDH1* promoter leading to heterochromatinization of the locus by displacing the CTCF chromatin insulator and facilitating the recruitment of histone deacetylase. As it has been shown for the *INK4/ARF* locus, an origin of replication is located upstream of the *CDH1* locus. Interestingly, overexpression of Cdc6 increased the firing efficiency of this origin in a human cell line. The activity of the origin could only be detected upon Cdc6 overexpression in a murine cell line, which suggests that it remains 'dormant' in conditions of physiological Cdc6 protein levels (Sideridou et al., 2011).

6. Identification of Cdt1 as an essential initiation gene

Cdt1 was originally identified in *S. pombe* in a screening to find new target genes of the Cdc10 transcription factor, which regulates the transcription of genes required for the initiation of DNA replication (Hofmann and Beach, 1994). In *S. pombe* and *X. laevis* egg extracts, the absence of Cdt1 inhibits DNA replication by preventing MCM chromatin

association. ORC and Cdc6 loading are not affected, suggesting that these proteins are recruited to origins separately (Maiorano et al., 2000; Nishitani et al., 2000). Cdt1 or functional homologues have been found in all eukaryotic organisms but not in *archaea*. In studies that aimed at the reconstitution of pre-RC *in vitro* with purified yeast proteins, MCM copurifies with Cdt1 and the molecular weight of the complex is consistent with a stoichiometric Cdt1·MCM2-7 heptamer. Once MCMs are loaded, both Cdt1 and Cdc6 are released from chromatin (Kawasaki et al., 2006; Remus et al., 2009; Frigola et al., 2013; Fernández-Cid et al., 2013).

7. Cell cycle regulation of Cdt1 function

Like ORC1, Cdc6 and MCM2-7, Cdt1 gene expression is controlled by the E2F transcription factors (reviewed by Fujita, 2006). In addition, Cdt1 protein activity is tightly regulated by overlapping mechanisms (reviewed by Diffley, 2011). In metazoans, Cdt1 protein is functional in G1 and is repressed in the subsequent phases of the cell cycle either by binding to an inhibiting protein called Geminin or by proteosomal degradation. Geminin was identified in a screening performed in *X. laevis* egg extracts to find new substrates of the APC/C complex. In human cells, Geminin accumulates from S-phase until the metaphase to anaphase transition. Geminin inhibited MCM chromatin loading, suggesting a mechanism to prevent unscheduled reassembly of pre-RC during S and G2 (McGarry and Kirschner, 1998).

Geminin is absent from yeasts but present in all metazoans. It physically binds to Cdt1 (Wohlschlegel et al., 2000; Tada et al., 2001) and exerts its anti-licensing function by inhibiting the MCM-Cdt1 interaction (Yanagi et al., 2002; Lee et al., 2004). In addition, it protects Cdt1 from ubiquitylation, especially during G2 and mitosis, allowing Cdt1 accumulation in an inactive form to facilitate pre-RC assembly in the next cell cycle, after Geminin is degraded (Ballabeni et al., 2004).

An X-ray based structural study has shown that the Cdt1:Geminin complex can exist in two different forms. A heterotrimeric ‘permissive form’ composed of two Geminin molecules per Cdt1 molecule and an ‘inhibitory form’ that consists in a dimer of heterotrimers in a head-to-tail configuration (**Fig. 4A**). In the latter, Geminin shields several conserved Cdt1 residues, two of which are important for licensing. Thus, Geminin activity may involve a cell cycle-regulated equilibrium between heterotrimers and heterohexamers

(De Marco et al., 2009). Interestingly, in mitotic cell extracts, at a stage when Cdt1 has to engage in replication licensing, both Cdt1 and Geminin are hyperphosphorylated (Ballabeni et al., 2004) and Geminin is inactivated upon exit from metaphase through a CDK- and ubiquitination-dependent mechanism (Li and Blow, 2004). Some of the posttranslational modifications on the inhibitory heterohexamers may promote reformation of the permissive heterotrimer (De Marco et al., 2009).

The second regulatory level on Cdt1 activity consists on its targeting for proteasomal degradation in S-phase. Cdt1 has an N-terminal PCNA-interacting motif (PIP). PCNA protein, a sliding clamp that acts as a processivity factor for DNA polymerases, attracts Cdt1 to chromatin where it is ubiquitylated by the E3 ubiquitin ligase CUL4-DDB1. The CUL4-dependent Cdt1 degradation is conserved from yeast through metazoans (Zhong et al., 2003; reviewed by Arias and Walter, 2007; Diffley, 2011).

At least in humans, a second proteosomal pathway acts redundantly with the CUL4-DDB1 complex. In this case, phosphorylation by CDKs promotes Cdt1 recognition by the SCF^{Skp2} ubiquitin ligase, which subsequently targets Cdt1 for degradation (**Fig. 4B**) (reviewed by Kim and Kipreos, 2007). Both pathways are involved in targeting Cdt1 for degradation in response to IR or UV-induced DNA damage. IR-induced Cdt1 degradation driven by CUL4-DDB1 complex is independent of ATM/ATR kinases, whereas UV-mediated destruction of Cdt1 is dependent on ATR activity and mediated by the E3 SCF complex (Higa et al., 2003; Kondo et al., 2004).

Apart from its role in DNA replication, a function of Cdt1 in mitosis has been recently described in human cells. Cdt1 downregulation in G2 induces a metaphase arrest. Cdt1 localizes to the mitotic kinetochores and stabilizes the kinetochore-to-microtubule attachment through direct interaction with the Ndc80 protein complex. Although the exact regulation of this interaction has not yet been characterized, Geminin was not found at centromeres, suggesting that its release from Cdt1 should occur early in mitosis (Varma et al., 2012).

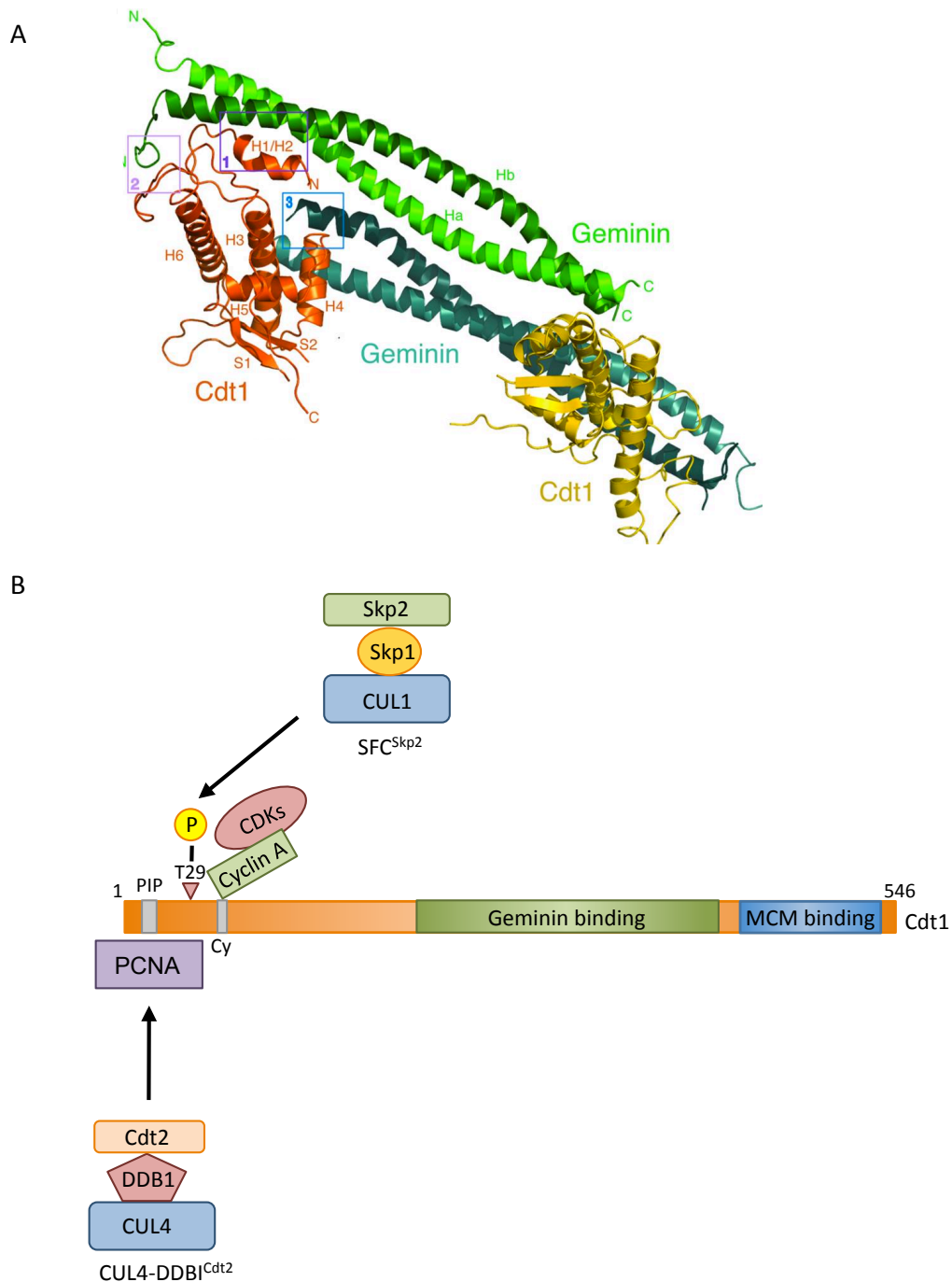


Figure 4. A. Structure of the human Cdt1:Geminin interaction. Fragments of Cdt1 are colored in yellow and orange. Fragments of Geminin are shown in green and blue. The interphase regions are shown in boxes (taken from De Marco, 2009). **B. Pathways that promote the proteolytic degradation of Cdt1.** The domains in Cdt1 responsible for the interaction with PCNA, cyclins, Geminin and MCM are indicated in colored boxes. During S-phase, Cdt1 is attracted to chromatin through its PCNA-interacting domain (PIP) and targeted for proteolysis by the CUL4-DDB1^{Cdt2} E3 ubiquitin ligase complex. In this way, Cdt1 ubiquitylation is coupled to DNA replication, limiting inappropriate origin licensing during the S-phase. SCF^{Skp2}-mediated proteolysis occurs throughout the cell cycle. Cdt1 has a cyclin-binding motif, which is essential for Cyclin A-CDK-mediated phosphorylation of Threonine 29. This phosphorylation event is essential for Skp2 recognition and subsequent ubiquitylation and proteasome degradation of Cdt1 (Adapted from Fujita, 2006).

8. Prevention of DNA re-replication

The activity of the origin licensing machinery is controlled to prevent replicated DNA from becoming re-licensed in S or G2 phases of the cell cycle. Partial DNA re-replication is normally detrimental and contributes to genomic instability (reviewed by Blow and Dutta, 2005). Re-replication is different from endoreduplication, in which a cell may undergo several rounds of complete DNA replication without intervening mitosis. A striking example is the trophoblast giant cells of the placenta, which can accumulate up to 1000N DNA content in rodents (reviewed by Hu and Cross, 2009). Cdc6, Cdt1 and geminin regulation has been affects physiological endoreduplication in megakaryoblastic cell lines, in which geminin is downregulated, Cdt1 levels are maintained and Cdc6 presence is the key event to trigger endoreduplication (Bermejo et al., 2002).

Eukaryotes have evolved multiple mechanisms to prevent re-replication. Possibly the most conserved one relays on the fluctuations of CDK activity in the cell cycle. From late mitosis to early G1, CDK activity is kept low and pre-RCs can be assembled. At the G1/S transition, increased CDK activity prevents further origin licensing by inhibiting different pre-RC components and at the same time promotes the initiation of replication (reviewed by Arias and Walter, 2007; Diffley, 2011). In *S. pombe*, inhibiting CDK activity in G2 promotes re-replication. CDKs phosphorylate ORC and keep it in an inactive state during S and G2, while Cdc18 (Cdc6) and Cdt1 are targeted for degradation in S-phase. Cdc18 overexpression also promotes extensive re-replication, which is enhanced by Cdt1 co-expression. In *S. cerevisiae*, CDK phosphorylation acts redundantly on several pre-RC members to prevent re-replication. ORC is inactivated, Cdc6 is targeted for degradation, and Cdt1 and the MCM complex are exported from the nucleus to the cytosol (reviewed by Arias and Walter, 2007; Diffley, 2011). In contrast to *S. pombe*, only when all three inhibitory pathways are disrupted can origins efficiently re-initiate in G2/M (Nguyen, et al., 2001).

In human cells, CDK phosphorylation promotes SCF-Skp2-mediated proteolytic degradation of ORC in S-phase and partial Cdc6 re-localization to the cytosol (Méndez et al., 2002; Tatsumi et al., 2003). Still, the main control in metazoans to prevent re-replication is exerted towards downregulating Cdt1 activity. The relative contribution of Geminin-mediated inhibition and proteosomal degradation of Cdt1 varies depending on the organism (Hall et al., 2008; Lin et al., 2010; reviewed by Kim and Kipreos, 2007). In *Drosophila*, loss of Geminin or Cdt1 overexpression is sufficient to promote re-replication. In *C. elegans* and *X.*

laevis, loss of Geminin does not lead to re-replication whereas overexpression of Cdt1 either by downregulating the activity of CUL4-DDB1 (Zhong et al., 2003; Lin et al., 2010; Milhollen et al., 2011) or by deleting the PIP motif (Arias and Walter, 2006) of Cdt1 is sufficient to promote re-replication. In human cells both Geminin depletion and Cdt1 overexpression promote re-replication. Tumor cells lacking p53 undergo re-replication upon Cdt1 overexpression, which is much enhanced by Cdc6 co-expression (Vaziri et al., 2003). Downregulation of Geminin induces re-replication in normal and tumor cells independently of p53 (Melixetian et al., 2004; Zhu et al., 2004). In these studies, re-replication activated a DNA damage response (DDR) that prevented cells from entering mitosis. Abrogation of the checkpoint by caffeine or UCN-01 resulted in cell death. A more recent study showed that Geminin-induced re-replication originated in G2, when Cdt1 protein levels start to build-up and the anti-licensing role of Geminin is essential (Klotz-Noack et al., 2012).

The DNA damage response may be activated upon high levels of Cdt1 even in the absence of extensive re-replication, highlighting the sensitivity of mammalian cells to licensing control disruption (Tatsumi et al., 2006; Liu et al., 2007). In addition, Geminin depletion in human or *Drosophila* cells promotes Cdt1 and Cdc6 destabilization by proteosomal degradation as a response to minimize the extent of re-replication (Hall et al., 2008).

9. Deregulated DNA replication activates the DDR and may promote senescence

As mentioned before, overexpression of Cdt1 and Cdc6 in tissue culture cells activates the DDR to restrain the cell cycle (Vaziri et al., 2003; Melixetian et al., 2004; Zhu et al., 2004). This may be one of the first barriers to prevent the progression from preneoplastic lesion to neoplasia (Bartkova et al., 2005; Gorgulis et al., 2005). The DDR is activated from the earliest stages of malignant transformation in human samples and drives cells into apoptosis or senescence (Bartkova et al., 2006; DiMicco et al., 2006). At the same time, a chronic DDR activation may create a selective pressure that eventually favors the outgrowth of malignant clones with genetic or epigenetic defects in the genome maintenance machinery (reviewed by Bartek et al., 2007). The link between defective DNA replication, activated DDR and the promotion of senescence has been reinforced by expressing different oncogenes in human tissue culture cells. Upon Cyclin E, Mos, Cdc6 or H-RasV12 expression, cells undergo senescence independently of p16 that could be overcome by inactivating the

DDR machinery. Analysis of the DNA replication dynamics at the molecular level showed that oncogene-expressing cells presented an increased rate of prematurely terminated forks, which can lead to DSB (Bartkova et al., 2006). In addition, re-replicated regions of the genome have been detected by *Fluorescence in situ Hybridization* (FISH) in cells expressing oncogenic *Ras* (**Fig. 5**) (DiMicco et al., 2006).

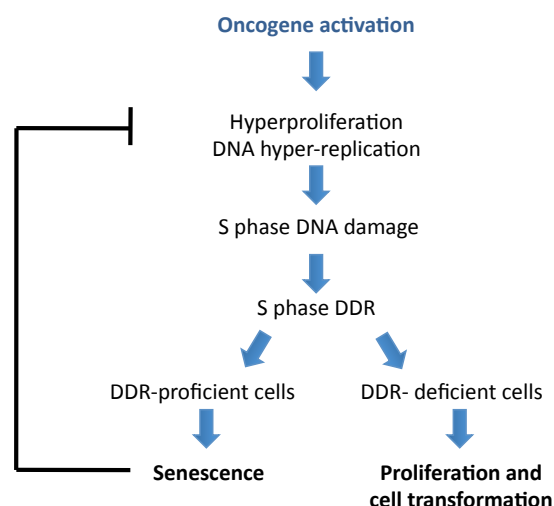


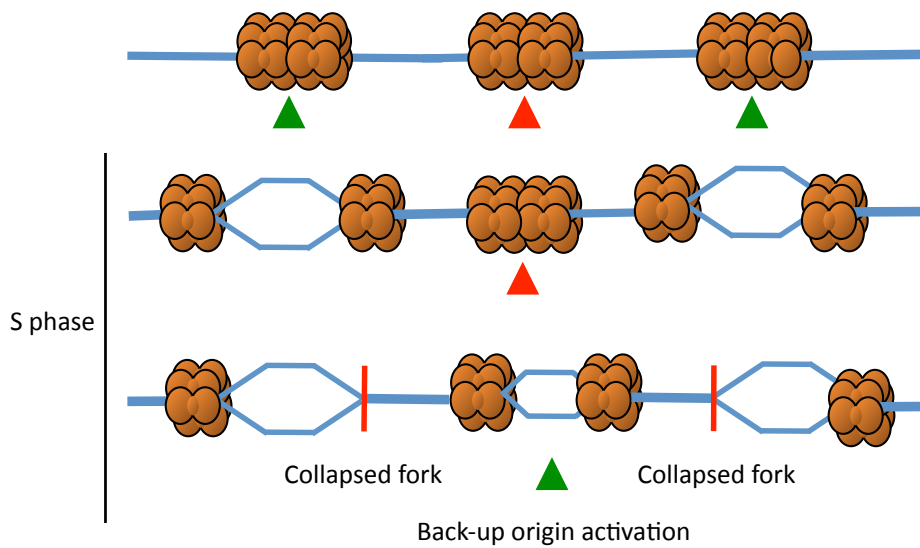
Figure 5. Proposed model for the events after oncogene expression. Taken from DiMicco et al., 2006.

In this context, continuous overexpression of Cdt1 and Cdc6 could contribute to overcome such a barrier by inducing genomic instability. Increased levels of Cdc6 and Cdt1 proteins have been found in human lung dysplasias and gene amplifications were found in the tumors (Liontos et al., 2007). The initial activation of the DDR probably might have resulted in the selection of clones with high proliferation potential, invasive properties and genomic instability.

10. Origin licensing machinery is deregulated in cancer

Failure to maintain a tight control on the licensing system has been linked to oncogenesis (reviewed by Blow and Gillespie, 2008). Insufficient origin licensing causes genomic instability (reviewed by Blow et al., 2011). As previously commented, MCMs are loaded in excess compared to the number of active origins in a normal S-phase. Several studies in *Xenopus* and human cells have shown that cells can still undergo an apparently normal S-phase with a reduced MCM pool. Nevertheless, the ‘excess’ of MCM complexes is essential for the licensing of ‘dormant origins’ that may be activated to complete DNA replication if ongoing forks stall or collapse (**Fig 6**).

Normal licensing



Minimum licensing

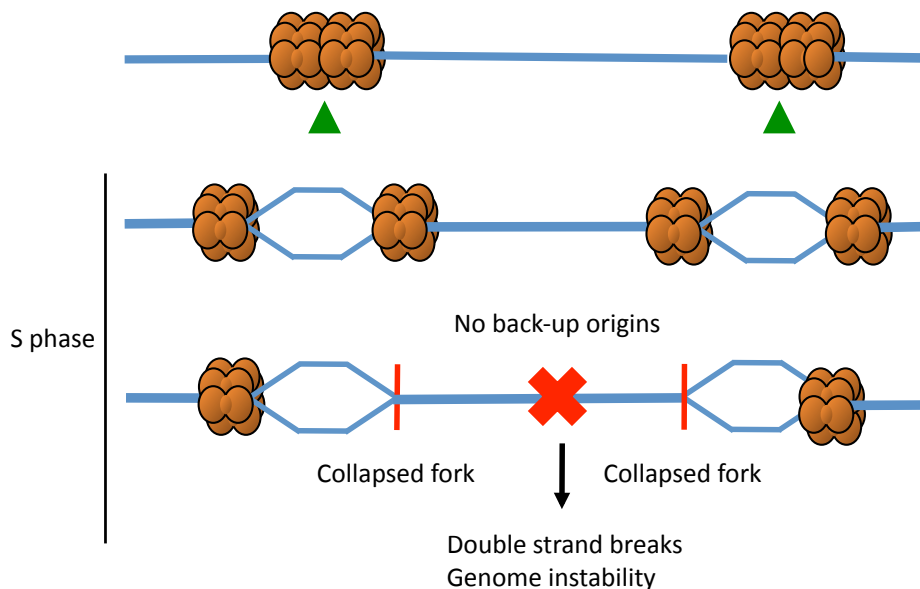


Figure 6. Dormant origins and replication fork stalling. Many more origins are licensed in G1 than activated in a normal S-phase. The inactive origins remain 'dormant' unless a nearby fork stalls or collapses, a situation that can be artificially induced by replication stress-inducing agents such as HU. Under these conditions, activation of dormant origins ensures complete genome replication. A reduced pool of MCMs, allows replication to proceed at normal rates, but cells become hypersensitive to replicative stress in terms of proliferation, reduced origin activation and DNA damage accumulation.

Cells with low MCM content become hypersensitive to replicative stress-inducing agents, accumulating DNA damage and chromosomal aberrations (Ge et al., 2007; Ibarra et al., 2008; reviewed by Blow et al., 2011). This model has been further validated *in vivo*. Mice hypomorphic for MCM2 and MCM4 affect the total amount of MCM2-7 loaded onto DNA and show a reduction in dormant origin activation in conditions of replicative stress (Pruitt

et al., 2007; Shima et al., 2007). Even in the absence of replicative stress, fibroblasts derived from these mice displayed signs of DNA damage and both strains are cancer-prone (Kunnev et al., 2010; Kawabata et al., 2011). Combination of the hypomorphic MCM4 mutation with hemizygoty of MCM2, MCM6 or MCM7 further increased genetic instability and the rate of tumor formation (Chuang et al., 2010).

Recently, mutations in different members of the pre-RC (ORC1, ORC4, ORC6, Cdt1 and Cdc6) have been found in patients suffering from Meier-Gorlin syndrome (MGS), an autosomal recessive primordial dwarfism syndrome (Bicknell et al., 2011a; Bicknell et al., 2011b; Gernsey et al., 2011). In spite of the marked genetic heterogeneity of this disorder, the underlying functional homology supports a causal link between impaired replication licensing and growth failure. Cells isolated from MGS patients with the different mutations grew effectively *in vitro* with different S-phase rates. These cells also displayed alterations in centrosome and centriole copy number that cause a defect in cilia formation and impairs cartilage formation (Stiff et al., 2013).

In addition, misregulation of the licensing system due to overexpression of pre-RC components, such as Cdc6 or Cdt1 has been also related to genomic instability although less is known about its consequences *in vivo*. Because genes such as Cdc6, Cdt1 or MCM2-7 are E2F-regulated and this pathway is frequently deregulated during cell transformation, an increased number of cells expressing these replication factors may be observed in otherwise quiescent tissues. This fact has provided clinical value to the immunohistochemical detection of Cdc6 or MCMs in early malignancies and also as a prognostic marker in several types of cancer including oral, laryngeal, oesophageal, mammary, ovarian, renal, prostatic, urothelial and colorectal cancers (reviewed by González et al., 2005; Williams and Stoeber, 2007; Blow and Gilliespie, 2008). Cdc6 is overexpressed in 55% of brain tumors and in a subset of mantle cell lymphomas (Ohta et al., 2001; Pinyol et al., 2006). A subset of non-small cell lung carcinomas is characterized by the overexpression of Cdc6 and Cdt1 (Karakaidos et al., 2004). In addition, oncogenic potential of Cdc6 has also been inferred *in vitro* through the transcriptional repression of the *INK4/ARF* locus (González et al., 2006) or the *CDH1* locus (Sideridou et al., 2011) as commented before.

Cells overexpressing Cdt1 form tumors in immunodeficient mice (Arentson et al., 2002). A mouse model overexpressing Cdt1 in thymocytes developed lymphoblastic

lymphoma in a p53-null background with a 100% incidence and the tumors presented numerical and structural chromosomal aberrations (Seo et al., 2005). In addition, a mouse model that expresses a constitutively active version of Cyclin D1 in the lymphoid compartment, displayed Cdt1-mediated re-replication and developed lymphomas, which turned out to be more aggressive and genetically unstable in a p53-null background (Aggarwal et al., 2007).

Given the importance of a precise regulation of the licensing system in eukaryotes, in this work we decided to investigate the *in vivo* consequences of overexpressing Cdc6 and Cdt1. We describe for the first time mouse models that allow the conditional overexpression of Cdc6 and Cdt1 alone or in combination as well as another model in which Cdc6 overexpression is restricted to stratified epithelia. We have used these new mouse strains to evaluate the effects of Cdc6 and/or Cdt1 overexpression in DNA replication dynamics, genome stability, ageing and cancer susceptibility.

OBJECTIVES

- To generate mouse models for tissue-specific and ubiquitous inducible Cdc6 and Cdt1 overexpression.
- To characterize the effects of Cdc6 and Cdc6/Cdt1 overexpression, in terms of DNA replication dynamics, cell proliferation and genome stability.
- To evaluate the impact of Cdc6 and Cdc6/Cdt1 overexpression *in vivo*, particularly in cancer susceptibility and ageing.

MATERIALS AND METHODS

1. Generation of genetically-modified mouse strains

1.1. Ethical statement

Mice were kept in the Animal Facility at CNIO in accordance with institutional policies and the 'Federation for Laboratory Animal Science Associations' (FELASA) guidelines. Animal procedures were approved by the Animal Experimental Ethics Committee of the Instituto de Salud Carlos III (Madrid, Spain).

1.2. K5-CDC6^{tg} mouse generation

Murine CDC6 cDNA (isoform b) was cloned into the pBluescript K5 plasmid, originally generated in Dr. J.L. Jorcano's lab (CIEMAT, Madrid, Spain). This plasmid contains the 5' regulatory fragment of the bovine keratin 5 gene (K5), the intron 2 of the rabbit β -globin gene and the SV40 early polyA signal (named K5-CDC6 plasmid). CDC6 was inserted 3' downstream of the bovine keratin 5 promoter, which has been shown to behave as the endogenous murine K5 promoter (Ramírez et al., 1994; Murillas et al., 1995). CDC6 cDNA was verified by sequencing after cloning. K5-CDC6 transgene was excised from the plasmid by *NotI* digestion, purified after agarose electrophoresis and microinjected into the pronuclei of C57BL/6J X CBA/J oocytes by the Transgenic Mice Unit at CNIO. Transgene insertion was screened in the progeny by Southern blot from genomic DNA isolated from tail clips. DNA was digested with *NheI* and hybridized to a specific CDC6 140 bp probe that allows detection of endogenous and transgenic CDC6 generated with the following primers Fw: 5' GTATTGCTAATACCCTAGATCTCA 3' and Rv: 5' CTGACTAAGTCGATCCTGCAAGA 3'. Two individuals showed integration of K5-CDC6 construct (founders 1 and 2) although only founder 1 overexpressed Cdc6. Founder 2 was dropped from the study. K5-CDC6^{tg} (founder 1) mice were maintained in heterozygosity by crossbreeding K5-CDC6^{tg} mice with C57BL/6J wt individuals.

1.2. Gene walking by unpredictably primed (UP) PCR

Genomic DNA from K5-CDC6^{tg} mice was isolated by ethanol precipitation and subjected to UP-PCR-based gene walking to determine the transgene integration site (Domínguez and López-Larrea, 1994).

1.3. Generation of *Lox-CDH1*; *K5-Cre^{tg}*; *K5-CDC6^{tg}* mice

Cdh1 conditional knock-out strain was provided by the Cell Division and Cancer group at CNIO. In this mouse strain exons 2 and 3 of Cdh1 (*Fzr1* locus) are flanked by loxP sites (García-Higuera et al., 2008) and Cre recombinase-mediated Cdh1 ablation is under the control of the K5 promoter. We crossbred animals bearing lox-Cdh1 in homozygosity and K5-Cre^{tg} in heterozygosity with K5-CDC6^{tg} animals. Lox-Cdh1 heterozygous mice (lox-Cdh1/+) were subsequently crossbred to generate homozygous animals for lox-Cdh1 and heterozygous for K5-Cre and K5-CDC6.

1.4. Generation of *K5-CDC6^{tg}* mice in a *p53*-null background

p53-null (p53 -/-) mice in C57BL/6J background (strain B6.129S2-Trp53tm1Tyj/J) were provided by the Animal Facility at CNIO to obtain K5-CDC6^{tg};p53 -/+ and K5-CDC6^{tg}; p53 -/- mice.

1.5. *Tet^{ON}-CDC6* and *Tet^{ON}-CDT1* mouse generation

Inducible mouse models for Cdc6 or Cdt1 overexpression were generated using recombinase-mediated single-copy transgene integration in a genetically modified Embryonic Stem cell line (KH2) previously described (Beard et al., 2006). The M2 reverse tetracycline transactivator (M2-rtTA) is constitutively expressed from the *ROSA26* locus. In addition, a modification downstream of the *Collagen 1 α1* locus (*Col1a1*) allows frt-mediated single-copy transgene integration. Co-electroporation of KH2 cells with a fpl-in vector carrying the transgenes (pBS31) and a vector that expresses flipase recombinase (FLPe) allowed specific transgene integration 3' of the *Col1a1* locus. A tetracycline-responsive element located upstream of the PGK ubiquitous promoter controls transgene expression. Different levels of expression can be achieved by modulating the concentration of tetracycline or one of its derivatives such as doxycycline (dox) (Gossen and Bujard, 1992).

N-terminally tagged HA-CDC6 cDNA was generated by PCR amplification from the murine CDC6 cDNA (b isoform) obtained from the IMAGE Consortium (Integrated Molecular Analysis of Genomes and their Expression; Clone #6837113). The PCR product was designed to include *MluI* restriction sites to allow insertion into the pBS31 plasmid, which was kindly provided by the Genes, Development and Disease Group at CNIO. C-terminally Flag-tagged CDT1 (CDT1-FLAG) was also generated by PCR amplification from the murine CDT1 cDNA obtained from the IMAGE Consortium (Clone #6307476). In this case, the PCR product

contained *EcoRI* restriction sites. The primers used for transgene generation are listed in **table 1**. DNA sequences of the HA-CDC6 and CDT1-FLAG constructs were verified after insertion into the pBS31. Electroporation of KH2 ES cells was carried out by the Transgenic Mice Unit at CNIO. Correct insertion of the transgenes was verified by Southern blot using the strategy described in Beard et al., 2006. Dox-induced HA-CDC6 and CDT1-FLAG expression was tested in ES cells before mouse generation. Correctly targeted KH2 clones for HA-CDC6 and CDT1-FLAG transgenes were used for ES cell aggregation. The resultant strains have a mixed genetic background (C57BL/6J X 6x129). Modified *ROSA26* and *Col1a1* alleles were maintained in heterozygosis by crossbreeding Tet^{ON}-mice with C57BL/6J wt individuals.

1.6. Tet^{ON}-CDC6/CDT1 mouse generation.

To obtain Tet^{ON}-CDC6/CDT1 mice, heterozygous Tet^{ON}-CDC6 or Tet^{ON}-CDT1 were first crossbred to obtain homozygous mice in the *Col1a1* locus for CDC6 or CDT1 transgenes. Subsequently homozygous Tet^{ON}-CDC6 and Tet^{ON}-CDT1 were crossbred between them to obtain descendants bearing both alleles in the *Col1a1* locus. For the studies with Tet^{ON}-CDC6/CDT1 mice, the *ROSA26-M2rtTA* was maintained in heterozygosity.

2. Mice genotyping

Genotyping was performed by PCR analyses of genomic DNA isolated from tail clips (Malumbres et al., 1997). Tails were lysed in PCR-K buffer (50 mM KCl, 1.5 mM MgCl₂, 10 mM Tris-HCl pH 8.5, 0.01% gelatin, 0.45% NP-40, 0.45% Tween-20, 100 µg/mL proteinase K (Roche)) for 2 h at 55°C in agitation and proteinase K was inactivated at 95°C for 15 min. Each PCR reaction was done with 2 µL of genomic DNA, 0.2 µL of Taq polymerase (Ecogen), 2.5 µL of 10X Taq reaction buffer (Ecogen), 1.5 µL of 50mM MgCl₂ (Ecogen), 1 µL of each primer from a 10 µM dilution in H₂O, 1 µL of 10mM dNTPs (Fermentas), and H₂O to a final volume of 25 µL. The different primers used for mice genotyping and expected DNA fragments are listed in **table 2**.

3. Mouse procedures

3.1. TPA-induced skin hyperplasia

Four doses (12.5 µg in 200 µL acetone) of 12-O- tetradecanoylphorbol 13-acetate (TPA)(Sigma-Aldrich) were applied to the tail skin of 2 month-old mice every 48h. One animal per genotype was administered acetone as control. At the end of the experiment, mice were sacrificed and the tail skin was subjected to histological examination. The degree of hyperplasia was estimated using ImageJ software (<http://rsb.info.nih.gov/ij/>) (US National Institutes of Health, Bethesda, Maryland, USA) on pictures of Hematoxylin-Eosin (H-E)-stained tail skin sections.

3.2. DMBA-TPA skin chemical carcinogenesis assay

Mice (1 to 3 month-old) were shaved and subjected to a single application of DMBA (Sigma-Aldrich) (20 µg in 200 µL of acetone). Starting 7 days later, mice were treated twice a week with TPA (12.5 µg in 200 µL of acetone) for 25 weeks. 2 mice per genotype were treated with acetone as control. The size and number of papillomas were weekly monitored. Mice were kept in the study for a total of 35 weeks.

3.3. Wound-healing

Four 4 mm² punch biopsies extending through the epidermis and dermis were performed in the back skin of 24 month-old mice 12, 8, 6 and 3 days before sacrifice. A punch biopsy was also performed on the day of sacrifice (day 0) and 2 hours before, mice were intraperitoneally injected with BrdU (5 mg of BrdU (Sigma-Aldrich) in 300 µL of NaCl 0.9%). The wound-healing rate was calculated as percentage of wounded area relative to the initial wound (day 0). Wound areas were measured on pictures taken at the end point with ImageJ software. When indicated, tissues surrounding the wounds were processed for histological analysis. The percentage of BrdU-positive cells was manually scored using ImageJ software.

4. Cell culture experiments

4.1. Primary keratinocyte isolation from adult mice

Mice were sacrificed by hypoxia in CO₂ chamber and the back skin was shaved and excised. The epidermis was separated from the dermis by treatment in the skin in 0.25% trypsin solution without EDTA (Sigma-Aldrich) overnight at 4°C. The epidermis was peeled

off the dermis, minced with a scalpel blade, collected in 10 mL of DMEM (Lonza) supplemented with 10% FBS and filtered through a 70 μ m cell strainer (BD Falcon). Keratinocytes for biochemical analysis were washed with PBS, collected by centrifugation (500 g/8 min) and snap-frozen.

In order to put keratinocytes in culture the procedure was performed in a laminar flow hood. The tail skin was soaked for 3 min in 70% ethanol, in 10% iodide solution in PBS and finally in sterile PBS prior to skin floating on trypsin as indicated above. Keratinocyte isolation growth medium was CnT-07 (CellInTec) supplemented with antibiotic/antimycotic solution (Invitrogen). Keratinocytes were seeded in dishes with Coating Matrix Kit (Cascade Biologics) according to the manufacturer's instructions. Cells were grown at 37°C and 5 %CO₂.

4.2. Isolation and culture of keratinocytes from newborn mice

Experiments with newborn-isolated keratinocytes were performed by Dr. Mirna-Pérez Moreno, Head of the Epithelial Biology Group at CNIO. Newborn animals were sacrificed and keratinocytes were isolated from the back skin using dispase (Sigma-Aldrich) and trypsin (Gibco). After filtration in 40 μ m cell strainers, cells were cultured in Low Calcium Medium (0.05 mM Ca⁺⁺) containing 15% Ca⁺⁺-depleted FBS, as described in Nowak and Fuchs, 2009. Cells were grown at 37°C and 5 %CO₂. For proliferation curves, 20000 cells were seeded per time point. When indicated 0.1 μ M aphidicolin was added 24 h after plating. For clonogenic assays 1500 cells were plated in triplicate and after 10 days cells were fix with 4% PFA and stained with cristal violet for colony quantification.

4.3. Primary Mouse Embryonic Fibroblasts (MEFs) isolation

Mouse embryos were obtained at E13.5 days. Pregnant females were sacrificed by cervical dislocation and uterine horns containing the embryos were removed and transferred to a sterile PBS solution. In a laminar flow hood, embryos were removed from the uterus, fetal liver was excised and a fragment of tissue was taken for subsequent genotyping. The rest of embryonic tissue was minced and treated with 0.25% trypsin-EDTA (Sigma-Aldrich) for 20 min at 37°C. Cells were further disaggregated by pipetting, transferred to 9mL medium (DMEM complete (Lonza), 15%FBS, 10% penicillin/streptomycin solution (Invitrogen)), seeded in tissue culture plates and grown at 37°C and 5 %CO₂. Cells

were expanded and frozen at passage 1 in 90% FBS, 10% dimethyl sulfoxide (DMSO). All experiments with primary MEFs were performed at low passage number (≤ 4).

4.4. Proliferation curves with MEFs

50000 cells for each time point were seeded in 6-well plates in duplicate. Transgene expression was induced with 1 $\mu\text{g}/\mu\text{L}$ dox. To induce replicative stress, 24h after dox-induction, 0.05 μM , 0.1 μM or 0.2 μM aphidicolin (Sigma-Aldrich) was added to the cell culture medium. To estimate the proliferation rate, cells were counted using a Neubauer hemocytometer.

4.5. Serum starvation and cell cycle re-entry

Cells were grown until nearly confluent and serum starved (0,1%FBS) for 72 h to induce a quiescent G0 state. 24 h before cell cycle re-entry, 1 $\mu\text{g}/\mu\text{L}$ dox was added to induce transgene expression. Cells were split and FBS was increased to 15% to promote cell cycle re-entry. To determine the percentage of cells entering S-phase. cells were pulsed with 10 μM BrdU for 30 min at 0, 15, 18, 21 and 24 h after serum stimulation.

4.6. MTT survival assay

1500 cells per well were seeded in triplicate in 96 well plates. 24 hours after seeding 1 $\mu\text{g}/\mu\text{L}$ of dox was added to induce transgene expression. 24 hours later, aphidicolin and HU (HU) were added. 3 days later, cells were treated for 6 h with 0.5 $\mu\text{g}/\mu\text{L}$ thiazolyl blue tetrazolium bromide (MTT-formazan, Sigma-Aldrich) and the resulting formazan was subsequently solubilized with a detergent solution (10% SDS, 10Mm HCl) for 24 h after measuring absorbance at 590 nm. In the case of UV light, MTT was added 3 days after irradiation. For methyl methanesulfonate (MMS) and neocarzinostatin (NCS), cells were treated for 24h, washed and allowed to grow for further 3 days before MTT addition. Survival was relativized to the absorbance of untreated controls.

4.7. Single-molecule analysis of DNA replication in stretched fibers

Exponentially growing cells were sequentially pulse-labeled for 20 min with 50 μM chlorodeoxyuridine (CldU) and 250 μM iododeoxyuridine (IdU). DNA spreads were made as described (Terret et al., 2009) with slight modifications. Cells were harvested and resuspended in cold PBS at $0.25 \cdot 10^6$ cells/mL. 2 μL of cell suspension were placed on a microscope slide and lysed for 6 min in 10 μL of pre-warmed (30°C) spreading buffer (0.5%

SDS, 200 mM Tris-HCl pH 7.4, 50 mM EDTA). Slides were tilted at a 15° angle to allow DNA suspension to run slowly down the slide, and the resulting DNA spreads were air-dried, fixed in cold 3:1 methanol: acetic acid for 2 min and refrigerated.

Slides were treated with 2.5 N HCl for 30 min, washed 3 times with PBS and blocked in 1% BSA, 0.1% Triton X-100 in PBS for 1 h before incubation with CldU, IdU and ssDNA primary antibodies (listed in **table 4**) diluted in blocking solution (1/100) for 1 h. Fluorophore-conjugated secondary antibodies were added for 30 min. ProLong Gold antifade reagent (Invitrogen) was used as mounting media for IF. For detecting re-replication events a 15 min treatment with 10 mM Tris-HCl pH 7.4, 400 mM NaCl, 0.2% Tween-20, 0.2% NP-40 was performed between primary and secondary antibody incubations according to the protocol described in Dorn et al., 2009.

Microscopy was carried out using a Leica DFC350 FX microscope and DNA staining was used to confirm fiber integrity. Fork progression rate was monitored in second-labeled (IdU) tracks. The length of 200-300 tracks was measured per condition using ImageJ software and conversion factor 1µm = 2.59 kb (Petermann et al., 2010). Inter-origin distances (IODs) were measured between two contiguous origins (green-red-green signals) in the same fiber. The length of 30-50 IODs was measured per condition.

4.8. Oncogenic transformation assay

pBabe (empty), pBabe-*H-RasV12* and pBabe-*H-RasV12/E1A* retroviral supernatants were produced by calcium phosphate transfection of 293T cells following a standard protocol (Wigler et al., 1977). MEFs were grown until nearly confluent and induced with 1 µg/µL dox 24 h before infection with retroviral supernatant. 24 h later the medium was changed and 10 days post-infection plates were fixed with 1% glutaraldehyde, stained with 0.1% crystal violet in 10% ethanol and scored for number of foci.

4.9. Chromatid breaks and Sister Chromatid Exchange (SCE) analyses

Cells were treated with 1 µg/µL dox 24 h after seeding to induce corresponding transgene. For analysis of aphidicolin-induced breaks, cells were treated for 24 h with 0.5 µM aphidicolin. 6 hours before collection 0.1 µg/µL of colcemid was added to the medium to arrest cells in metaphase. For SCE, 24 after dox cells were labeled for 48 h with 10 µM

BrdU. During the last 24 h of labeling, 0.5 μ M aphidicolin or 2.5 nM camptothecin were added to induce SCE.

For metaphase spread preparation, cells were subjected to an osmotic shock (75 mM KCl for 20 min at 37°C), centrifuged for 10 min at 200 g and fixed by drop-wise addition of Carnoy's fixative solution (ice-cold 3:1 methanol-acetic acid). Cells were subjected to 3 cycles of centrifugation and Carnoy's solution addition before storing them at -20°C. For chromosome spreading, microscope slides were soaked in 45% acetic acid and drops of the cell suspension were let to fall and spread on the slide. After air-drying, spread chromosomes were stained with 1 μ g/ μ L DAPI (Sigma) diluted in Vectashield (Vector laboratories) mounting media. Chromatid breaks and SCE events were scored and normalized to the total number of analyzed chromosomes.

4.10. Flow cytometry analyses

For BrdU incorporation analysis, cells were pulsed-labeled with 10 μ M BrdU for 30 min. Primary keratinocytes were labeled for 2 h. Cells were trypsinized, washed with PBS and fixed overnight at 4°C in 70% ethanol. DNA denaturation and cell permeabilization was carried out with 2N HCL 0.5% Triton X-100 for 20 min at 37°C. Cells were subsequently washed twice with 1 M Tris-HCl pH 7.5 for HCl neutralization and incubated for 1 h with FITC-BrdU antibody (BD Biosciences Pharmigen) in 1% BSA PBS- 0.05% Tween-20. For DNA content analysis, cells were incubated overnight in DNA staining solution (25 μ g/mL propidium iodide (Sigma-Aldrich), 10 μ g/mL RNase A (Qiagen)). For quantification of apoptosis, cells were incubated with 40 nM tetramethylrhodamine ethyl ester (TMRE, Sigma) for 10 min at 37°C and washed with PBS. DAPI dye exclusion was used to differentiate dead (permeable) from alive cells.

Data acquisition was carried out in a FACsCanto II cytometer (Becton-Dickinson) and data were analyzed using Flow Jo software (Tree Star). For cell sorting based on DNA content, cells were stained with Hoechst 33342 (Invitrogen) for 30 min at 37°C in DMEM, 3% FBS. Subsequently cells were washed and resuspended in 0.1% BSA, 3 mM EDTA in PBS at $1 \cdot 10^7$ cells/mL. Cell sorting was performed by the Cytometry Unit at CNIO in a BD Influx sorter (Becton-Dickinson).

5. RNA expression analyses

5.1. RNA isolation, retrotranscription and quantitative PCR (RT-qPCR)

Tissues were disrupted and homogenized in Trizol using a bead-beating system (Precellys). Total RNA was isolated using Trizol (Invitrogen) according to the manufacturer's instructions. Potential genomic DNA contamination was removed by DNaseI digestion (Roche). cDNA was obtained with Maxima First Strand cDNA kit (Thermo) according to the manufacturer's instructions. cDNAs were diluted 1/100 and qPCR was performed in triplicates using SYBR green-Real Time PCR master mix (Applied Biosystems). Primers used for RT-qPCR analysis are shown in **table 3**. The $2\Delta\Delta^{Ct}$ method was used to quantify amplified fragments. Expression levels were normalized to GAPDH housekeeping gene. qPCR analysis were done in a Applied Biosystems 7900HT Fast Real Time PCR System equipment and analyzed with 7900HT Sequence Detection System (Applied Biosystems).

6. Protein analysis

6.1. Whole cell extracts

Keratinocytes were lysed in RIPA lysis buffer (1% NP-40, 0.1% SDS, 50 mM Tris-HCL pH 7.4, 150 mM NaCl, 0.5% Sodium Deoxycholate, 1mM EDTA, 1mM NaVO₄, 0.5mM NaF, 0.1mM PMSF, protease inhibitors (Complete Mini EDTA, Roche), for 20 min on ice and sonicated (Branson sonicator 102C) for 30 seconds at 20% amplitude. Extracts were clarified by high-speed centrifugation (15 min/16000 g/ 4°C). Protein was quantified using BCA kit (Pierce) according to the manufacturer's instructions. For whole cell extracts intended for immunoblot analysis, cells were trypsinized, collected by centrifugation (290 g/5 min) washed with PBS, lysed in Laemmli Sample Buffer (50 mM Tris-HCL pH 6.8, 10% glycerol 3% SDS, 0.006% w/v bromophenol blue and 5% 2-mercaptoethanol) at 5000 cells/ μ L and subsequently sonicated.

6.2. Biochemical fractionation

Biochemical fractionations were performed as described in Méndez and Stillman, 2000. Cells were resuspended at $2 \cdot 10^7$ cells/mL in buffer A (10mM HEPES pH 7.9, 10mM KCl, 1.5mM MgCl₂, 0.34M sucrose, 10% glycerol, 1m MDTT, 1mM NaVO₄, 0.5mM NaF, 5mM β -glycerophosphate, 0.1mM PMSF, protease inhibitors cocktail), and incubated on ice for 5 min in the presence of 0.1% Triton X-100. Low-speed centrifugation (4 min/600 g/4°C)

allowed the separation of the cytosolic fraction (supernatant) and nuclei (pellet). The cytosolic fraction was clarified by high-speed centrifugation (15 min/16000 g /4°C). Nuclei were first washed with buffer A and subsequently subjected to hypotonic lysis in buffer B (3mM EDTA, 0.2mM EGTA, 1mM DTT, 1mM NaVO₄, 0.5mM NaF, 5mM β- glycerophosphate, 0.1mM PMSF, protease inhibitors cocktail) 30 min on ice. Nucleoplasmic and chromatin fractions were separated after centrifugation (4 min/600 g/4°C). Chromatin was resuspended in Laemmli Sample Buffer and sonicated twice for 30 seconds at 15% amplitude.

6.3. Antibody generation

Specific antibodies for Mcm3, Mcm4 and Mcm6 murine proteins were generated by injecting the following peptides into NZW rabbits according to a standard immunization protocol (Sigma-Aldrich).

MCM3: CSQEDTEQKRKRRK

MCM4: SLRSEESRSPNRRRC

MCM6: AGSQHPEVRDEVAEKC

6.4. Immunoblots

SDS-polyacrylamide gels and immunoblotting were performed following standard protocols (Harlow and Lane, 1999). The primary antibodies used are listed in **table 4**. Horseradish peroxidase (HRP)-conjugated secondary antibodies (Amersham Biosciences) and ECL developing reagent (Amersham Biosciences) were used. When indicated, signals were quantified using the Odyssey Imaging System (LI-COR) in which secondary antibodies are conjugated to Alexa-680 fluorophores (Invitrogen).

6.5. Immunofluorescence

Cells grown on poly-lysine were fixed with 4% paraformaldehyde (PFA) in PBS for 15 min, permeabilized with 0.5% Triton X-100 in PBS for 5 min and treated with blocking solution (3% BSA, 5% normal donkey serum (Jackson ImmunoResearch) and 0.05% Tween-20 in PBS) for 30 min. Primary and fluorophore conjugated-secondary antibodies were diluted in blocking solution. The primary antibodies used for IF are listed in **table 4**. Nuclei were stained with 1 μg/μL DAPI (Sigma) in PBS for 1 minute. ProLong Gold antifade reagent was used as mounting media for IF. To visualize chromatin-bound proteins, cells were subjected to a pre-extraction step with 0.5% Triton X-100 in CSK buffer buffer (10 mM PIPES pH 7.0,

0.1 M NaCl, 0.3M sacarose and 3 mM MgCl₂, 0.5 mM PMSF) for 5 min at 4°C. For PCNA IF, after pre-extraction an additional treatment with methanol for 10 min at -20°C was used. For BrdU detection under native conditions, cells were fixed with methanol for 1 h at -20°C. EdU detection was performed using Click-it detection kit (Invitrogen) according to the manufacturer's instructions.

Images were acquired in a Leica DFC350 FX microscope or a SP2 AOBS LEICA confocal. In the latter case, image analysis was performed at the Confocal Microscopy Unit at CNIO, using pre-designed routines for nuclei and foci detection in the Definiens software (Definiens, Germany). For high-throughput assays, cells were grown on glass-bottom 96 well plates (Greiner Bio One) pretreated with 0.1 % gelatin. After IF detection, cells were analyzed in an Opera HTS spinning disk confocal microscope (Perkin Elmer). A routine was designed in Acapella software (Perkin Elmer) for nuclei identification and nuclei intensity measurements.

7. Histological analysis

Tissue processing for histological analysis of formalin-fixed tissues was done by the Histopathology Unit at CNIO. Briefly, tissues were fixed overnight in 10% buffered formaline, embedded in paraffine and sectioned (5 µm). Samples were deparaffinized, re-hydrated and stained with H-E for histological examination. For immunohistochemistry (IHC) tissues were submitted to antigen retrieval and blocking of endogenous enzymatic activities. Tissue slides were digitalized using a Mirax scanner (Carl Zeiss) and equivalent areas per tissue and group were analyzed using the AxioVision digital image processing software (Carl Zeiss). Staining-positive areas were normalized to total analyzed areas. When indicated, skin samples were embedded in optimal cutting temperature (OCT) compound (Tissue-Tek), snap-frozen and sent to Cédric Blanpain's lab (Université Libre, Brussels) for histological analysis as described in Sotiropoulou et al., 2013.

Table 1. Primers for Tet^{ON} mouse generation

Mouse strain	Primers	Sequence (5'→3')
Tet ^{ON} -CDC6	MLuI-HA-CDC6 Fw	GACTACGCGTACCATGTACCCATACGATG TTCCAGATTACGCTCCTCAAACCAGATCCCAG
	CDC6-MLuI Rv	AGTCACGCGTTCAGGGCAGACCAGCAGC
Tet ^{ON} -CDT1	CDT1-EcoRI-Fw	ACGTGAATTCATGGCGCAAAGTCGTG
	CDT1-FLAG-EcoRI-Rv	ACGTGAATTCTCACTTGTGCGTCATCGTCTT TGTAAGTCCAGCCCCTCGGCGTGGACG

Table 2. Primers for mice genotyping and PCR fragments

Mouse strain	Primer name	Sequence (5'→3')	Expected DNA fragment
K5-CDC6 ^{tg}	K5	CTTCTTGCTTGAACAGTCTTATA	wt → no amplification
	Cdc6	CTTCTTGCTTGAACAGTCTTATA	tg → 1.2 kb
Lox-Cdh1	Cdh1-A	AGCATGGTGACCGCTTCATCC	wt → 170 bp
	Cdh1-B	GCTGGGGGACTTCTCATTTTCC	lox-Cdh1 → 290 bp
p53-null	p53-A	TGGTTTGTGCGTCTTAGAGACAGT	wt → 480 bp
	p53-B	AAGGATAGGTCGGCGGTTTCAT	null → 330 bp
	p53-C	CCAGCTATTCTCCCACTCA	
Tet ^{ON} -mice	Col-A	GCACAGCATTGCGGACATGC	<u>Co1a1 locus</u>
	Col-B	CCCTCCATGTGTGACCAAGG	wt → 300 bp
	Col-C	GCAGAAGCGCGCCGTCTGG	targeted → 500 bp
	Rosa-1	GCGAAGAGTTTGTCTCAACC	<u>Rosa locus</u>
	Rosa-2	GGAGCGGGAGAAATGGATATG	wt → band 600 bp
	Rosa-3	AAAGTCGCTCTGAGTTGTTAT	targeted → 300 bp

Table 3. Primer sequences for gene expression analysis by RT-qPCR

Gene	Primer	Sequence (5'→3')
CDC6	CDC6-Fw	ACAACTGTTTGAGTGGCCGT
	CDC6-Rv	GCTTCAAGTCTCGGCAGAATT C
CDT1	CDT1-Fw	TAGTACCCAGATGCCAAGG
	CDT1-Rv	GTAGGACAAGCCTGGGAGA
INK4 ^a	INK4 ^a -Fw	TACCCGATTGAGGTGAT
	INK4 ^a -Rv	TTGAGCAGAAGAGCTGCTACGT
ARF	ARF-Fw	GCCGCACCGGAATCCT
	ARF-Rv	TTGAGCAGAAGAGCTGCTACGT
GAPDH	GAPDH-Fw	TGAAGCAGGCATCTGAGGG
	GAPDH-Rv	CGAAGGTGGAAGAGTGGGAG

Table 4. Antibodies used in this study

Antibody	Use	Supplier	Reference/Catalogue #
α -tubulin	WB	Sigma	T9026
BrdU-FITC	FACs	BD-Biosciences	BD 556028
Cdc6	WB	Millipore	05-550
Cdh1	WB	Neomarkers	MS-1116-P
Cdt1	WB	Millipore	07-1383
CldU (BrdU-clone BU1/75)	IF	Abcam	AB6326
DYKDDDDK-tag (Flag)	WB	Cell Signaling	#2368
HA-tag	WB, IHC	Cell Signaling	#2367
H3	WB	Abcam	AB1791
IdU (BrdU-clone B44)	IF	BD Biosciences	BD 347580
Mcm2	WB	Bruce Stillman, CSHL	Ekholm-Reed et al.,2004
Mcm3	IF, WB	Méndez lab	
Mcm4	WB, IHC	Méndez lab	
Mcm6	WB, IHC	Méndez lab	
Mek2	WB	BD Transduction	610235
PCNA	IF WB	Santa Cruz	SC-56
p16	WB	Neomarkers	MS-887-P0
pSer139 H2AX (γ H2AX)	IF, WB, IHC	Millipore	07-164
pS15-p53	WB	Cell Signaling	#9284S
RPA	IF	Cell Signaling	2208
SA1	WB	Losada lab (CNIO)	Remeseiro et al., 2012
Smc1	WB	Bethyl	A300-055A
ssDNA	IF	Millipore	MAB3034
53BP1	IF	Novus Biological	NB-100-304

RESULTS

Chapter 1. K5-CDC6 transgenic mouse

1.1. Generation of a K5-CDC6 transgenic mouse

In order to study the effects of overexpressing Cdc6 *in vivo*, we first decided to generate a transgenic mouse that expressed Cdc6 under the control of the keratin 5 promoter (K5). This promoter constitutively drives the expression of the transgene to the basal layer of stratified epithelia located in the skin, esophagus and stomach (Ramírez et al., 1994; Murillas et al., 1995). Albeit at lower levels, keratin 5 is also expressed in tracheal epithelium, some myoepithelial cells that conform glandular epithelia, thymic reticulum cells and certain pancreatic duct cells (Moll et al., 1989).

The skin is a complex organ that has been extensively used to study proliferation, differentiation, ageing, wound healing or tumorigenesis with the advantage of its inherent accessibility (reviewed by Blanpain and Fuchs, 2006). Thus, we considered of interest to study the overexpression of a replication factor such as Cdc6 in this context. A schematic of the skin structure is shown in **figure 7**.

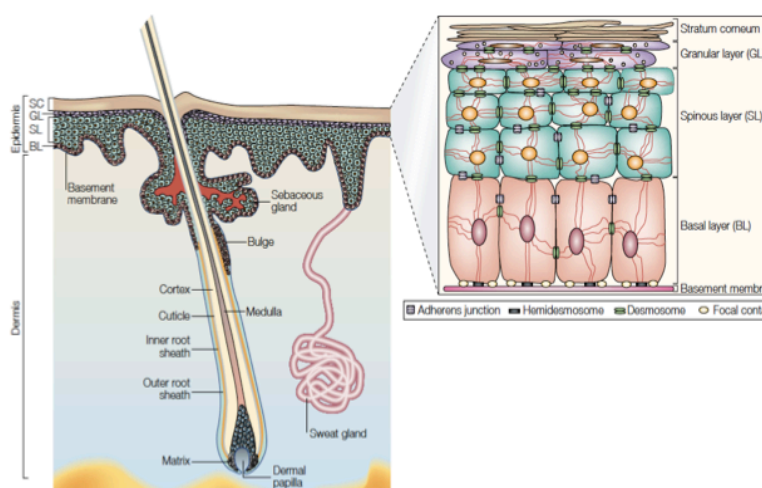


Figure 7. The skin and its appendages. Mammalian skin consists of epidermis and dermis, separated by the basement membrane. The epidermis is a stratified squamous epithelia. The basal layer is the proliferative compartment and expresses keratin 5 and keratin 14. As cells migrate towards the surface they differentiate forming the spinous and granular layers until they are finally enucleated and shed out from the body. The hair follicle consists of an outer rootsheath that is contiguous with the basal epidermal layer. At the bottom of the follicle is the hair bulb, made from proliferating matrix cells. The transit-amplifying matrix cells terminally differentiate to generate the different cell types of the follicle. Epidermal stem cells reside at the bulge. The dermal component of the hair follicle is the dermal papilla, which consists of specialized mesenchymal cells surrounded by hair matrix cells (taken from Fuchs and Raghavan, 2002).

The construct used for K5-CDC6^{tg} mice generation contains the regulatory sequence of the bovine keratin 5 gene, the intron 2 of the rabbit β -globin gene, the murine CDC6 cDNA (b- isoform) and the SV40 early polyA signal (**Fig. 8A**). In mice Cdc6 has two isoforms, which differ in a 27 aa-extension in the N-terminus. We chose the shorter isoform (b) for its similarity to human Cdc6. The construct was microinjected in the pronuclei of fertilized oocytes and integration of the transgene in the progeny was tested by Southern blot of genomic DNA isolated from tail clips. Digestion of genomic DNA with the *NheI* restriction enzyme and subsequent hybridization with a specific Cdc6 probe allowed the detection of a 4.9 Kb fragment (endogenous Cdc6) and 1.6 Kb fragment corresponding to the transgenic construct (**Fig. 8B**). Out of a total of 73 animals screened, only two of them (named founder 1 and 2) showed integration and germline transmission of the transgene. In founder 2, the transgene was integrated in the Y chromosome as it was only inherited by male descendants. This mouse did not overexpress Cdc6 possibly due to the heterochromatic nature of the insertion site (reviewed by Ohtsuka et al., 2012). Hence, this founder was dropped from the study, and we concentrated on founder 1 (**Fig. 8C**).

The high signal intensity of the transgenic band compared to the endogenous one indicate that multiple copies had been integrated, which is a frequent event in models generated by DNA microinjection in fertilized eggs (reviewed by Ohtsuka et al., 2012).

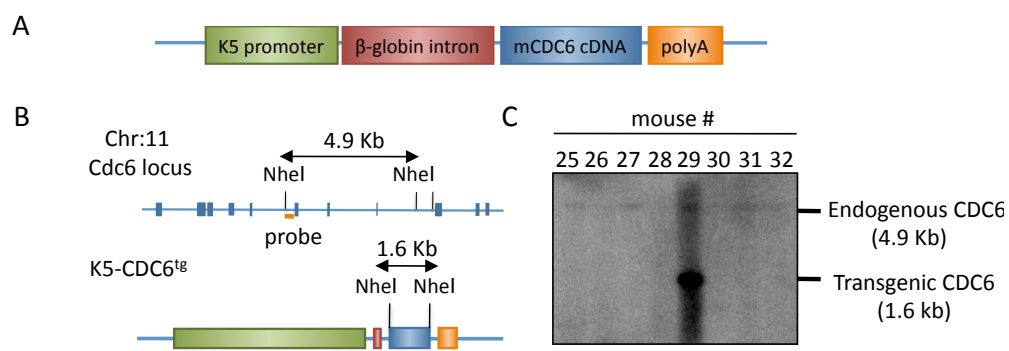


Figure 8. K5-CDC6^{tg} mouse model. **A.** The K5-CDC6 construct contains the regulatory sequences of the bovine keratin 5 gene (K5 promoter), intron 2 of rabbit beta-globin, murine CDC6 coding sequence (b isoform) and the SV40 early polyA signal. **B.** Strategy for transgene integration screening by Southern blot. **C.** Southern blot showing the screening of 8 potential founder lines (#25-32). Only # 29 (henceforth named founder 1) was positive for the transgene.

Because of the risk of secondary effects caused by the integration of the transgene, we decided to map the integration site by PCR-based gene walking (Domínguez and López-Larrea, 1994; Materials and Methods) in collaboration with the Genomics Unit at CNIO. The integration site was mapped to the intron 4 of the gene coding for vesicle-trafficking protein SEC22a (*Sec22a*) located in chromosome 16. The integration site of the 5' end (K5 promoter) has been further confirmed by PCR. Confirmation for the 3' end and expression levels of the *SEC22a* gene is currently underway but its intronic location strongly suggest that it does not interfere with *Sec22a* expression or function. A colony of mice bearing the K5-CDC6^{tg} was established. The animals are fertile, born at Mendelian rates and do not display any gross differences with their wt littermates.

1.2. Overexpression levels of CDC6 transgene in the skin and other organs

As the K5 promoter is active in several organs besides the epidermis, we first checked the expression levels of Cdc6 by retrotranscription and quantitative PCR (RT-qPCR) on total RNA isolated from different organs. Cdc6 overexpression was found in the skin, esophagus, stomach, kidney, lung, salivary gland, brain and to a much lesser extent in heart, muscle, liver and large intestine (**Fig. 9A**). We next analyzed the overexpression levels of Cdc6 by western-blot on keratinocytes isolated from the back skin of the animals (**Fig. 9B**). Quantification of signal intensity in four wt and four K5-CDC6^{tg} mice revealed a 6 to 8 fold overexpression of Cdc6 in K5-CDC6^{tg} mice (**Fig. 9C**).

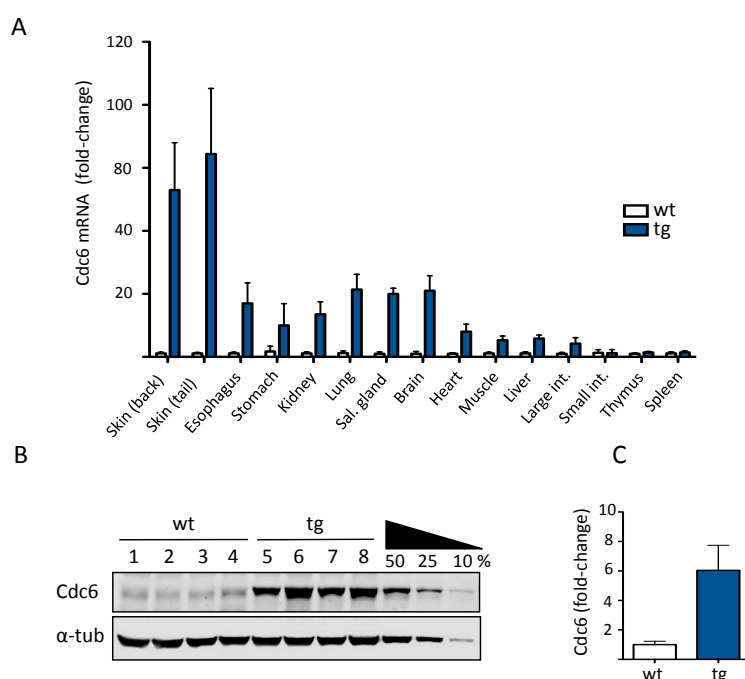


Figure 9. Cdc6 overexpression levels in K5-CDC6^{tg} mice. **A.** CDC6 mRNA level in different tissues of K5-CDC6^{tg} mice. Increased CDC6 expression was higher in organs containing stratified epithelia such as skin, esophagus and stomach but also detected in other organs (n=2 wt and 2 tg mice). **B.** Western blot analysis of Cdc6 protein in extracts prepared from keratinocytes isolated from the back skin of young wt and K5-CDC6^{tg} animals. α -tubulin, loading control (n=4 wt and 4 tg mice). **C.** Cdc6 protein level quantified from part A using the LI-COR Odyssey imaging system. Cdc6 was normalized by its corresponding α -tubulin signal.

1.3. Cdc6 overexpression leads to increased chromatin association of MCM proteins

Given the role of Cdc6 in MCM2-7 loading at replication origins, we first considered that Cdc6 overexpression could promote higher level of chromatin association of MCM proteins with DNA. A biochemical fractionation method (Méndez and Stillman, 2000) was used on back skin-isolated keratinocytes. We analyzed the levels of different MCM subunits in whole keratinocyte, cytosolic and chromatin-enriched fractions. A sharp increase in chromatin-bound MCM proteins is observed in K5-CDC6^{tg} keratinocytes (**Fig. 10A**, left panels). A slight but reproducible increase in MCM content is detected in the whole keratinocyte extract and in the cytosolic fraction of transgenic keratinocytes (**Fig. 10A**, middle and right panels). Quantification of MCM levels in the different fractions (**Fig. 10B**) confirms that the K5-CDC6^{tg} strain represents a true Cdc6 gain-of-function model for MCM loading.

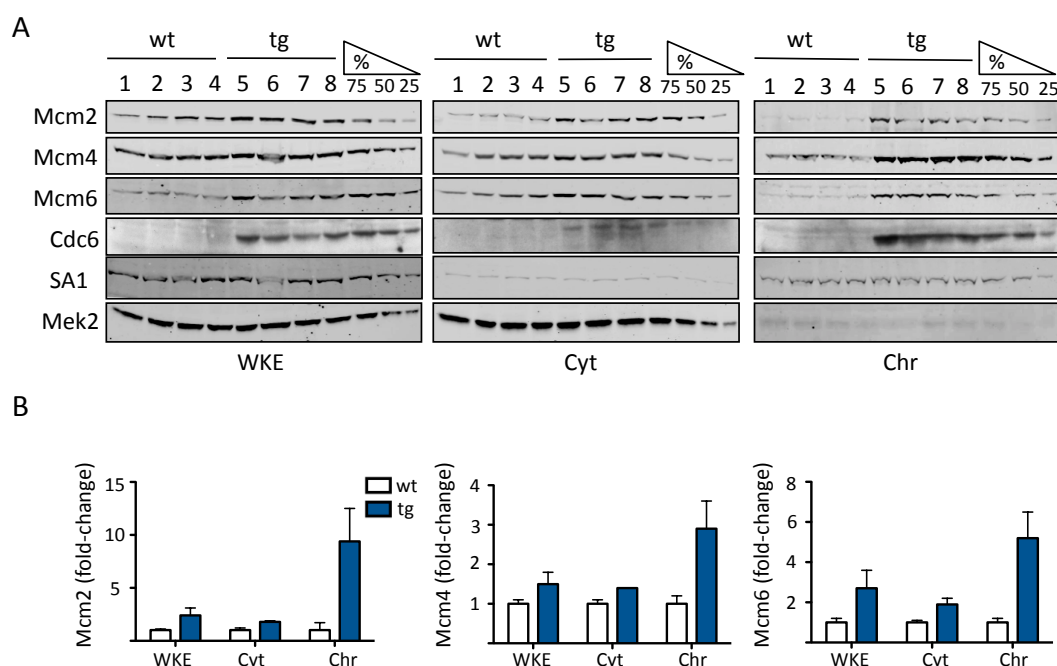


Figure 10. Increased MCM loading on chromatin in K5-CDC6 keratinocytes.

A. Western-blot for Cdc6 and MCM in whole keratinocyte extracts, cytosolic and chromatin fractions. SA1 and Mek2 serve as loading controls and as markers of chromatin-bound and cytosolic proteins, respectively (n=4 wt and 4 tg mice). **B.** Quantification of indicated MCM subunit using the LI-COR Odyssey imaging system. MCM signals were normalized to their respective loading control and fold-change was calculated for each K5-CDC6^{tg} over the average of wt mice.

A similar analysis was performed in keratinocytes isolated from the skin of mice at different ages (**Fig. 11A and B**). From newborn to 24 month-old, K5-CDC6^{tg} mice showed increased levels of chromatin-bound MCMs. Nevertheless the difference was attenuated in

newborn mice, most likely because postnatal skin is more proliferative than adult skin and expresses higher levels of Cdc6 (Costarelis et al., 1990).

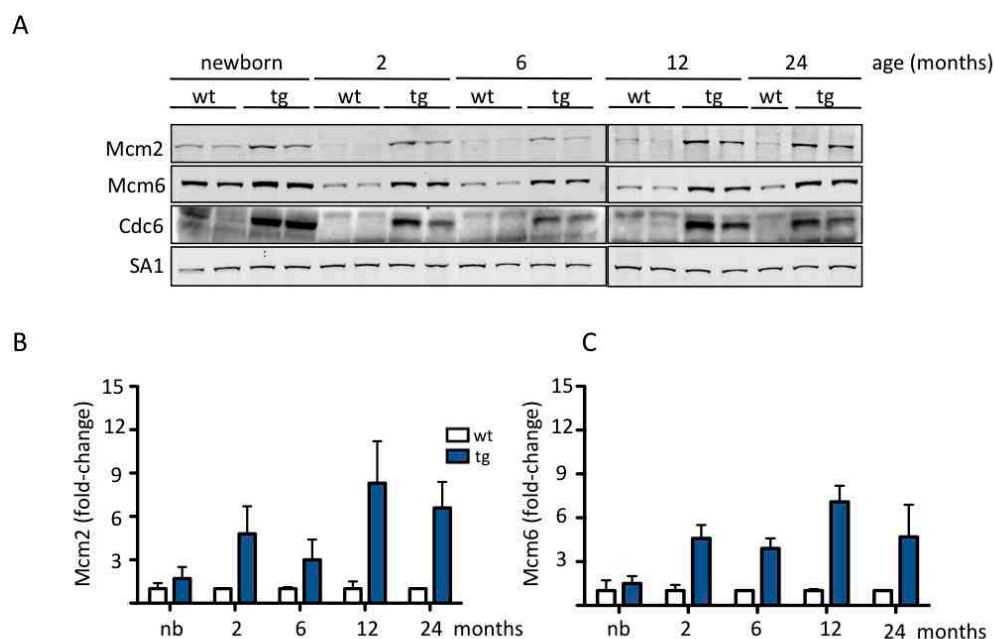


Figure 11. MCM chromatin enrichment in keratinocytes during the lifespan of K5-CDC6^{tg} mice.

A. Western blot of the chromatin fraction in keratinocytes isolated from newborn and adult mice (2, 6, 12 and 24 month-old). SA1, loading control. **B.** Quantification of MCM fold-change using the LI-COR Odyssey imaging system. MCM signals were normalized by their respective loading control and fold-change was calculated over the averaged wt mice at each timepoint.

1.4. Cdc6 overexpression does not confer a cell proliferation advantage in vitro

We next analyzed the proliferation potential of keratinocytes isolated from newborn animals in collaboration with Mirna Pérez-Moreno, Head of the Epithelial Cell Biology Group at CNIO. Wt and transgenic keratinocytes grew at similar rates in culture, either in normal growth medium or in the presence of aphidicolin, an agent that induces replicative stress by slowing down fork progression (**Fig. 12A**). A clonogenic assay was performed in which the colony forming efficiency reflects the proliferation potential of epidermal stem cells (ESCs) and progenitor cells (PCs) (Barrandon and Green, 1987). No differences were found between wt and transgenic animals (**Fig. 12B**).

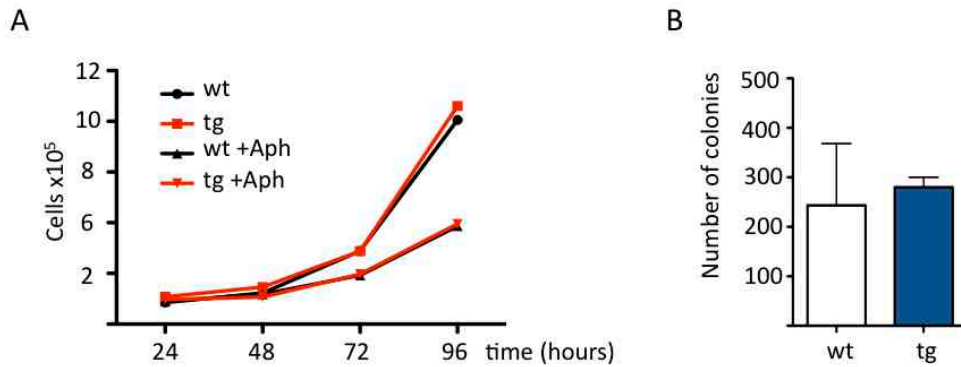


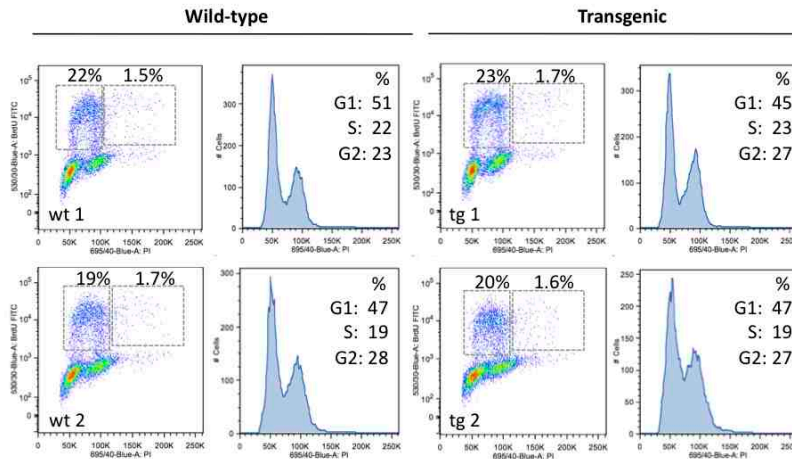
Figure 12. Keratinocytes isolated from newborn mice display normal cell proliferation and colony formation efficiency. **A.** Proliferation curve of keratinocytes isolated from newborn mice in the presence or in the absence of aphidicolin 0.1 uM (n=1 wt and 1 tg). **B.** Colony formation assay quantification (n= 2 wt and 4 tg).

Because the largest difference in the amount of chromatin-bound MCM was observed in adult skin, we next tried to evaluate the proliferation and colony formation efficiency in keratinocytes isolated from adult mice. Unfortunately, primary keratinocytes could not be established in culture as most cells died upon the first passage. Still, short-term *in vitro* studies that did not imply passage of the cells showed no differences in cell cycle distribution or BrdU incorporation between wt and transgenic animals (**Fig 13A and B**). A small population of keratinocytes was polyploid but this effect was not related to Cdc6 overexpression (**Fig. 13A**). These results show that the increased levels of Cdc6 and chromatin-bound MCM do not affect cell cycle dynamics or cell proliferation capacity.

1.5. Histopathological characterization of the skin of K5-CDC6^{tg} mice

Following the evaluation of Cdc6 and MCM levels in isolated keratinocytes, we next analyzed the levels of MCM proteins and proliferation in the epidermis of K5-CDC6^{tg} mice using immunohistochemistry (IHC). Histological analysis of skin sections stained with hematoxylin-eosin (H-E) did not show any morphological abnormalities from young (2 month-old) to old (24 month-old) animals (**Fig 14A**). Mcm4 and Mcm6 IHC staining on skin sections were used to estimate the percentage of MCM-expressing cells in the interfollicular epidermis. In K5-CDC6^{tg} individuals, a 1.5-fold increase in the percentage of MCM-positive cells was consistently observed (**Fig. 14B and C**).

A



B

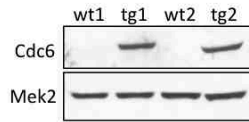


Figure 13. BrdU incorporation and cell cycle profile in keratinocytes isolated from 2 month-old animals. A. BrdU incorporation and cell cycle profiles (n=2 wt and 2 tg). **B.** Western blot for Cdc6 overexpression in keratinocytes from part A. Mek2, loading control.

Cell proliferation index was determined by Ki-67 and BrdU IHCs, the latter injected intraperitoneally 4 hours before sacrifice. Wt and transgenic animals showed similar percentage of both markers (**Fig. 14 D and E**), consistent with what it had been observed with keratinocytes *in vitro*. Also, overexpression of Cdc6 did not increase the percentage of γ H2AX-positive cells, a marker of DNA damage (Ward and Chen, 2001; Celeste et al., 2002; reviewed by Ciccia and Elledge, 2010) (**Fig. 14F**).

1.6. Further increase of Cdc6 overexpression does not increase MCM loading

The APC/C cofactor Cdh1 targets Cdc6 for proteolysis during G1 (Petersen et al., 2000; Mailand and Diffley, 2005). In a Cdh1 conditional knock-out mouse model, the levels of Cdc6 were elevated (García-Higuera et al., 2008). We reasoned that the level of Cdc6 overexpression (and thus, MCM-chromatin association) in K5-CDC6^{tg} mice could be limited by this proteolytic pathway. To test this possibility, K5-CDC6^{tg} mice were crossbred with a K5-specific Cdh1 knock-out mouse strain (K5-Cre;loxCdh1, referred to as K5- Δ Cdh1) generated in the Cell Division and Cancer Group at CNIO. Indeed, Cdc6 protein levels were higher in the skin of K5- Δ Cdh1 (**Fig. 15A**, compare lanes 1-2 and 8-9).

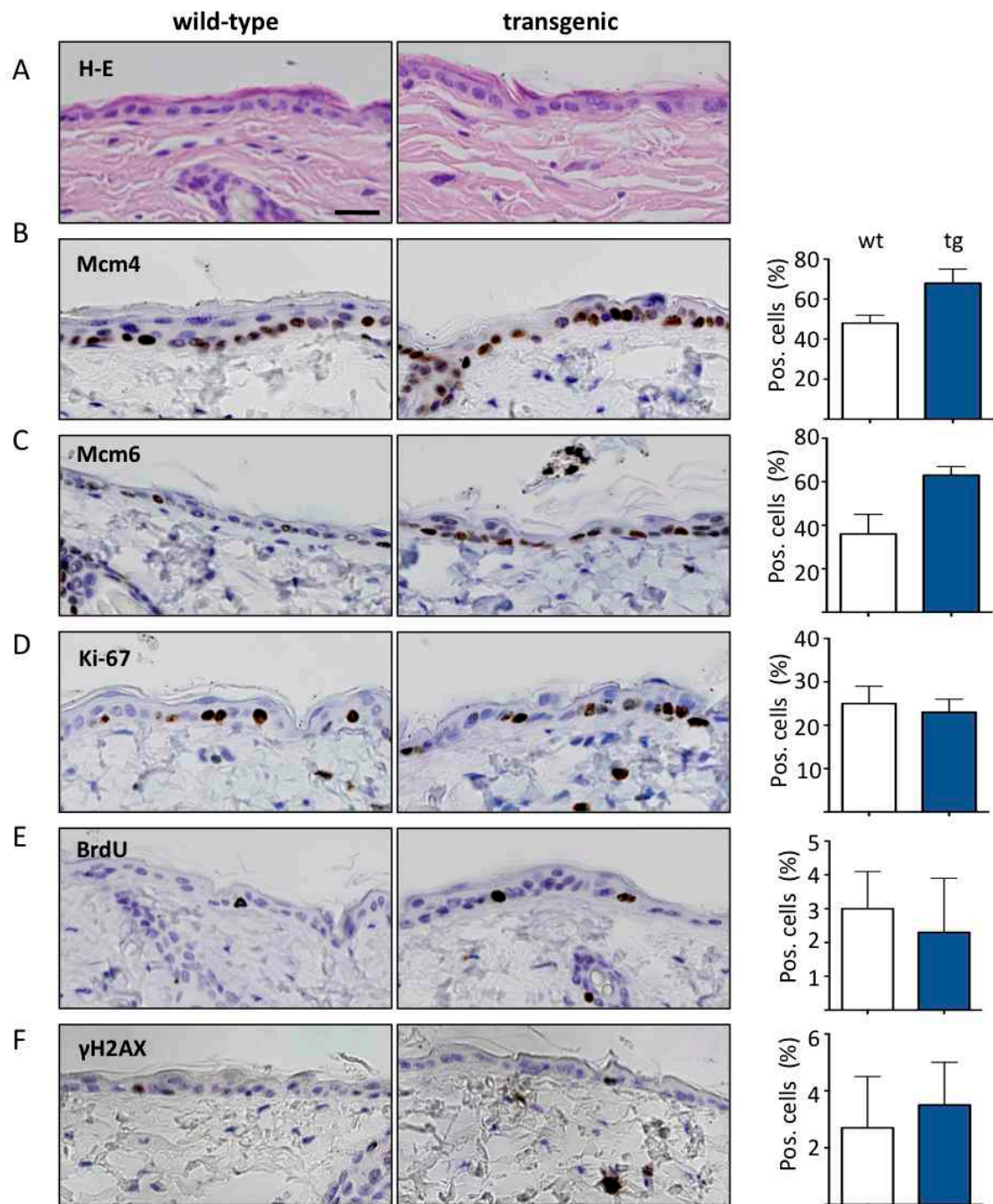


Figure 14. Characterization of the skin in K5-Cdc6^{tg} mice. **A.** Hematoxylin-Eosin (H-E) staining of skin sections do not show tissue architecture abnormalities. **B -F.** IHC detection of Mcm4 (**B**), Mcm6 (**C**), Ki-67 (**D**), BrdU (**E**) and γH2AX (**F**). Quantifications are shown on the right upon counting 500 cells in each case (n= 4 wt and 4 tg). Scale bar 12.5 μm.

Furthermore, the levels of Cdc6 were strikingly increased in the skin of K5-ΔCdh1 animals carrying the Cdc6 transgene (compare lanes 3 and 10). Nevertheless, the chromatin-bound MCM levels in K5-ΔCdh1/Cdc6^{tg} were no further increased (**Fig. 15B**), suggesting that

Cdc6 overexpression levels in the K5-CDC6^{tg} already allow maximal MCM chromatin-association.

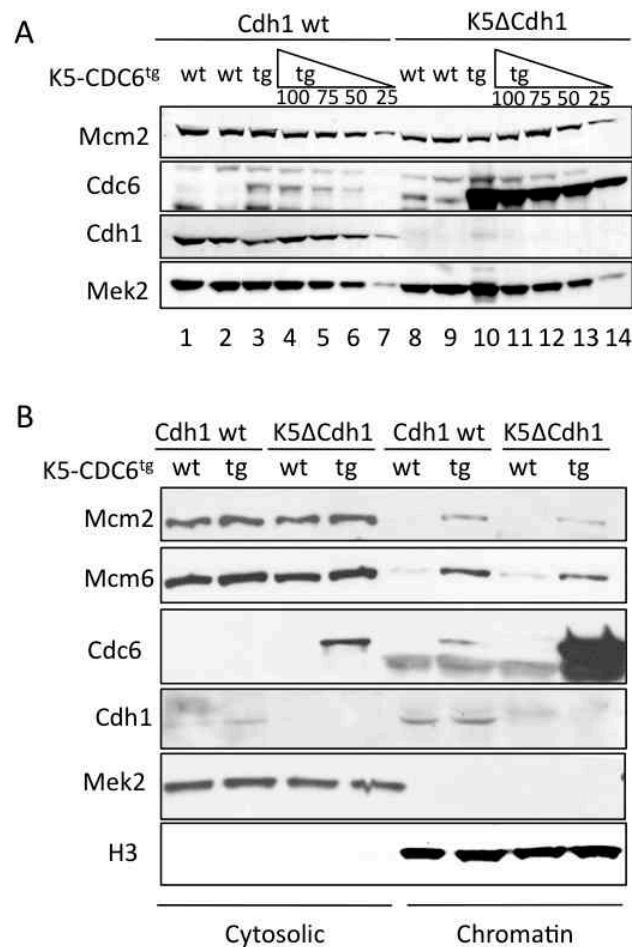


Figure 15. Further increase of Cdc6 overexpression does not enhance MCM chromatin loading. K5-Cdc6^{tg} animals were introduced into a K5-Cre/loxCdh1 background (K5ΔCdh1). **A.** Western blot for Mcm2, Cdc6, Cdh1 in keratinocytes isolated from back skin. Mek2, loading control. n=2 animals per genotype. **B.** Western blot for Mcm2, Mcm6, Cdc6 and Cdh1 after biochemical fractionation of keratinocytes. Mek2 and H3 are cytosolic and chromatin-bound proteins respectively (n=1 animal per genotype).

To confirm this observation, we analyzed the MCM content and proliferation rate in the skin of these animals. K5-ΔCdh1 showed increased percentage of MCM, Ki-67 and BrdU-positive cells compared to wt animals (**Fig. 16A-C**, compare white bars). Nevertheless, the increase of MCM-positive cells due to Cdc6 overexpression was similar, regardless of Cdh1 (**Fig. 16A**). In addition, Cdc6 overexpression in the K5-ΔCdh1 background did not affect the cell proliferation rate (**Fig. 16 B and C**).

Taking into account the technical difficulties of maintaining this genetic combination (lox-Cdh1;K5-Cre; K5-CDC6^{tg}) and the fact that the extra levels of Cdc6 do not translate into higher MCM loading or proliferation rate, this strain was discontinued.

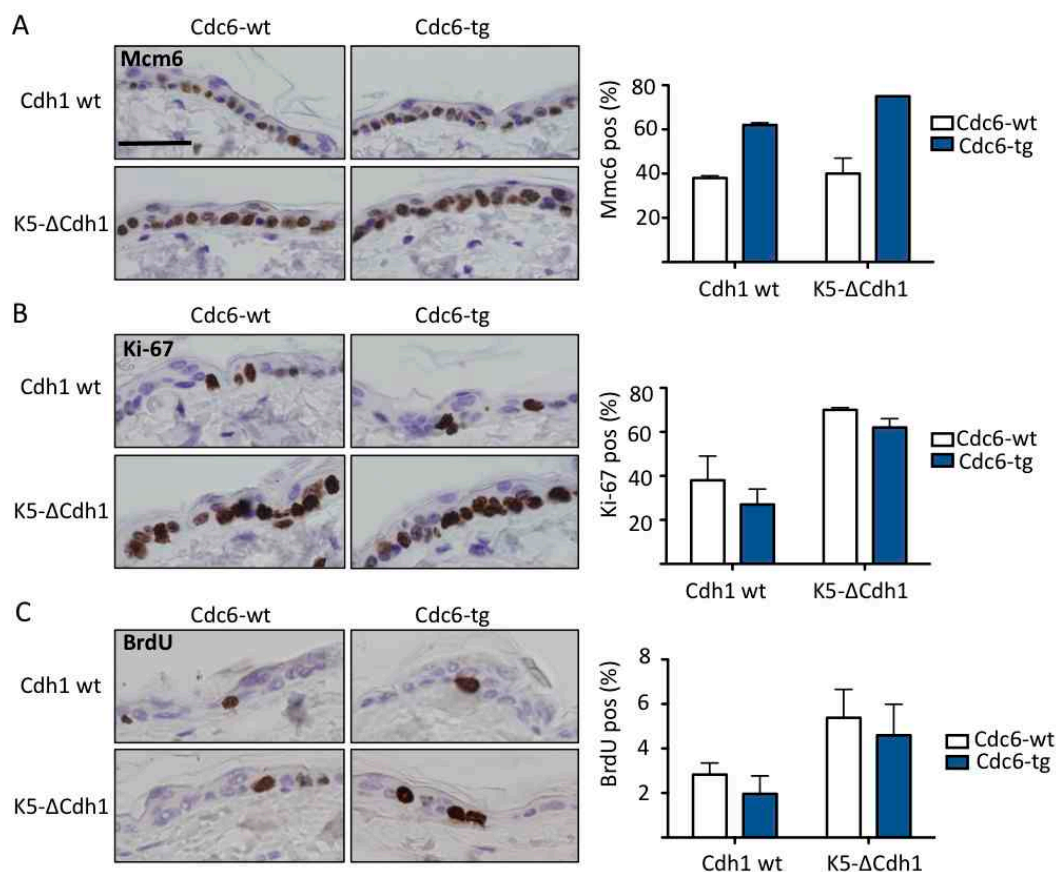


Figure 16. MCM-positive cells and proliferation upon Cdc6 overexpression in a K5-ΔCdh1 background. A-C. IHC in back skin for detection (left) and quantification (right) of Mmc6 (A), Ki-67 (B) and BrdU (C). BrdU was injected intraperitoneally 4 h before sacrifice (n=2 animals per genotype). Scale bar 20 μm.

1.7. Susceptibility of K5-CDC6^{tg} mice to skin carcinogenesis

12-O- tetradecanoylphorbol 13-acetate (TPA) is a potent tumor promoter that induces cell proliferation, skin hyperplasia and entry of HFs in the anagen (growing-phase) phase of the hair cycle. In the skin it mobilizes slow-cycling cells such as epidermal stem cells (ESCs) and progenitor cells (PCs) (Flores et al., 2005). We first analyzed whether Cdc6 overexpression would affect the skin hyperplasia induced by TPA treatment. Four doses were applied to the tail skin of each mouse (**Fig. 17A**). One week later, the degree of hyperplasia measured as the thickening of the epidermis was similar in both genotypes (**Fig. 17B-D**).

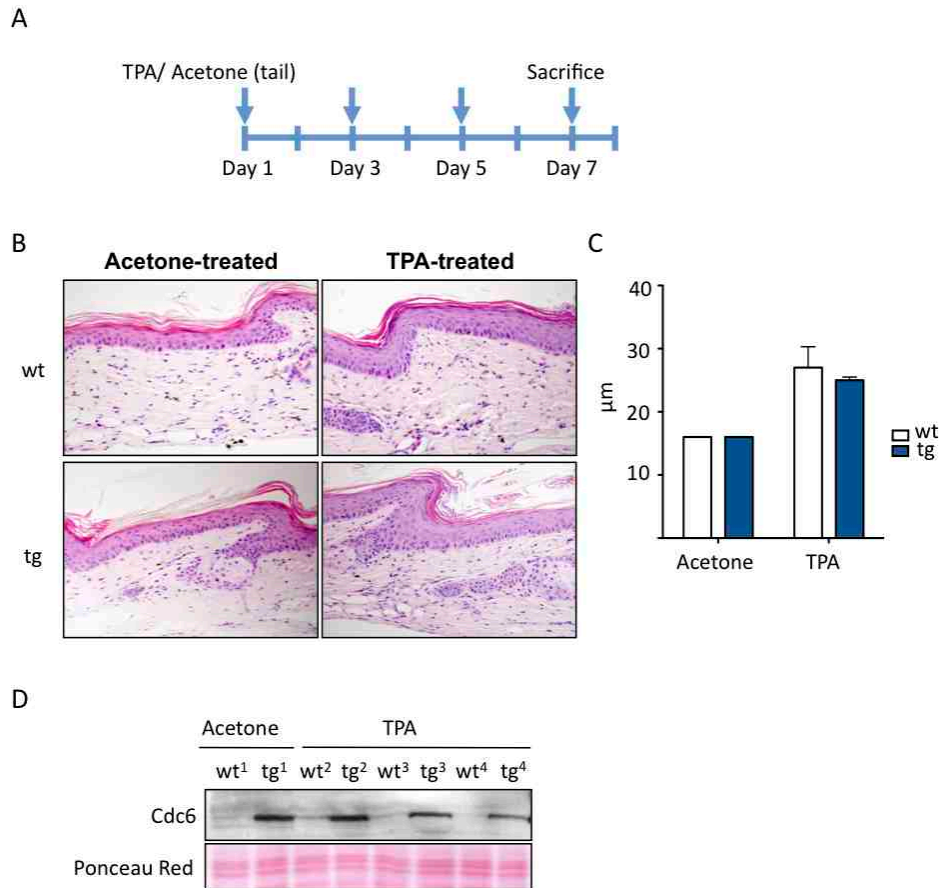


Figure 17. Acute TPA treatment in K5-CDC6^{tg} mice. **A.** Outline of the protocol for TPA-induced skin hyperplasia. **B.** Representative H-E tail skin sections of acetone-treated (control for hyperplasia induction) and TPA-treated animals. 20X fields. **C.** Epidermal thickening measurement. (Acetone n=1 wt and 1 tg. TPA n= 3 wt and 3 tg). **D.** Western-blot for Cdc6 in the skin of the animals used in the experiment. Red ponceau staining, loading control.

Next we subjected wt and K5-CDC6^{tg} animals to a classic two-stage chemical skin carcinogenesis protocol (reviewed by DiGionvanni, 1992). ‘Initiation’ is driven by a single dose of 7,12-dimethylbenz[α]anthracene (DMBA), which in 90% of the cases induces a mutation in the codon 61 of the *H-ras* gene (Balmain et al., 1984; Quintanilla et al., 1986). Subsequent ‘promotion’ with TPA results in the clonal expansion of the initiated cells and the appearance of benign papillomas, which might progress to squamous cell carcinoma (SCC) depending on the genetic background (Woodworth et al., 2004). Interestingly, when this protocol (**Fig. 18A**) was applied to young aged-matched mice, transgenic animals developed more papillomas than the wt counterparts. The size of the papillomas were similarly distributed between genotypes (**Fig. 18B**). On average, a 3-fold increase in the number of lesions was observed in transgenic animals at the end of TPA administration (**Fig. 18C**). No progression towards SCC was observed neither in wt nor in transgenic animals. Skin

papillomas express senescence markers such as p16 and p19 (Collado et al., 2005). Normal induction of these markers was confirmed in papillomas isolated from wt or transgenic mice (Fig. 18D).

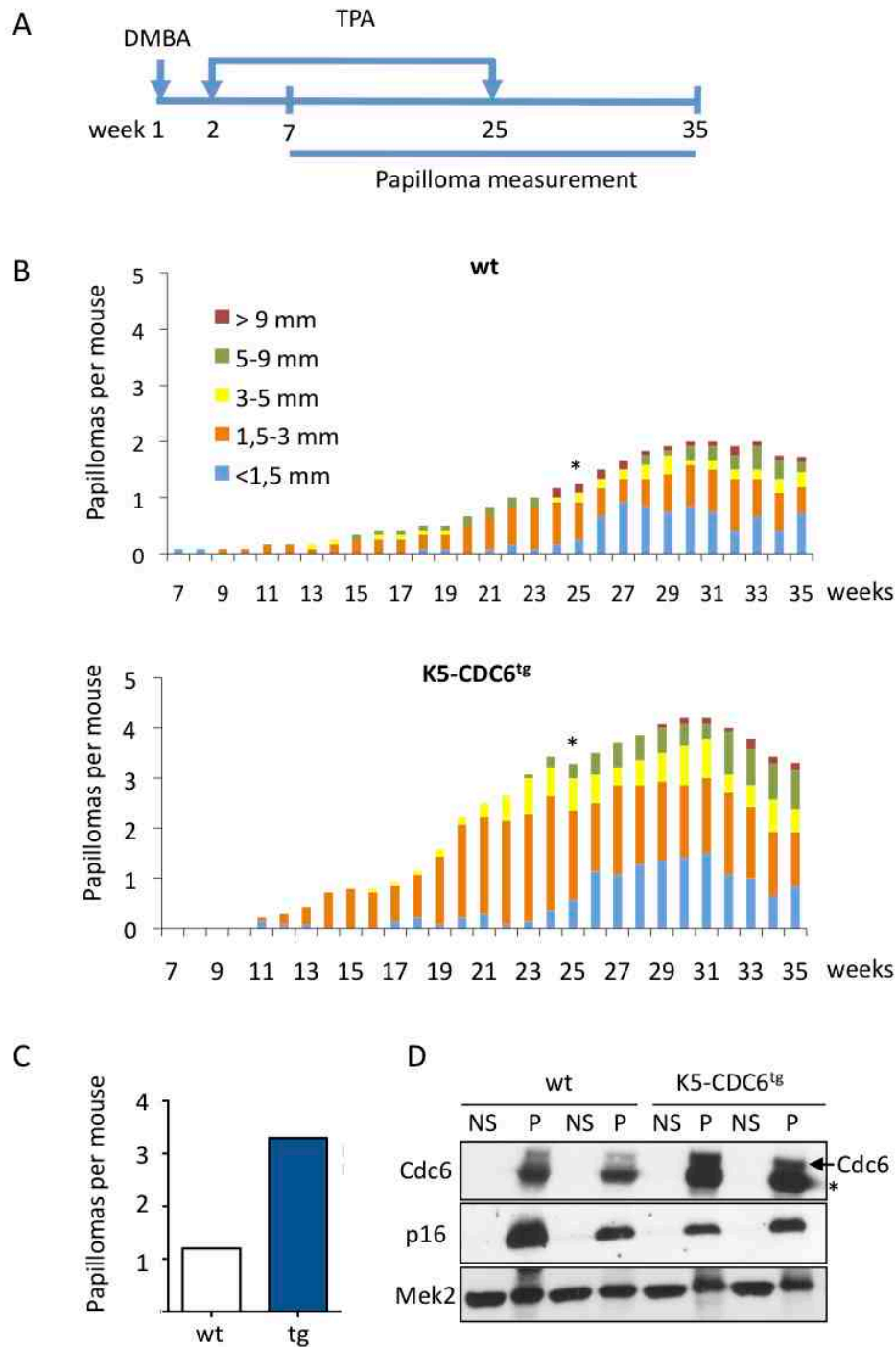


Figure 18. K5-CDC6^{tg} mice are more susceptible to DMBA/TPA- induced carcinogenesis. **A** Protocol outline. Animals were given a single dose of DMBA at week 1 and treated with TPA twice a week from week 2 to week 25. Animals were kept 10 weeks after the last application of TPA to evaluate any possible progression towards SCC. The number and size of papillomas were weekly measured. **B.** Number of papillomas and size distribution in wt and transgenic animals. The asterisk represents the last dose of TPA (n= 12 wt and 14 tg). **C.** Average number of papillomas per mouse at week 25. **D.** Western blot of Cdc6 and p16 in protein extracts prepared from papillomas. Mek2, loading control. NS, Normal Skin; P, papilloma. The asterisk marks an unspecific band below Cdc6 signal.

1.8. K5-CDC6^{tg} mice have a normal lifespan

Survival (Kaplan-Meier) curves indicated that K5-CDC6^{tg} animals had a mean overall lifespan of 107 weeks, similar to their wt littermates (**Fig.19**). Most mice suffered from standard age-related health problems, including the onset of spontaneous tumors (**Table 1**). A subset of mice of both genotypes were subjected to histopathological examination in collaboration with Dr. Marta Cañamero, Head of the Histopathology Unit at CNIO. A classification of the analyzed tumors is shown in (**Table 2**).

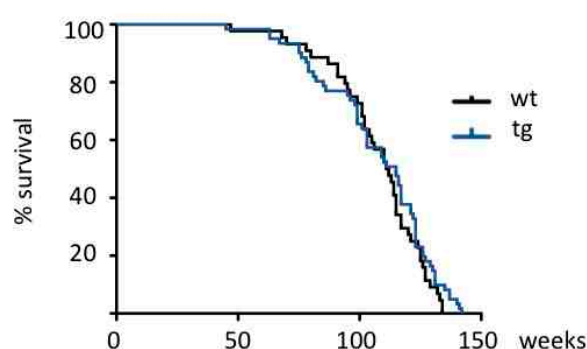


Figure 19. A. Kaplan-Meier survival curves show similar life expectancy for wt and transgenic animals (n=44 wt; 61 tg).

The most frequent tumors found were hematological (histiocytic sarcomas and B-cell lymphomas), followed by hepatocarcinomas, which are frequent in the C57BL/6J genetic background. A certain incidence of sarcomas was also observed in both genotypes. No significant differences in the percentage of tumor-prone animals or their tumor spectrum were found between wt and transgenic animals, indicating that K5-driven Cdc6 overexpression does not affect the frequency of spontaneous tumorigenesis.

Table 1. Causes of sacrifice in the K5-CDC6^{tg} colony. Percentages are calculated over the total number of animals included in the K5-CDC6^{tg} colony. Percentages are calculated over the total number of animals included in the Kaplan-Meier survival curve. Percentages corresponding to 'Seminal gland hyperplasia' and 'Ovary cysts' are calculated over the number of males (M) and females (F) respectively.

Pathology	Wild-type	K5- CDC6 ^{tg}
1. Tumors	32 (72.7%)	42 (68.8%)
2. Dermatitis	3 (6.8%)	6 (9.8%)
2. Liver hemorrhage/failure	3 (6.8%)	
3. Intestine obstruction/bleeding		2 (3.2%)
4. Reproductive tract anomalies	6 (13.6%)	10 (16.3%)
Seminal gland hyperplasia (M)	5 (15.6%)	8 (18.6%)
Ovary cysts (F)	1 (8.3%)	2 (11.1%)
Total mice (included in Kaplan-Meier curve)	44 (32 M; 12 F)	61 (43 M; 18F)

Table 2. A subset of tumors were histologically examined and classified in hematological neoplasias (histiocytic sarcomas, lymphomas), carcinomas or sarcomas. Some animals presented more than one tumor type.

Pathology	Wild-type	K5- CDC6 ^{tg}
1. Hematological neoplasias	5 (50%)	17 (70.8%)
2. Carcinomas (hepatocarcinomas)	4 (40%)	1 (4.2%)
3. Sarcomas (fibrosarcomas, leiomyosarcomas)	1 (10%)	4 (16.7%)
4. Hematological + hepatocarcinoma		1 (4.2 %)
5. Hematological + fibrosarcoma		1 (4.2%)
Total mice	10	24

1.9. Cdc6 overexpression in a p53-null background

After having evaluated the incidence of spontaneous tumors in K5-CDC6^{tg} mice, we introduced the K5-CDC6^{tg} in a p53-null background to evaluate possible phenotypes restrained by p53 activity in terms of proliferation and tumorigenesis. Cdc6 overexpression levels were slightly higher in the p53-null background but the MCM levels in whole

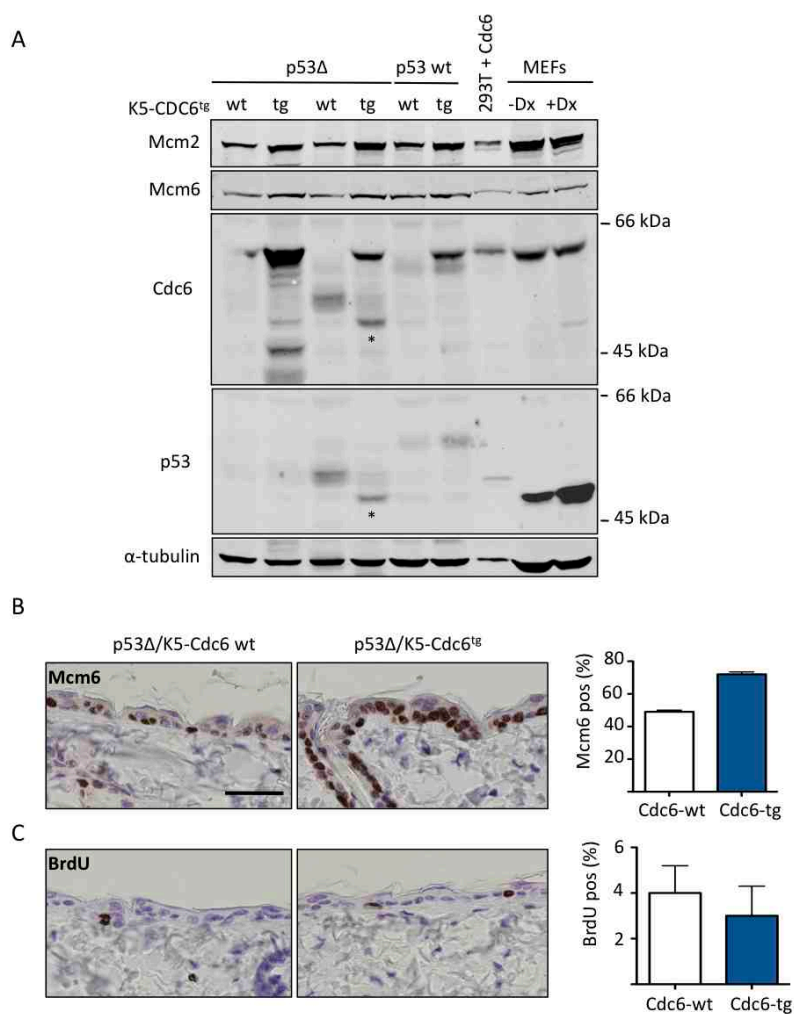


Figure 20. K5-Cdc6^{tg} in the p53Δ background. **A.** Western-blot in back-skin isolated keratinocytes for Mcm2, Mcm6, Cdc6 and p53. α -tubulin, loading control. MEFs treated with doxorubicin were used as a positive control for p53 detection. The asterisk marks an unspecific band. Mcm6 IHC in back skin and quantification of positive cells. **C.** BrdU IHC in back skin and quantification of positive cells. Scale bar 20 μ m.

keratinocyte extracts were not further increased compared to K5-CDC6^{tg} with p53 (**Fig. 20A**). Accordingly, the increase in MCM-positive cells due to Cdc6 overexpression was similar to that observed in the p53-proficient background (**Fig. 20B**). No significative differences were observed in the index of BrdU positive cells (**Fig. 20C**).

p53-null and hemizygous (p53 ^{-/+}) mice are tumor prone (Donehower et al., 1992; Jacks et al., 1994). While p53-null mice primarily develop lymphomas, p53^{+/-} mice exhibit a wider array of tumors, including soft tissue sarcomas, osteosarcomas and carcinomas of various types. We followed a cohort of K5-CDC6^{tg} mice in a p53 ^{-/+} (hemizygous) and p53-null backgrounds. In both cases, the overall lifespan (64 weeks in p53 ^{-/+} background and 20 weeks in the p53-null background) was not affected by Cdc6 overexpression (**Fig. 21 A and B**). We concluded that Cdc6 neither enhanced nor attenuated the phenotypes caused by loss of p53.

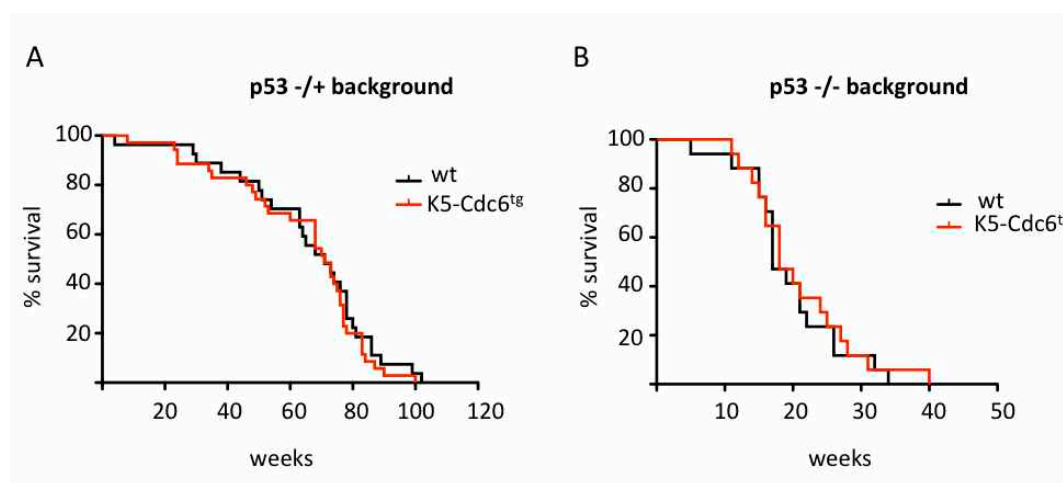


Figure 21. Survival (Kaplan-Meier) curves of K5-CDC6^{tg} in a p53-deficient background. A. Kaplan-Meier curves in hemizygous p53 background (n=27 wt; 35 K5-Cdc6^{tg}). **B.** Kaplan-Meier curves in a p53-null background (n=17 wt; 18 K5-Cdc6^{tg}).

1.10. Old K5-CDC6^{tg} mice show better skin/hair fitness

Through direct observation of the K5-CDC6^{tg} mice colony, we observed that older animals preserved their fur, in terms of color and density, better than age-matched wt animals. At one point, we systematically classified the mice into three phenotypic categories according to the general aspect of their fur. Mice with black hair and no signs of hair loss defined the 'fit group'. Those with localized regions of hair loss or hair graying were included in the 'aging-signs group'. Finally, animals with generalized hair loss and abundant grey hair were considered the 'aged group' (**Fig. 22A**). The distribution of wt and transgenic mice in

the three categories taking into account the age of each individual is shown in **figure 22B**. A 2.8-fold increase in the percentage of animals that retained a young-like aspect of the hair shaft was observed in transgenic animals ≥ 2 years old (59% vs. 21% of wt). Conversely, there was a 3.4-fold increase in the percentage of wt animals included in the ‘aged group’ (34% vs. 10% of transgenic animals). A decrease in the percentage of K5-CDC6^{tg} animals belonging to the ‘aging-signs group’ was also observed (31% compared to 45% of wt) (**Fig. 22C**).

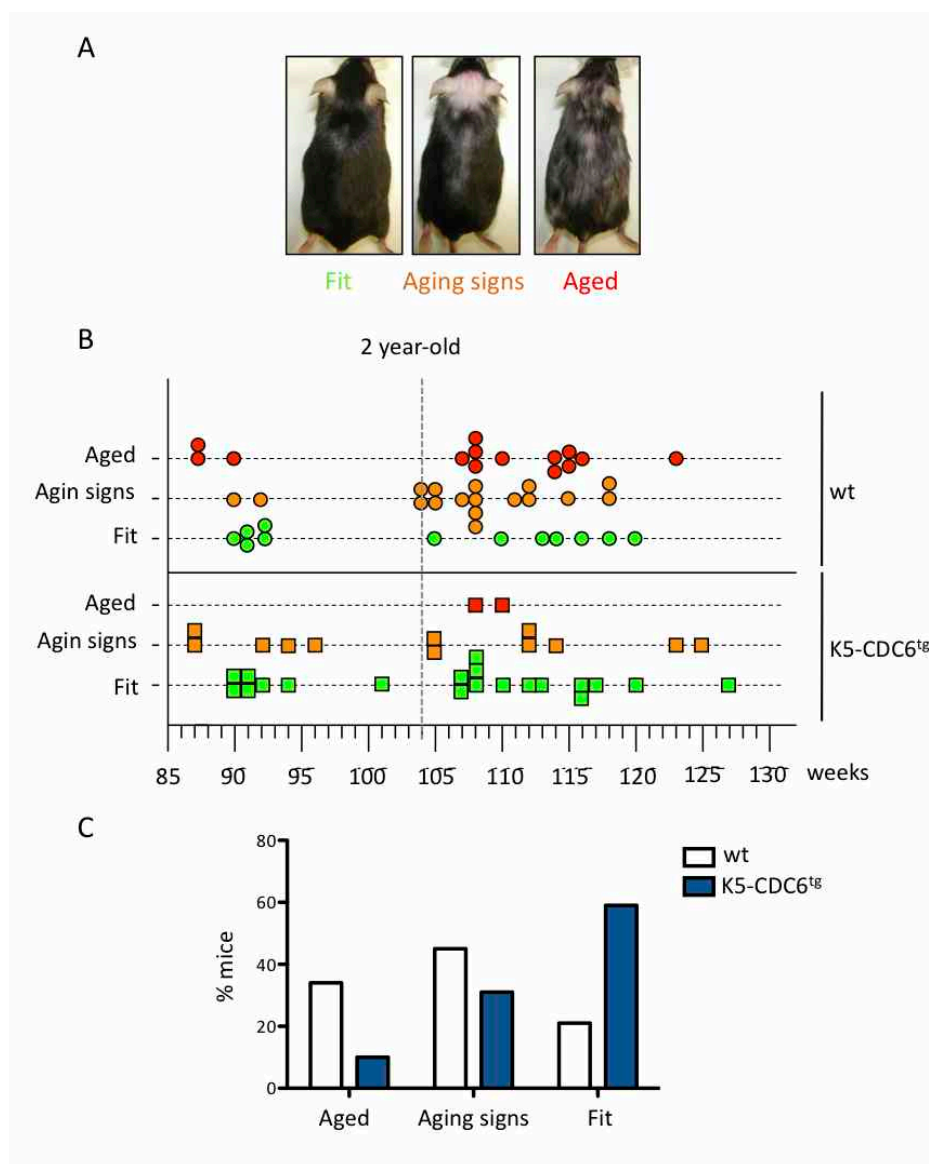


Figure 22. Better hair/skin fitness in old K5-CDC6^{tg} mice. **A.** Three categories were defined according to the aspect of the fur. Fit: black hair, no hair loss. Aging signs: localized grey hair or hair loss. Aged: generalized grey hair and hair loss. **B.** Graph showing the distribution of wt and transgenic mice in each group (n= 43 wt and 34 tg) taking into account their age. **C.** Percentage of wt and transgenic animals in each category (age ≥ 2 years old) (n=33 wt and 22 tg).

The percentage of MCM-positive cells in the epidermis of old animals was increased relative to wt mice, as it had been noted in young animals (**Fig. 23A**). No difference was observed regarding Ki67-positive cells (**Fig. 23B**). Interestingly, neither the percentage of MCM-positive cells nor the Ki-67 index decreased with age.

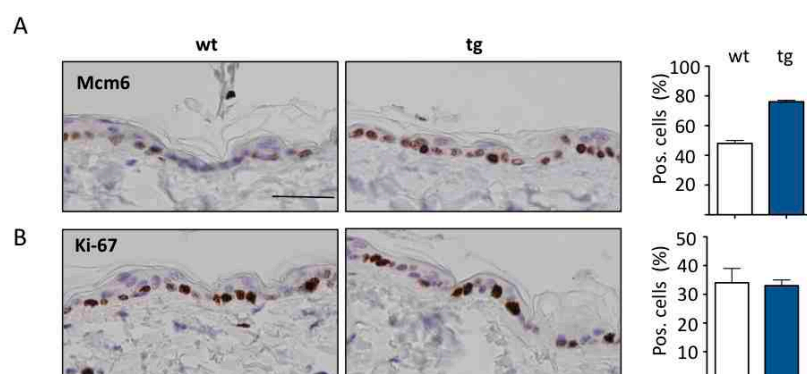


Figure 23. MCM content and proliferation in old K5-CDC6^{tg} mice. IHC in the back skin of old animals and quantification for Mcm6 (A) and Ki-67 (B) (n=4 wt and 4 tg). Scale bar 20 μ m.

To expand this observation and test whether it was restricted to the hair shaft, we analyzed the mRNA levels of p16^{INK4a} and p19^{ARF} in keratinocytes isolated from the epidermis of old animals (**Fig. 24A**). These proteins are well-established molecular ageing biomarkers (Zindy et al., 1997; Krishnamurthy et al., 2004; reviewed by Jenkins, 2002; Kim and Sharpless, 2006). 110 week-old transgenic animals showed lower mRNA levels of p16 and p19 compared to age-matched wt animals that phenotypically belonged to the 'aged group' (**Fig. 24B**). The decrease in p16 and p19 mRNA levels further support that K5-CDC6^{tg} mice retain features of a younger skin.

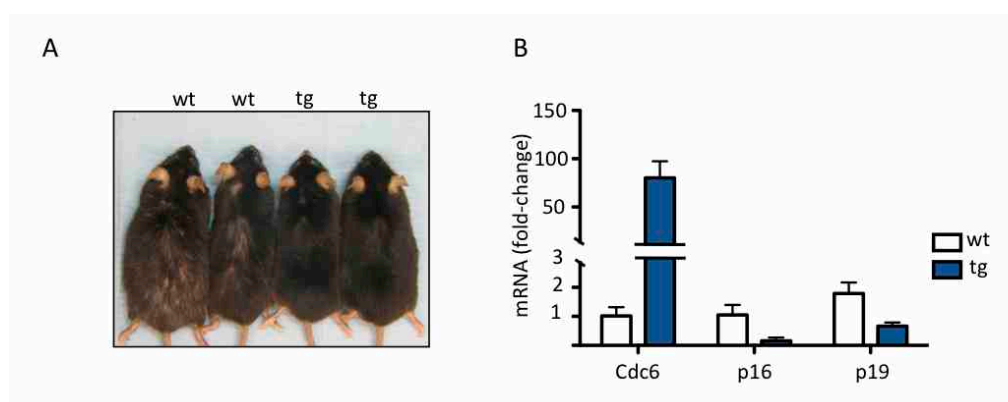


Figure 24. Aging biomarkers in keratinocytes from old K5-CDC6^{tg} mice. A. Fur phenotypes of the animals used in the experiment (wt=110 and tg =108 week-old). B. p16, p19 and Cdc6 mRNA expression levels in back-skin isolated keratinocytes. Fold-change was calculated over the averaged wt mice (n=2 wt and 2 tg).

1.11. Normal wound healing in K5-CDC6^{tg} skin

Loss of tissue regenerative potential and disrupted organ homeostasis are also hallmarks of aging in mice (Gannon et al, 2011; reviewed by Rodier et al., 2007). It has been shown that upon wounding, hair follicle (HF) stem cells are mobilized to the wound area and contribute to the repair of the damaged epidermis (Ito et al., 2005; Levy et al., 2007). Basal slow-cycling cells located in the interfollicular epidermis also contribute to wound healing (Mascre et al., 2012). In order to test whether the young-like skin features observed in transgenic animals affected the rate of tissue regeneration, a wound healing assay was performed with 4 mm² punch biopsies. The different time points analyzed encompass the phases of inflammation, keratinocyte migration and proliferation and formation of new stroma (reviewed by Clark, 1996; Martin, 1997) (**Fig. 25A**).

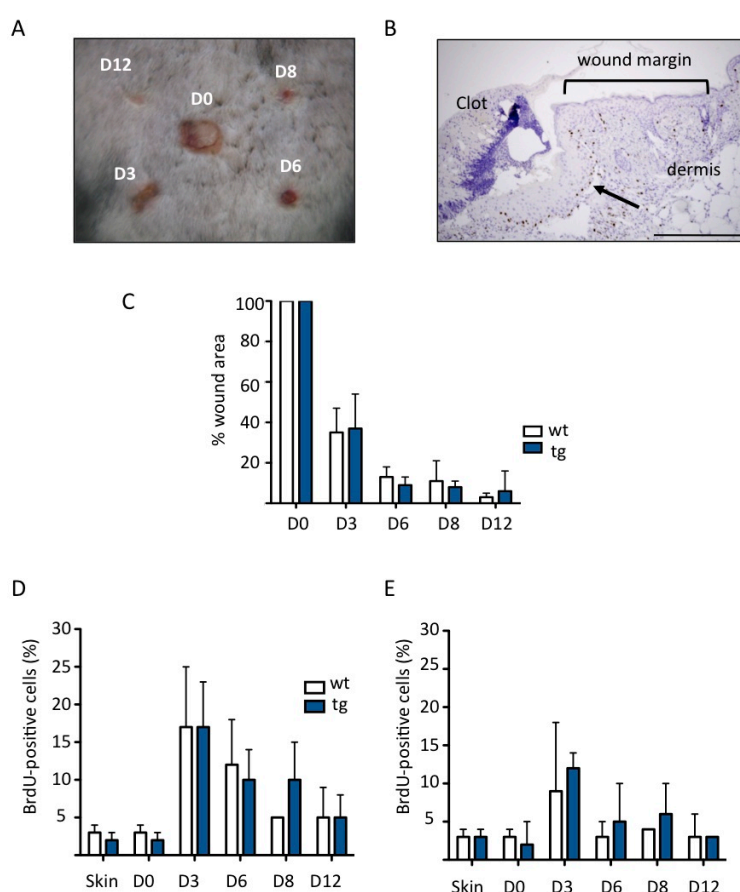


Figure 25. Wound-healing rate in old K5-CDC6^{tg} mice. **A.** Wound healing in the back of a wt mouse. 4 mm² punches were made at 12, 8, 6 and 3 days before the photograph was taken. D0, original size of the wound. **B.** BrdU IHC of a lesion at day 3. BrdU-positive cells in the wound margin and the keratinocyte migrating front (arrow) were quantified. Scale bar 200 μ m. **C.** Measurements of the wound area at each time point. After sacrifice pictures of the back skin were taken, areas were digitally measured using Image J software and normalized by D0 area. Animals were 24 month-old (n=3 wt and 3 tg). **D-E.** Quantification of BrdU-positive cells in the keratinocyte-migrating front (**D**) (wound margin) and wound surrounding area (**E**) at the different time points. Normal skin was also quantified as control of basal cell proliferation.

The wound area that remained open at each time point was measured (**Fig. 25B**). In addition, BrdU was injected i.p. to the animals 2 hours before sacrifice in order to estimate cell proliferation in the wound margin and the region immediately adjacent (**Fig. 25C**). Despite the better fur/skin fitness reported (**Fig. 22 and 24**), K5-CDC6^{tg} animals did not heal the wound faster than the wt counterparts (**Fig. 25B**) and no difference in the percentage of BrdU-positive cells was observed at or near the wound at any of the time points tested (**Fig. 25D and E**).

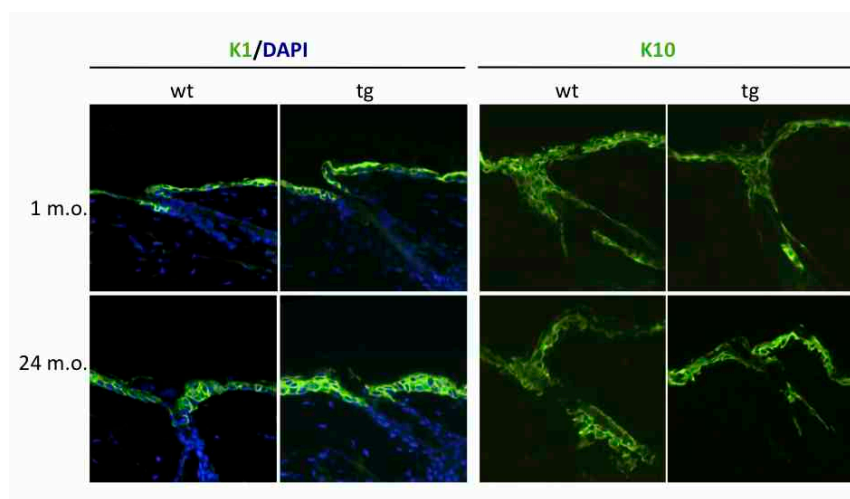


Figure 26. Wt and K5-CDC6^{tg} animals show similar staining pattern of skin differentiation markers. Keratin 1 (K1) and Keratin 10 (K10) staining in 1 and 24 month-old animals. Nuclei are stained with DAPI. (n=2 wt and 2 tg per time point).

To further study the ‘delayed ageing’ observed in the old K5-CDC6^{tg} animals, we established a collaboration with the laboratory of Dr. Cédric Blanpain (Université Libre, Brussels), a leading group in the epidermal stem cell field. First, different epidermal differentiation markers were analyzed without finding differences between genotypes neither in young nor in old animals. In **figure 26**, staining for keratin 1 and 10, markers of suprabasal epidermal cells expressed in the spinous layer (reviewed by Blanpain and Fuchs, 2006), are shown as an example.

Similarly, no differences were found in the staining profile of Lrg1 and MTS24 markers, which characterize resident progenitors that control the maintenance of the sebaceous gland and the infundibulum (the region that connects the HF to the IFE; Nijhof et al., 2006; Jensen et al., 2009) (**Fig. 27A**). The profile of HF stem cells characterized by the CD34 marker (reviewed by Fuchs and Raghavan, 2002), was also identical between genotypes (**Fig. 27B**). It should be noted that these analyses are qualitative. Accurate

quantification of these cell populations would require flow cytometric analysis using fresh tissue, which we may undertake in the future.

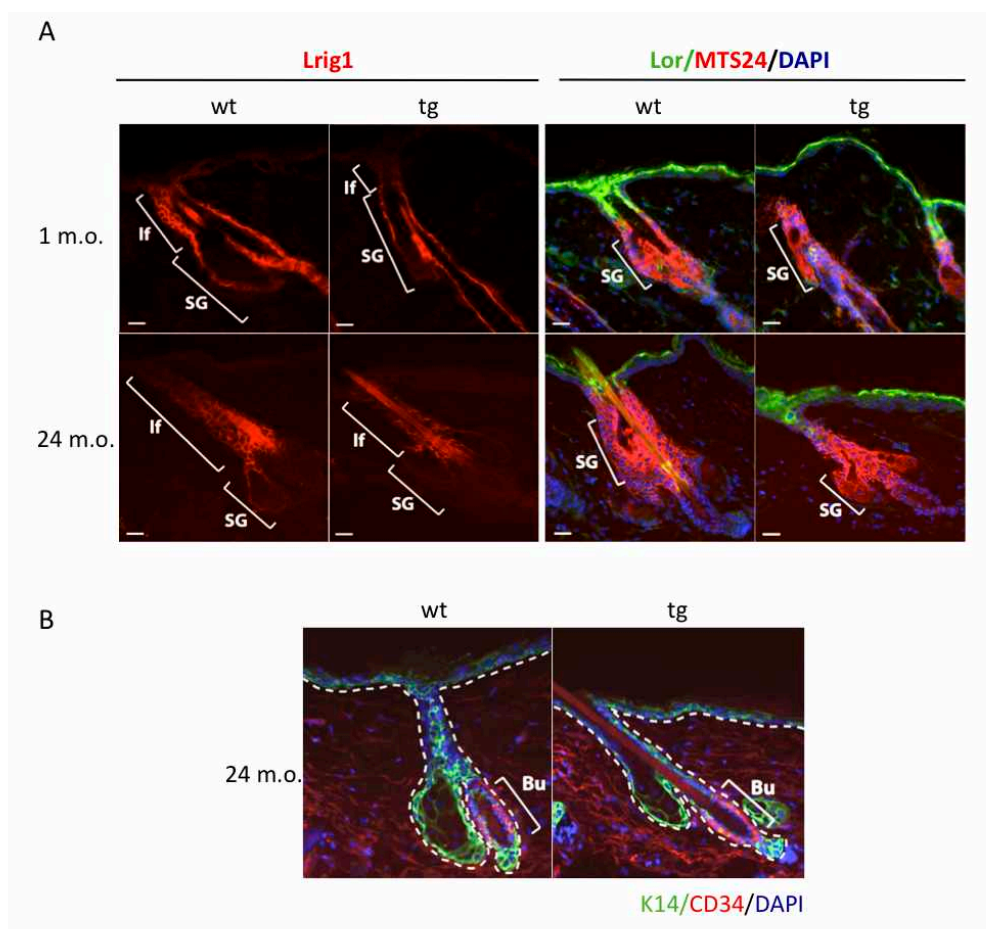


Figure 27. Wt and K5-CDC6^{tg} animals show similar staining pattern of skin progenitor cells. A. Infundibulum (If) and sebaceous gland (SG) progenitors staining (Lrig1 and MTS24) in 1 and 24 month-old animals (n=2 wt and 2 tg). Loricrin (Lor) stains the granular layer of the epidermis. Nuclei are stained with DAPI. **B.** CD34 staining marks the epidermal stem cells in the bulge (Bu) region of the hair follicle. Keratin 14 stains the basal layer. Nuclei are stained with DAPI.

The levels of proliferation and apoptosis were also analyzed in the skin samples from wt and K5-CDC6^{tg} mice. Few apoptotic cells measured by active caspase 3 were found in either genotype (**Fig. 28A**). Proliferation was analyzed by Ki-67 staining paying special attention to the HF compartment. Interestingly, Ki-67 positive cells could neither be found in the infundibulum of young K5-CDC6^{tg} animals nor in the hair germ of old K5-CDC6^{tg} mice (**Fig. 28B**). Owing to the strict coupling of follicular melanogenesis, which controls the color of the hair shaft, and HF cycling (Slominski and Paus, 1993) these results are compatible with the hypothesis of transgenic HF and melanocyte stem cells undergoing less cycles during the lifespan of the animals, possibly leading to an enhanced fitness of the hair shaft in old K5-CDC6^{tg} mice.

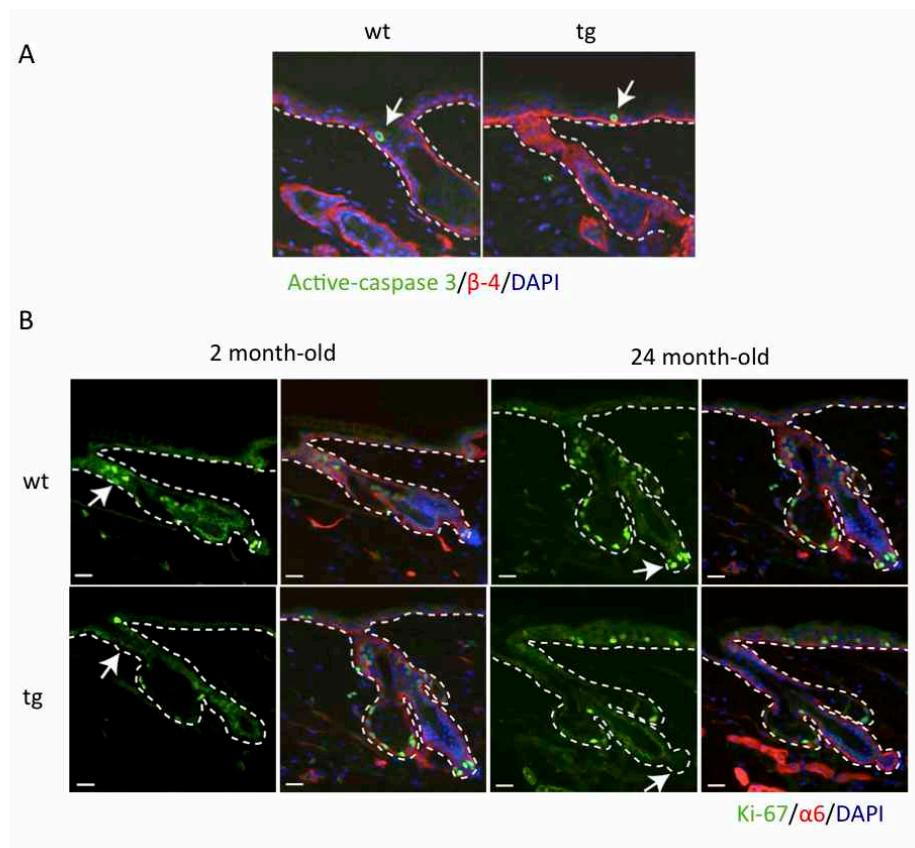


Figure 28. Proliferation is decreased in the HF of K5-CDC6^{tg} mice. **A.** No difference in apoptosis is found in transgenic animals by activated-caspase 3 staining. β 4 integrin (β 4) stains the basal lamina. Nuclei are stained with DAPI. **B.** Proliferation in the hair follicle of transgenic animals is reduced as measured by Ki-67 staining. Arrows mark the infundibulum in 2 month-old animals and the hair germ in 24 month-old mice. α 6 integrin (α 6) stains the basal lamina. Nuclei are stained with DAPI.

Hair regeneration follows a precise cycle that encompasses a rapid growth of the hair shaft (anagen), an apoptosis-driven regression of the lower HF ‘cycling’ portion (catagen) and a resting phase (telogen) (reviewed by Alonso and Fuchs, 2006). In mice, the hair cycle is synchronized in the 14 weeks after birth and is lost in subsequent hair cycles (reviewed by Stenn and Paus, 2001). We decided to analyze the dynamics of the hair follicle cycle during the first weeks of life of the wt and K5-CDC6^{tg} animals, selecting precise time points (4,6,7,8,9 weeks) in which most of the follicles are found in anagen, catagen or telogen.

Indeed, an altered dynamic of HF cycle entry was found in K5-CDC6^{tg} animals. In each timepoint, HF were classified according to their structure into early anagen, full anagen, catagen or telogen (Müller-Rover et al., 2001). At 4 weeks, most of the wt HF were in full anagen, whereas in K5-CDC6^{tg} animals most of HF were still in telogen or early anagen

(Fig. 29). At 6 weeks, when most of the wt follicles were in telogen and catagen, a considerable population of K5-CDC6^{tg} HF was still in full anagen. At 9 weeks, almost 100% of the wt follicles had reached early anagen, whereas > 50% of K5-CDC6^{tg} were still in telogen. These results show that the HF of K5-CDC6^{tg} mice have an altered hair cycle consistent with the possibility of an extended lifespan of the HF stem cells.

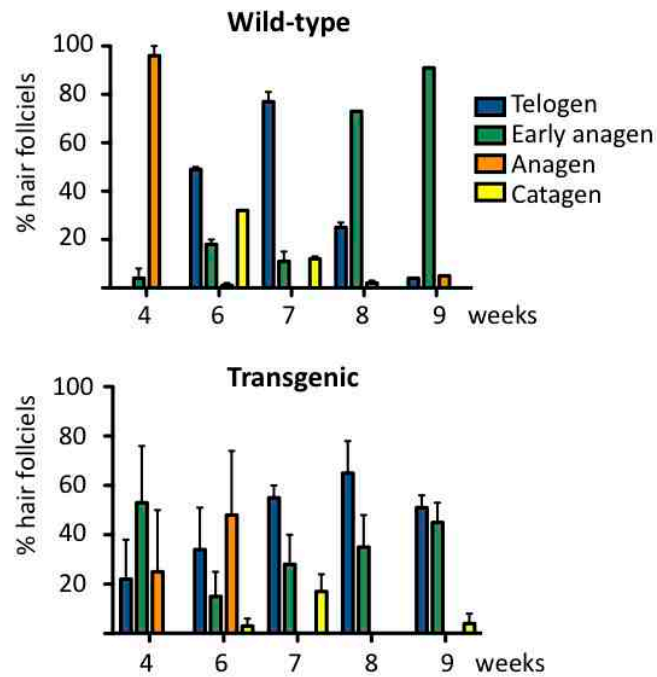


Figure 29. The hair cycle is delayed K5-CDC6^{tg} mice. Percentage of hair follicles at the different stages of the hair cycle. More than 500 hair follicles per animal were classified (n=2 wt and 2-4 tg).

Chapter 2. Tet^{ON}-CDC6 mouse model

2.1. Generation of a mouse model for inducible Cdc6 overexpression

To study the effects of Cdc6 overexpression in other tissues, we decided to generate a mouse model in which Cdc6 overexpression would be ubiquitous and inducible. For this purpose we made use of an engineered Embryonic Stem (ES) cell line that expresses the M2 reverse tetracycline transactivator (M2-rtTA) constitutively from the *ROSA26* locus. In addition, this ES cell line has a modification downstream of the *Collagen 1 a1* locus (*Col1a1*) that allows recombinase-mediated single-copy transgene integration. A tetracycline-responsive element located upstream of the PGK ubiquitous promoter controls expression of the transgene (Beard et al., 2006). Titratable expression can be achieved by modulating the concentration of tetracycline or one of its derivatives such as doxycycline (dox) (Gossen and Bujard, 1992). We used this system to introduce a HA-tagged version of Cdc6 to be able to distinguish it from the endogenous protein (**Fig. 20A**). Correct transgene insertion and dox-induced Cdc6 expression in ES cells were tested (data not shown). Tet^{ON}-CDC6 mouse was generated in the CNIO Transgenic Mice Unit.

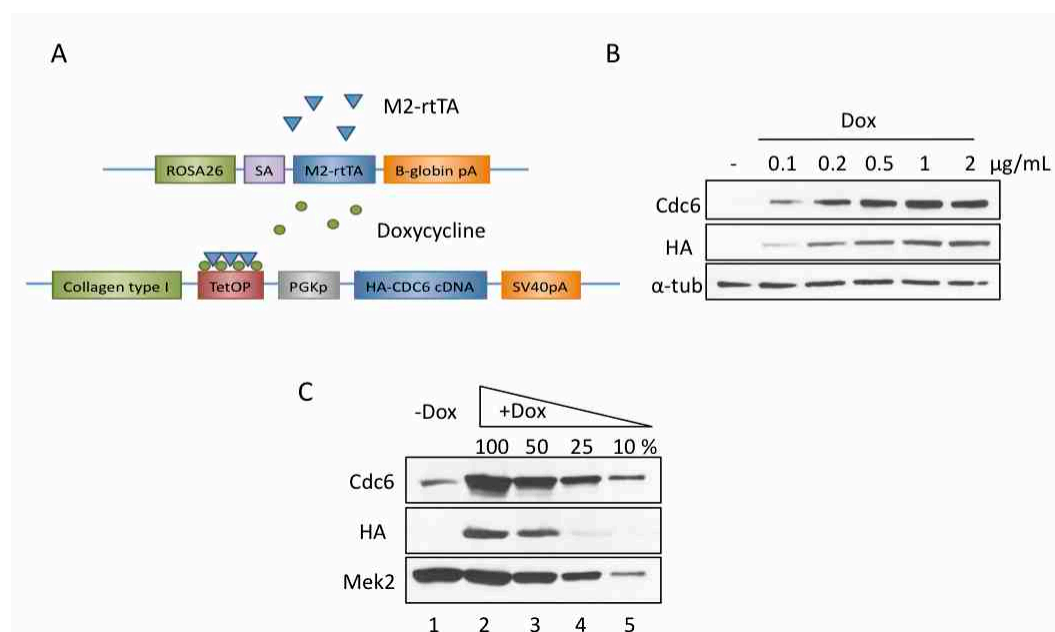


Figure 20. Tet^{ON}-CDC6 mouse model for Cdc6 overexpression. A. Two-transgene design for for Cdc6 overexpression. rtTA is inserted into the *ROSA26* locus under the control of the *ROSA* promoter. A cassette containing HA-tagged Cdc6 (isoform b) under the control of the dox-responsive promoter was inserted in the *Col1a1* locus by site specific recombination. SA, splice acceptor; pA, polyadenylation signal; TetOP, tetracycline/doxycycline responsive operator. Black arrows indicate transcriptional start sites. B. Dox titration experiment in MEFs. Cells were treated for 24 h at the indicated dox concentrations. Cdc6 and HA tag were detected by immunoblot. Alpha tubulin, loading control. C. Cdc6 overexpression levels were determined by immunoblot in MEFs by comparing the signal corresponding to endogenous (lane 1) with that corresponding to cells treated with dox for 24 h in serial dilution (lanes 2-5).

Mouse Embryonic Fibroblasts (MEFs) were obtained at E13.5 and tested for levels of Cdc6 expression in response to different dox concentrations. The response to dox was linear up to 1 $\mu\text{g/mL}$, which was chosen as working concentration for subsequent experiments (**Fig. 20B**). We determined that HA-Cdc6 was overexpressed approximately 10-fold relative to endogenous Cdc6, 24 h after dox addition (**Fig. 20C**).

2.2. Cdc6 overexpression increases MCM-chromatin loading in MEFs

Next we addressed whether Cdc6 overexpression in this new model led to increased MCM chromatin association, as previously observed in keratinocytes from the K5-CDC6^{tg} strain. MEFs were treated with dox for 24 h and 48 h and subjected to biochemical fractionation. Increased amounts of Mcm2, Mcm4, and Mcm6 proteins were found in the chromatin-enriched fraction (**Fig. 21A**, lanes 5-6 and 11-12).

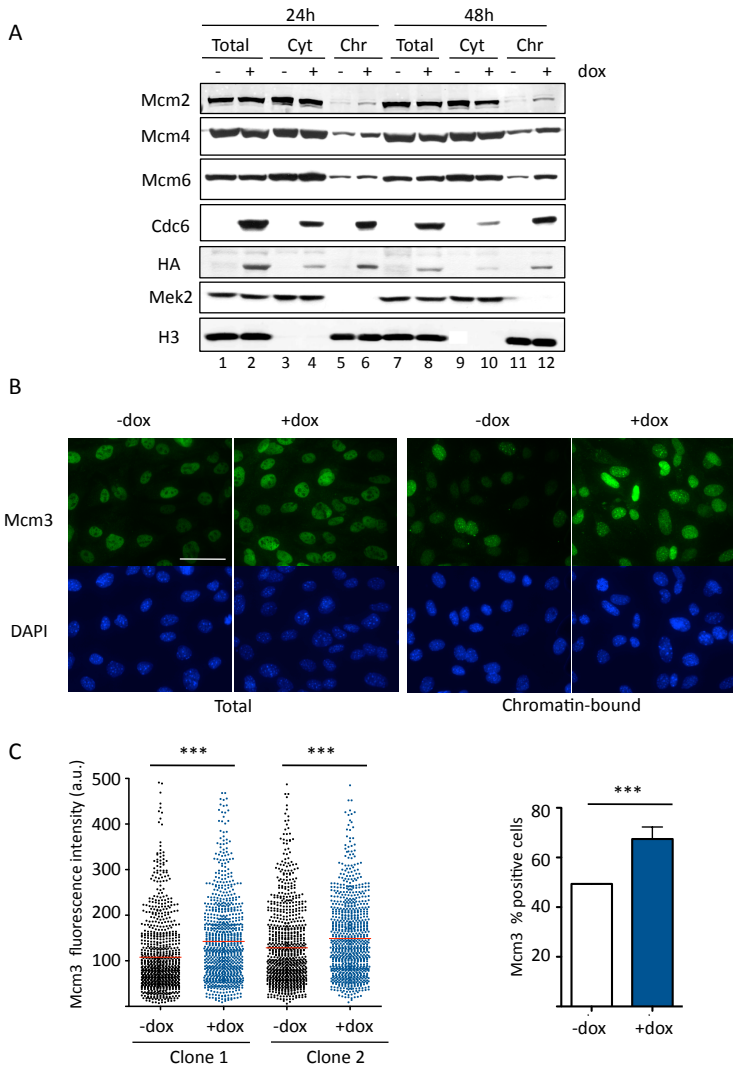


Figure 21. Increased MCM-chromatin association upon Cdc6 overexpression.

A. Western blot for the indicated proteins after biochemical fractionation of MEFs treated for 24 or 48 h with dox. Total cell extracts, cytosolic (Cyt) and chromatin-bound (Chr) fractions were analyzed. Mek2 and H3 serve as markers of cytosolic and chromatin-bound proteins, respectively.

B. Immunofluorescence (IF) of total and chromatin-bound (pre-extracted) Mcm3 (green) on MEFs -/+ dox treated (48 h). Nuclei are stained with DAPI (blue). Scale bar 50 μm . **C.** High-throughput microscopy (HTM) analysis showing Mcm3 fluorescence intensity in individual cells (left) and percentage of cells positive for chromatin-bound MCM3 (right; n=2 clones; 900 nuclei/clone). Statistically significant p values calculated using Mann-Whitney test (left) and Fisher's test (right); *** p<0.001.

This result was further confirmed by Mcm3 immunofluorescence (IF). In cells treated with detergent prior to fixation, the IF signal corresponds exclusively to chromatin-bound proteins (**Fig. 21B**). The presence of Mcm3 on chromatin was also analyzed by high-throughput microscopy (HTM). As shown in **figure 21C and D**, Cdc6 overexpression leads to increased Mcm3 nuclear intensity and higher percentage of Mcm3-positive cells.

As it was the case with K5-CDC6^{tg} keratinocytes, no differences were observed in the cell cycle profile and BrdU incorporation rate 24 or 48 h after dox addition, ruling out that the increased MCM-chromatin binding was due to an accumulation of cells in G1 (**Fig. 22**).

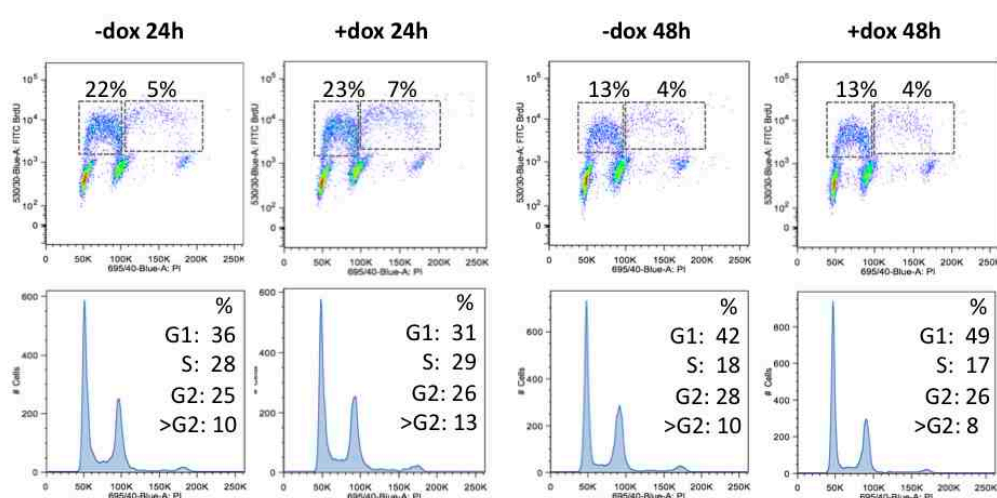


Figure 22. BrdU incorporation rate and cell cycle profile in Cdc6-overexpressing cells. Cells were pulse-labeled for 30 min with BrdU after 24 or 48 h of dox addition and processed for flow cytometry analysis of BrdU incorporation and DNA content, stained with propidium iodide (PI).

Accordingly, no differences were found in the number of EdU-positive cells, EdU nuclear intensity or chromatin-bound PCNA measured by HTM between control and dox-treated cells (**Fig. 23**).

2.3. Overexpressed Cdc6 protein is regulated in the cell cycle

We next studied whether Cdc6 overexpression would affect cell cycle re-entry after serum starvation in primary MEFs. Cells were grown until nearly confluent and serum-starved for 72 h to drive them into a quiescent G0 state. 24 h before induction of cell cycle re-entry, dox was added to induce HA-Cdc6 overexpression (**Fig. 24A**).

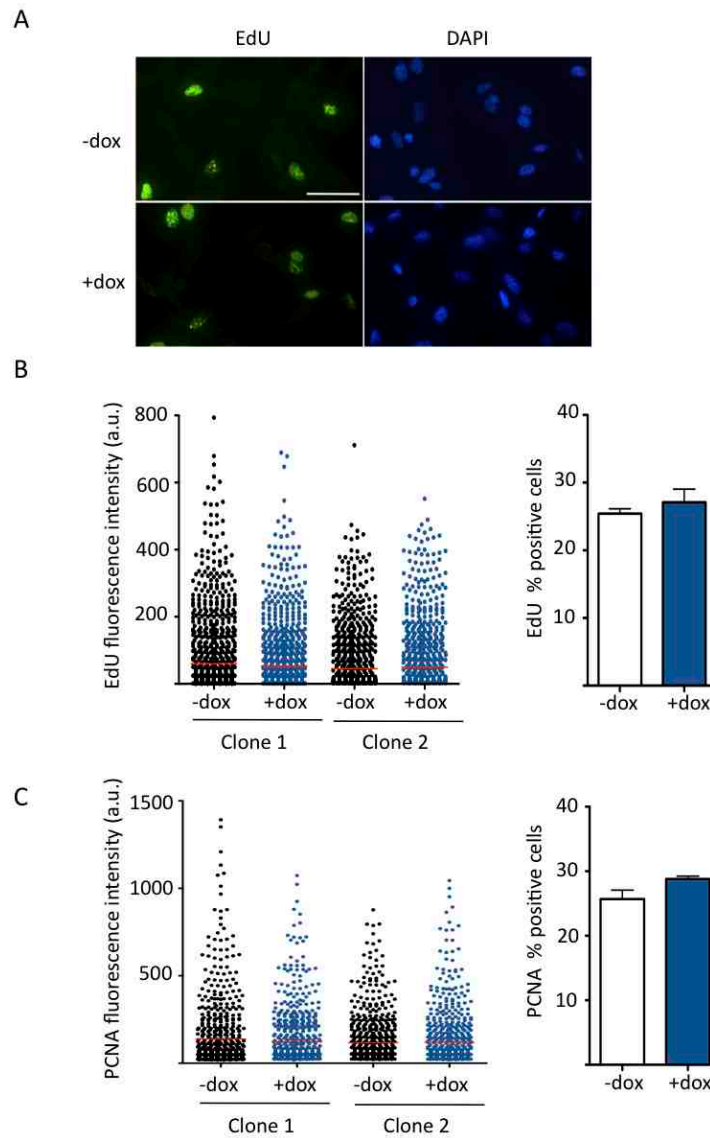


Figure 23. EdU and PCNA quantification by HTM-analysis. **A.** Representative images of EdU IF (green) in control and dox-treated cells. Nuclei are stained with DAPI (blue). Scale bar 50 μ m. **B.** HTM-mediated quantification revealed no differences in nuclear intensity (left) or percentage of EdU-positive cells (right) between control and dox-treated cells ($n = 2$ clones; 1000 nuclei are depicted). Error bars represent SD. **C.** HTM analysis of chromatin-bound PCNA resulted in similar nuclear intensity (left) or percentage of positive cells (right) in control and dox-treated cells ($n=2$ clones; 700 nuclei are shown). Error bars represent SD.

Interestingly, we noticed that even in the presence of dox, Cdc6 protein failed to accumulate in G0 cells, consistent with its reported downregulation in quiescence (Hateboer et al., 1998; Petersen et al., 2000) (**Fig. 24B**). Upon cell cycle re-entry, Cdc6 progressively accumulated both in control and dox-treated cells. In any case, cell cycle re-entry was not accelerated upon Cdc6 overexpression. No differences were found in the percentage of BrdU-incorporating cells at any of the time points tested after serum addition (**Fig 24C**).

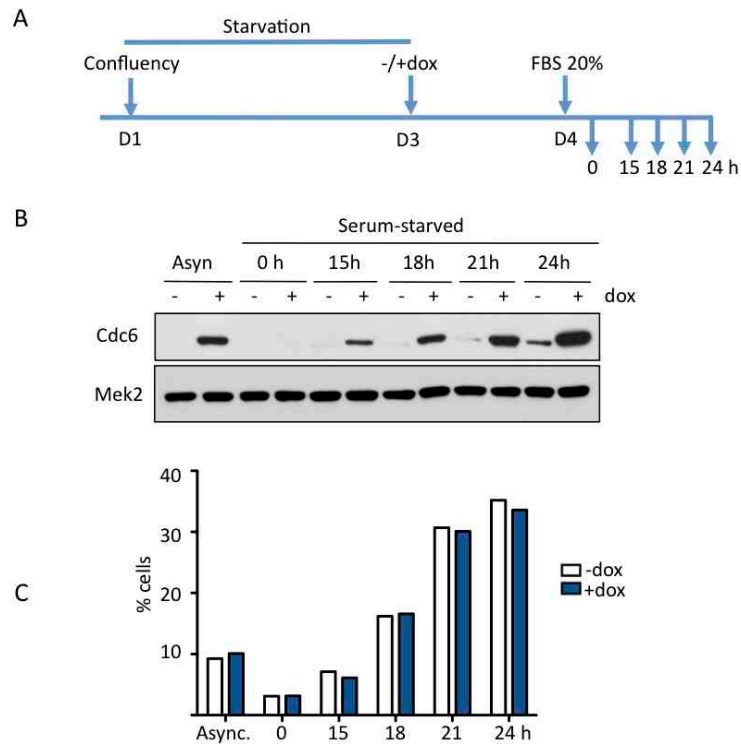


Figure 24. Effect of Cdc6 on cell cycle re-entry upon serum starvation. **A.** Outline of the serum-starvation and cell cycle re-entry induction protocol. **B.** Immunoblot showing Cdc6 protein for the duration of the experiment. Mek2, loading control. **C.** Cells were pulse-labeled for 30 min with BrdU at the indicated time points and the percentage of cells incorporating it into nascent DNA was estimated by flow cytometry. No differences were observed between control and dox-treated cells. An asynchronous culture is shown as a control.

The observation that exogenous Cdc6 did not accumulate in G0 cells prompted us to compare the accumulation of Cdc6 and the level of MCM chromatin association in cells enriched in G1, S and G2/M phases. Cells treated for 24 h with dox were submitted to FACS sorting based on their DNA content (**Fig. 25A**). The lowest Cdc6 expression level was detected in G1 (**Fig. 25B**). This probably reflects the fact that Cdc6 is a substrate of the Cdh1-APC/C proteolytic pathway (Méndez and Stillman, 2000; Petersen et al., 2000; Mailand and Diffley, 2005). In contrast, expression levels increased from S to G2/M (**Fig. 25B**). Higher levels of MCM chromatin association were seen in G1 and G2/M cells (**Fig. 25C**). In the latter, the enrichment probably corresponds to mitotic cells, when pre-RC proteins start to bind to DNA (Méndez and Stillman, 2000). The fact that no increased levels of MCM on chromatin are seen in S-phase suggests that overexpressed Cdc6 mainly exerts its licensing function in the expected phases of the cell cycle (telophase and G1).

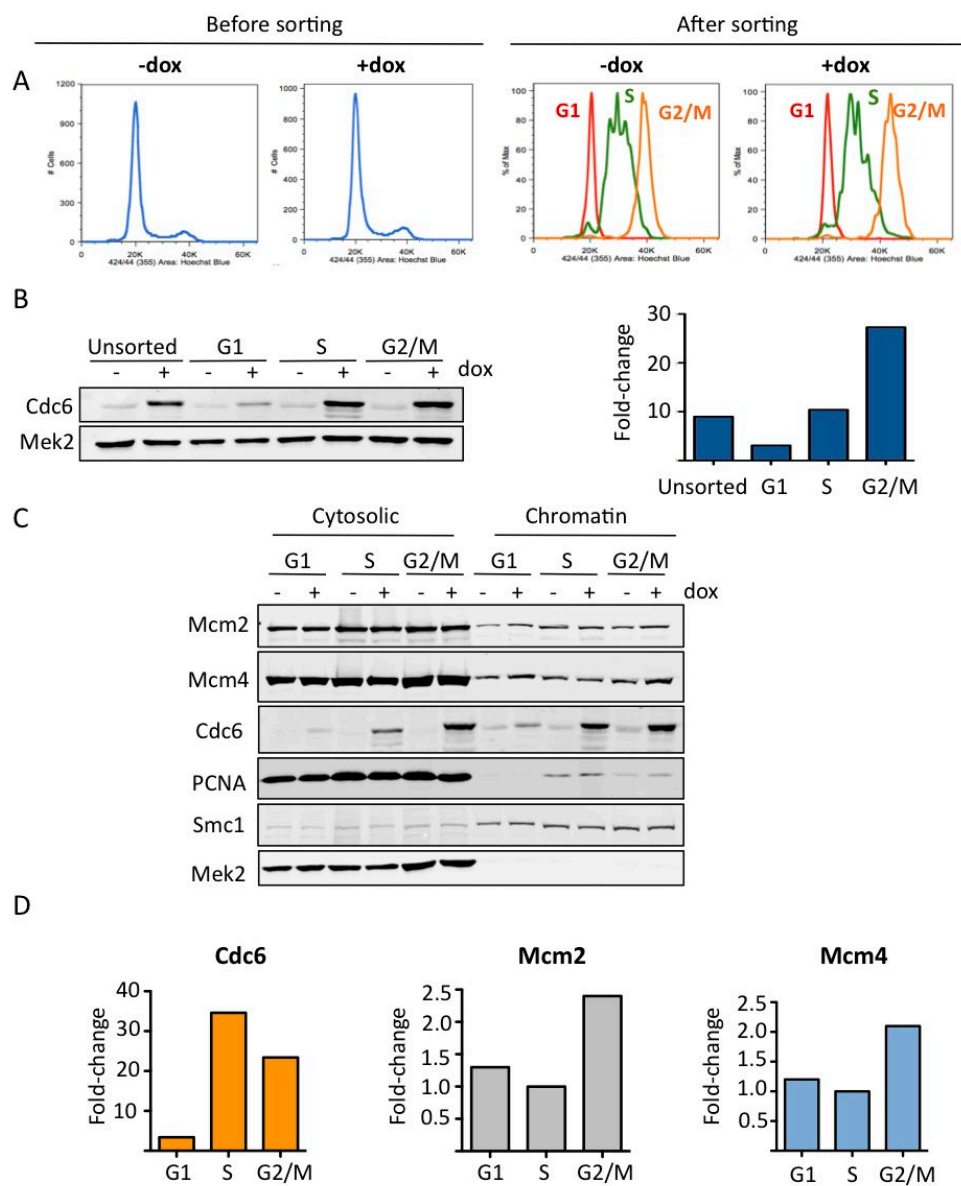


Figure 25. Cdc6 overexpression and MCM chromatin enrichment in the cell cycle. A. DNA content profile of control and dox-treated cells before sorting (left) and in the different cell fractions obtained after sorting (right). **B.** Cdc6 expression levels by western blot in an unsorted population of cells, G1, S and G2/M fractions (left). Mek2, loading control. Cdc6 overexpression levels quantified (right) using the LI-COR Odyssey Imaging system. Cdc6 was normalized by its corresponding Mek2 signal. Cdc6 overexpression accumulates from G1 to G2/M. **C.** Western blot for the indicated proteins after biochemical fractionation. **D.** Chromatin-bound fractions for Cdc6, Mcm2 and Mcm4 quantified using the LI-COR Odyssey system.

2.4. Cdc6 overexpression increases origin activity during S-phase

After having detected increased levels of MCM on chromatin due to Cdc6 overexpression, we next analyzed the DNA replication dynamics in terms of origin firing efficiency and fork progression rate. We reasoned that the increased efficiency of MCM loading could favor the activation of more DNA replication origins. Potential ‘new’ origins might be activated in a normal S-phase or perhaps reserved to be activated upon replicative-stress conditions as described for ‘dormant origins’ (Get at al., 2007; Ibarra et al., 2008). In the second case, Cdc6 overexpression might confer some resistance to replication stress.

The analysis of origin firing and fork progression was addressed by DNA fiber spreading, which allows the visualization of newly synthesized DNA tracks in individual molecules. To do so, cells were sequentially pulse-labeled with halogenated nucleosides chlorodeoxyuridine (CldU) and iododeoxyuridine (IdU) after which genomic DNA was extracted and stretched on glass slides, stained with IdU- and CldU-specific antibodies, and visualized by IF (see Materials and Methods).

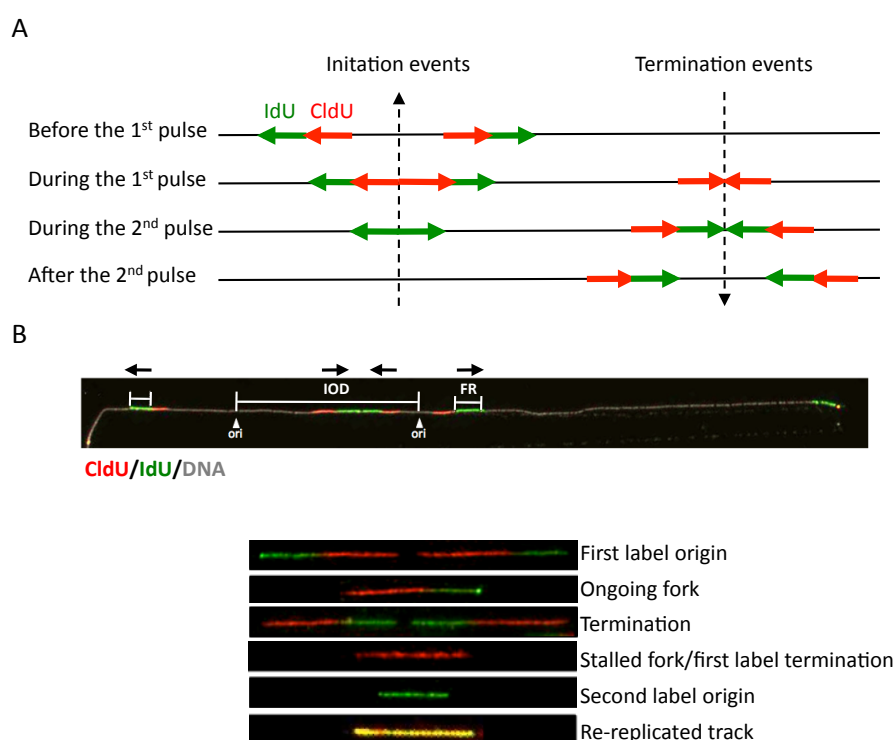


Figure 26. Replication structures detected by DNA fiber spreading. **A.** Schematic representation of the structures generated by sequential pulse labelling of cells with CldU (red) and IdU (green), depending on the timing of origin firing during the labelling period. **B.** The upper part shows a single DNA fiber with two active origins that allows the measurement of the inter-origin distance (IOD). Fork rate (FR) is calculated with second-labeled tracks. The bottom part shows representative pictures of the structures depicted in A plus a re-replicated track.

The configuration of replication tracks on single DNA molecules allows the identification of origins, ongoing forks, terminating forks and even re-replication events (**Fig. 26A-B**). To estimate the frequency of fired origins, we measured the inter-origin distance (IOD). Shorter IODs correlate with higher origin activity (Conti et al., 2007; Maya-Mendoza et al., 2007). Fork progression rate was monitored in second-labeled tracks, whose length is divided by the duration of the pulse (**Fig. 26B**). The same parameters can be measured under conditions of replicative stress. Here, cells were subjected either to a short (2 h), low-dose aphidicolin treatment (0.1 μ M) or to a longer (24 h), higher dose treatment (0.5 μ M) (**Fig. 27A**).

Interestingly, cells treated with dox for 24 h showed a 1.5-fold reduction in IOD, which suggests that Cdc6-overexpressing cells fired more origins in a normal S-phase (**Fig. 27B**). A similar effect was observed upon 48 h of dox treatment (1.8-fold decrease in IOD; **Fig. 27C**). We ruled out non-specific effects of dox by performing similar experiments wt MEFs (data not shown). The higher frequency of origin usage should in principle lead to faster DNA replication and shorter S-phase, but these effects were not observed (**Fig. 22**). This is probably because the increase in origin firing was accompanied by a parallel decrease in fork rate progression (**Fig. 27 C and 27 E**, left lanes). This ‘slowing’ of forks after excessive origin activity could indicate the existence of limiting factors for fork activity (Zhong et al., 2013; reviewed by Petermann and Helleday, 2010).

As expected, when control cells were treated for 2 h with aphidicolin, they activated more (approximately 3-fold) compared to a regular S-phase (**Fig. 27B**, lanes 1 and 3). The fork rate was reduced to a similar extent (**Fig. 27C**, lanes 1-3). In contrast, dox-treated cells only increased origin firing by 1.4-fold upon aphidicolin with a proportional decrease in the fork progression rate (**Fig. 27B, 8C** lanes 2-4). This result suggests that replication stress-induced new origin firing is partially inhibited in Cdc6-overexpressing cells (**Figs. 27B**, lanes 3-4). This observation was more apparent under conditions of continued replicative stress. After 24 h of aphidicolin, control cells increased origin firing by 2-fold, Cdc6-overexpressing cells showed the same IOD independently of aphidicolin, indicating that they had already fired all available origins, i.e. that virtually no origin was left dormant under these conditions (**Figs. 27D**).

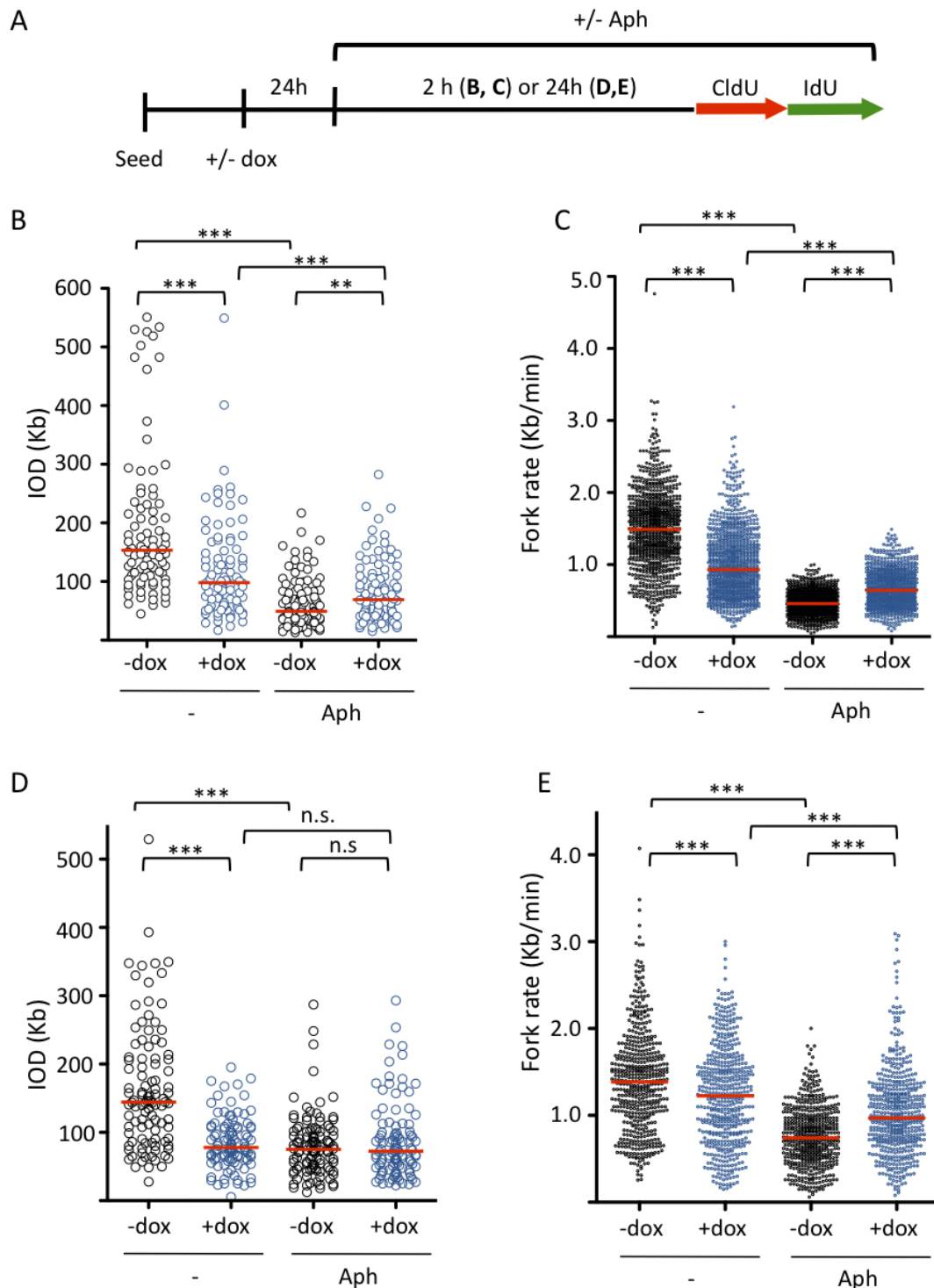


Figure 27. DNA fiber analysis shows increased origin activity in Cdc6 overexpressing cells. **A.** Outline of the experiment. Two different conditions of aphidicolin were used: 0.1 μ M of aphidicolin during 2 h (part B, C) and 0.5 μ M for 24 h (part D, E). Cells were sequentially pulsed-labeled for 20 min with CldU/IdU and subjected to DNA fiber spreading. **B.** Inter-origin distance (IOD) and fork progression rate measurements (FR) (**part C**) for dox-treated and control cells in a normal S-phase and upon short aphidicolin treatment ($n=3$ clones; IOD, ≈ 100 measurements/condition; FR, > 900 measurements/condition). **D-E.** Same as in parts B and C but upon long aphidicolin treatment ($n=2$ clones; IOD >100 measurements/condition; FR > 500 measurements/condition). Statistically significant p values calculated using Mann-Whitney test ***= $p<0.001$; ** $p<0.0055$; n.s. no significant.

2.5. Spatio-temporal regulation of DNA replication is not affected by Cdc6 overexpression

DNA replication follows a spatio-temporal program, by which large segments of the genome are coordinately replicated through the nearly synchronous firing of clusters of replication origins (reviewed by Gilbert, 2010; Aparicio, 2013). The molecular and genetic mechanisms that define this spatio-temporal coordination are not fully understood, and one hypothesis postulates the existence of rate-limiting proteins for origin firing (Mantiero et al., 2011). To check whether Cdc6 might alter the spatio-temporal replication program, we analyzed the distribution of the different EdU patterns observed during S-phase (Dimitrova and Berezney, 2002). No differences in the distribution of early, mid- and late S-phase EdU patterns between control and dox-treated cells were observed (**Fig. 28**), indicating that Cdc6 overexpression did not affect the large-scale replication timing programme.

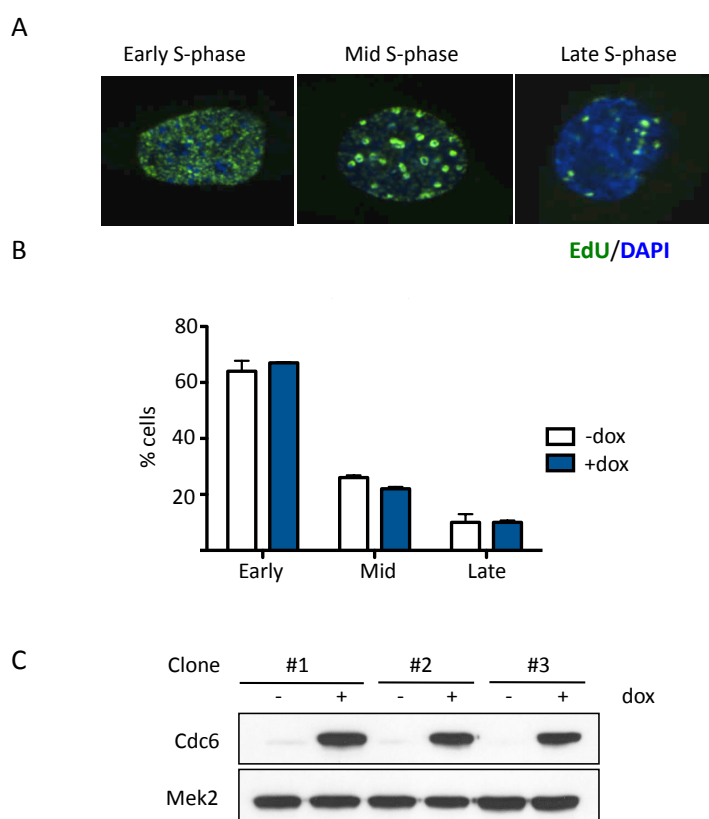


Figure 28. Cdc6 overexpression did not affect the distribution of replication foci during S-phase. A. Representative images of S-phase EdU patterns. Cdc6 overexpression was induced with dox for 48 h before EdU pulse-labeling for 30 min. EdU (green), DAPI (blue). **B.** Quantification of replication patterns (n= 3 clones, 150-200 nuclei per clone were counted). Error bars represent SD. **C.** Immunoblot showing Cdc6 overexpression levels. Mek2, loading control.

2.6. Cdc6 overexpressing-cells do not show signs of replicative stress

Promiscuous origin activity may lead to stress and activation of the DDR (Syljuasen et al., 2005; DiMicco et al., 2006; Maya-Mendoza et al., 2007). Given that Cdc6-overexpressing cells activate more origins in a normal S-phase, we checked for the activation of DDR markers. No changes were observed for the nuclear intensity and percentage of positive cells for chromatin-bound RPA (**Fig. 29A-B**) and γ H2AX (**Fig. 29C-D**) upon Cdc6 overexpression. As a control, cells treated with HU displayed RPA foci and γ H2AX fluorescence. Still, no differences were found by Cdc6 overexpression in the presence of HU. Similar results were obtained with aphidicolin (data not shown).

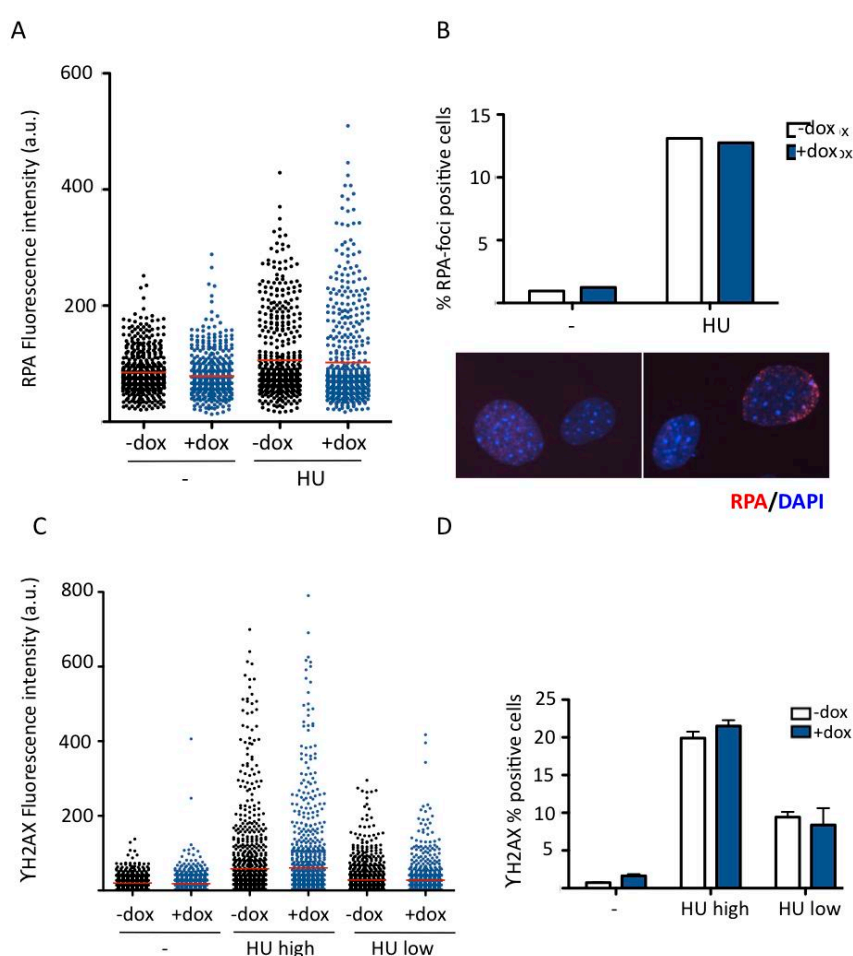


Figure 29. No signs of replicative stress in Cdc6-overexpressing MEFs. **A.** HTM-mediated quantification of nuclear signal intensity of RPA in normal conditions and upon a 3 h treatment with 0.5 mM HU. Cdc6 overexpression was induced with dox 24 h before the experiment (500 nuclei per condition are shown). **B.** Upper part: quantification of cells positive for RPA foci in normal and upon HU treatment as in part A (300-400 nuclei/condition). Bottom part: representative pictures of RPA IF (red) before and after HU treatment. DNA stained with DAPI (blue). **C.** HTM-mediated quantification of γ H2AX nuclear intensity in normal conditions and upon a 3 h treatment with different HU concentrations (high; 0.5 mM; low: 0.1 mM). Cdc6 overexpression was induced 24 h before the experiment. Data are representative of 2 independent analyses (1000 nuclei per condition). **D.** Quantification of γ H2AX-positive cells under the same experimental conditions (n=2 clones; >1000 nuclei per condition). Error bars represent SD.

Replicative stress-inducing agents increase the frequency of double strand breaks (DSB) (Saintigny et al., 2001; Lundin et al., 2002) that can be visualized by the colocalization of 53BP1 and γ H2AX foci (Shultz et al., 2000) (**Fig. 30A**). As expected, aphidicolin increased the number of cells positive for 53BP1 and γ H2AX foci, but no differences were observed between control and dox-treated cells (**Fig. 30B**).

DNA replication problems induced by long aphidicolin treatments can also be visualized in the form of chromatid breaks on metaphase spreads (**Fig. 30C**). Tet^{ON}-CDC6 MEFs were treated with aphidicolin for 24 h and the number of breaks per chromosome was quantified in metaphase spreads. Without aphidicolin, the number of breaks was very low,

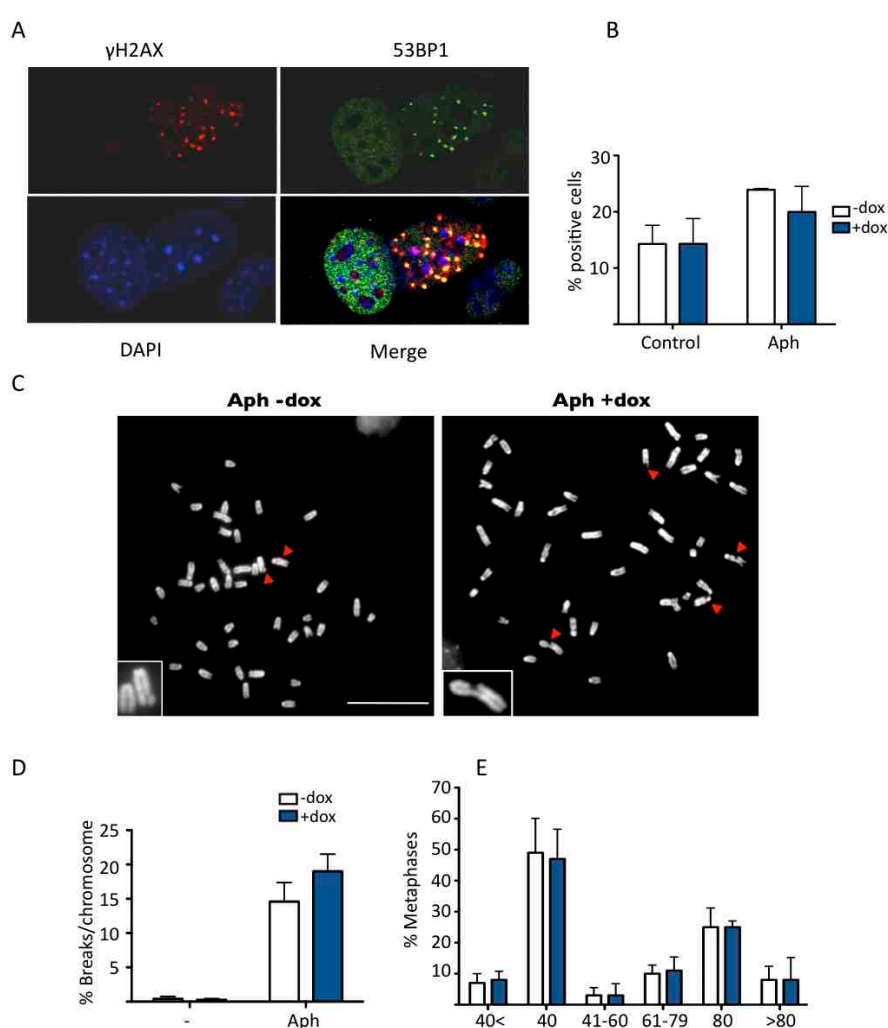


Figure 30. Cdc6 overexpression does not induce DSB. **A.** Confocal microscopy IF images for γ H2AX IF (red), 53BP1 IF (green) and nuclear DNA stained with DAPI (blue). **B.** Quantification of positive cells for γ H2AX and 53BP1 foci in normal conditions and upon aphidicolin treatment (0.5 μ M for 24 h). Cells with >2 foci were considered positive (n=2 clones; \approx 700 nuclei per condition). Error bars represent SD. **C.** Representative pictures of metaphase chromosomes obtained after aphidicolin treatment. Arrowheads mark chromatid breaks (see insets) Scale bar 25 μ m. **D.** Quantification of chromatid breaks per chromosome after 48 h of Cdc6 overexpression. During the last 24 h, 0.5 μ M aphidicolin was added. Variations were just under the limit of significance (p = 0.056) using Student t-test test (n=4 clones; >30 metaphases quantified per condition). **E.** Ploidy quantification on metaphase spreads. No differences were observed between control and dox-treated cells 48 h post-induction (n=4 clones; >50 metaphases were counted per condition). Error bars represent SD.

and no differences were observed between control and dox-treated cells. In the presence of aphidicolin, a modest increase in the frequency of breaks was observed in Cdc6-overexpressing cells, which was very close to the threshold of statistical significance ($p=0.056$; **Fig. 30D**). No changes in ploidy between control and dox-treated cells were observed (**Fig. 30E**).

2.7. Cdc6 overexpression does not affect homologous recombination rate

As indicated above, fork progression was slower after Cdc6 overexpression (**Fig. 27**). Short-labeled tracks could also indicate a higher frequency of stalled or collapsed replication forks. Upon fork collapse, replication can be rescued through the homologous recombination (HR)-mediated replication fork restart, which involves template switching to the undamaged sister chromatid (reviewed by Petermann and Helleday, 2010; Branzei, 2011). The resulting crossover events can be visualized as sister chromatid exchanges (SCE) on metaphase chromosomes (Sonoda et al., 1999).

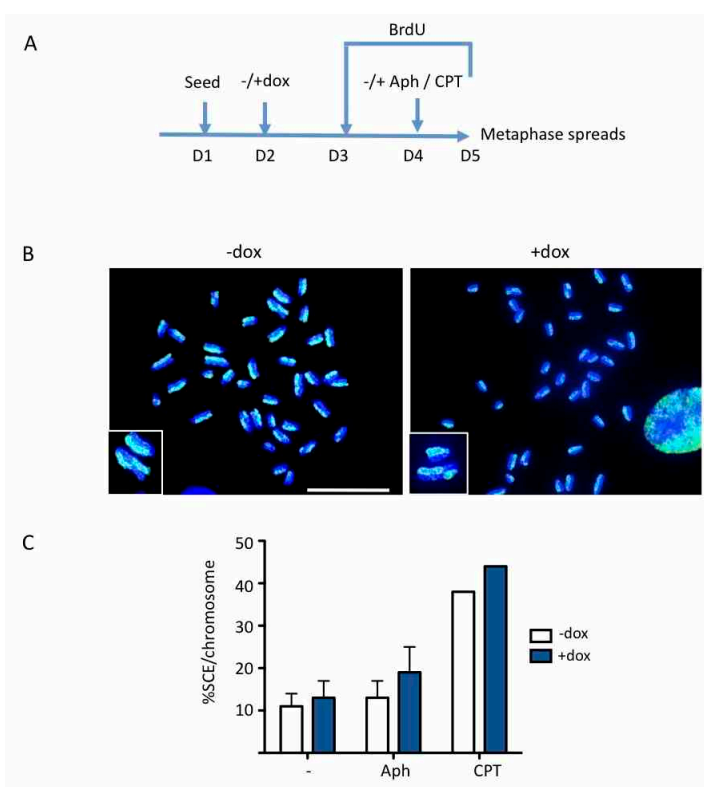


Figure 31. Sister-chromatid exchange analysis (SCE) showed similar HR events in dox-treated and control cells. **A.** Protocol for SCE analysis upon aphidicolin (0.5 μ M) or CPT (CPT, 2.5 nM). **B.** Representative pictures of BrdU IF to detect HR events on metaphase chromosomes. Scale bar 25 μ m. **C.** Quantification of HR events per chromosome. No statistically significant values were obtained using Mann-Whitney test ($n=3$ clones for aphidicolin; CPT $n=1$ clone; > 600 chromosomes/condition). Error bars represent SD.

For this reason, we analyzed the frequency of HR events in MEFs overexpressing Cdc6 under normal growth conditions or in the presence of aphidicolin or camptothecin

(CPT), two DNA replication inhibitors known to induce SCEs (**Fig. 31A**). Cells were labeled for 48 h with BrdU and its incorporation was visualized on metaphase chromosomes by IF (**Fig. 31B**). The frequency of HR events was similar in control and dox-treated cells. Aphidicolin and CPT induced a moderate increase in cells overexpressing Cdc6, although the differences were not statistically significant (**Fig. 31C**).

2.8. No effect of Cdc6 overexpression on cell growth or viability

The results shown in figures 29-31 indicate that short-term Cdc6 overexpression in MEFs did not have a negative impact on genomic integrity.

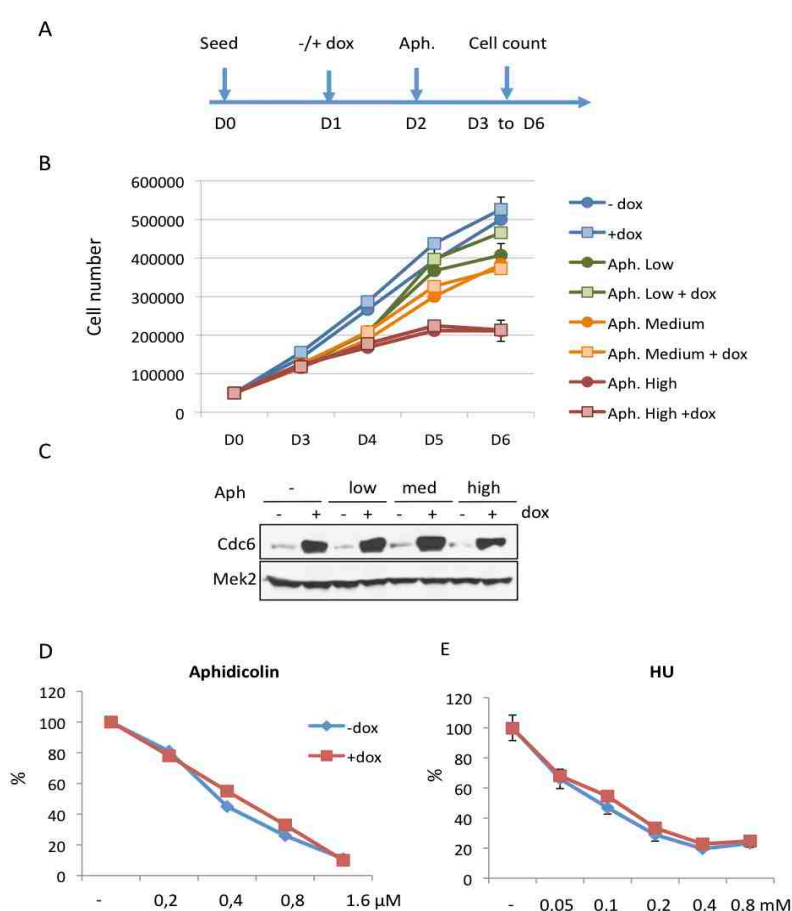


Figure 32. Cell proliferation under conditions of replicative stress. **A.** Outline of the cell proliferation assay. **B.** Proliferation curve. Circles represent control cells. Squares represent dox-treated cells. The colors correspond to control (blue lines) and different aphidicolin doses: green, 0.05 μ M; yellow, 0.1 μ M; red, 0.3 μ M. This curve is representative of 7 independent experiments. Error bars represent SD of duplicates in this experiment. **C.** Western blot for Cdc6 overexpression in cells at day 5. Mek2, loading control. **D.** MTT-based colorimetric cell proliferation assay. Cells were grown for three days in the presence of different doses of aphidicolin (**D**) or HU (**E**). Cell viability is calculated relative to the absorbance of the untreated samples. Error bars represent SD of duplicates in this experiment.

Next we considered the alternative possibility, namely that higher Cdc6 levels could have a protective effect in situations of replicative stress. However, Cdc6-overexpressing cells proliferated at the same rate than control cells in the presence of different doses of

aphidicolin (**Fig. 32**). Furthermore no differences in cell viability were obtained using a colorimetric MTT-based cell proliferation assay in the presence of other DNA damaging agents such as UV, methyl methanesulfonate (MMS) and Neocarzinostatin (NCS). Again, no differences in cell proliferation between control and dox-treated cells were observed (**Fig. 33**).

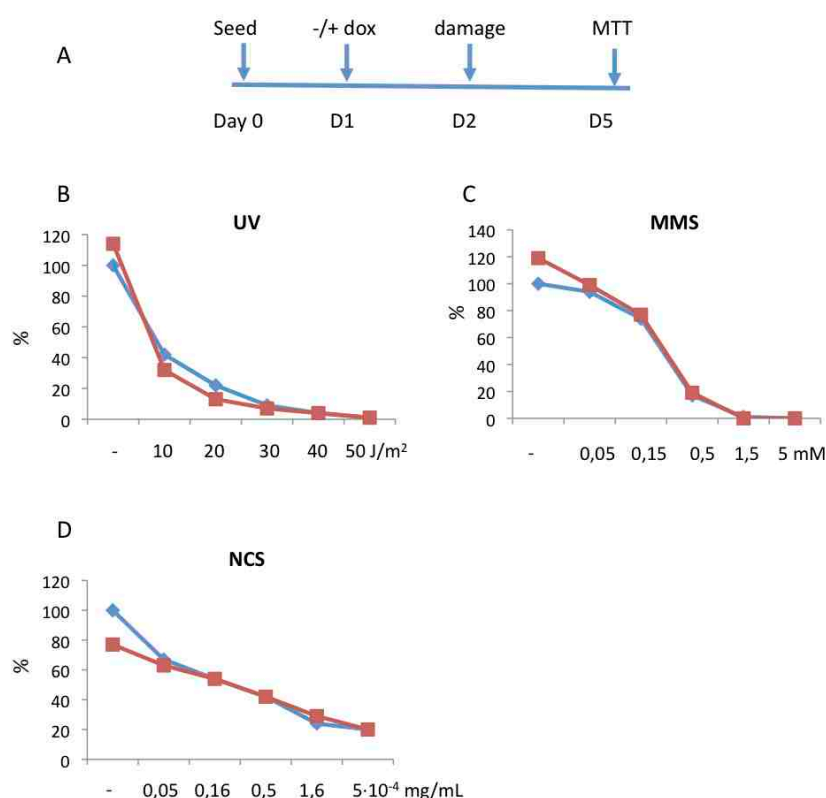


Figure 33. MTT-based colorimetric proliferation assay upon different DNA damaging agents. **A.** Outline of the experiment. Cells were given increasing doses of different insults for 24 hours, released the day after and kept in culture for 3 more days. **B, C and D.** Cell viability in control and dox-treated cells after UV (**B**), MMS (**C**) and NCS (**D**) treatment. Cell viability was calculated relative to the absorbance of the untreated samples.

2.9. Cdc6 overexpression does not facilitate transformation in MEFs

We also tested whether Cdc6 overexpression could contribute to spontaneous cell immortalization. Primary MEFs were subjected to a 3T3 protocol, in which cells grow exponentially the first 4-5 passages after which they reach a 'plateau' phase where further growth is limited by senescence. Upon the occurrence of spontaneous mutations in tumor suppressor genes such as p53 (Harvey and Levine, 1993) cells escape senescence and exponential growth is recovered. Three different clones of Cdc6 overexpressing MEFs reached and exited the plateau phase with similar kinetics regardless of Cdc6 overexpression. A wt clone of MEFs was analyzed in parallel to rule out possible unspecific

effects of dox addition (**Fig. 34A-B**). We also checked that Cdc6 did not increase the efficiency of cell transformation mediated by *H-RasV12* and *E1A* (**Fig. 34 C**)

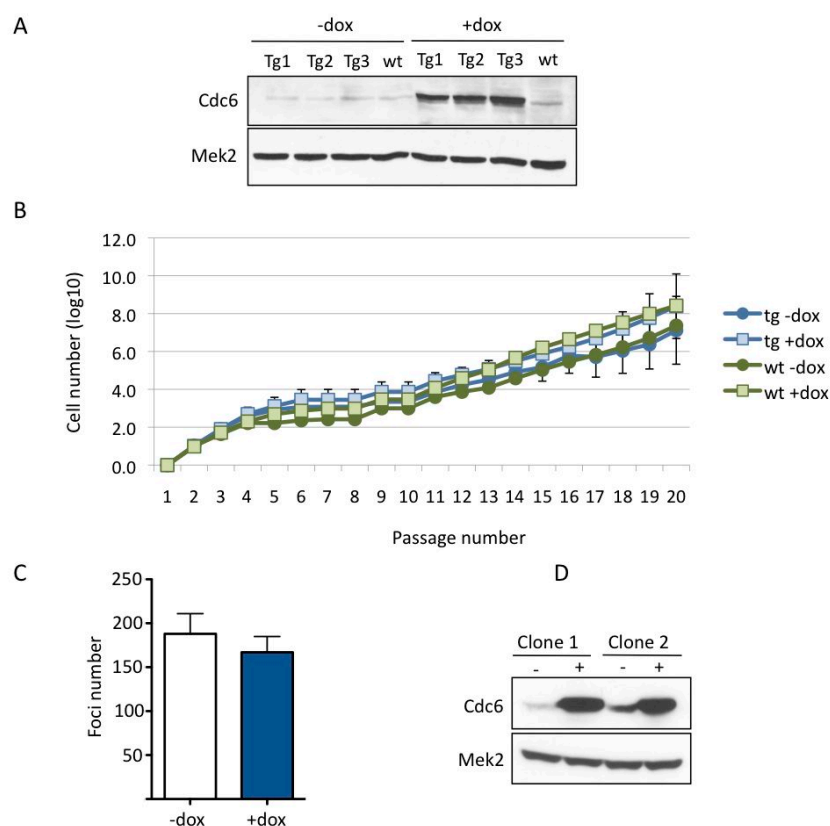


Figure 34. Cdc6 overexpression does not facilitate cell transformation. **A.** Western blot for Cdc6 overexpression for the different clones used in the 3T3 immortalization assay. **B.** Growth rate during the immortalization process (n=3 Tet^{ON}-CDC6 clones and 1 wt clone). Error bars represent SD between clones. **C.** Foci quantification in the *E1A/H-RasV12*-infected plates (n= 2 clones). **D.** Cdc6 overexpression was confirmed by western blot. Mek2, loading control.

2.10. Cdc6 overexpression increases MCM-content in proliferative tissues

The results presented in this chapter so far show that the Tet^{ON}-CDC6 strain is functional, leading to significant overexpression of Cdc6 and increased association of MCM proteins with chromatin (**Figs. 20, 21**). In MEFs, in a higher frequency of origin firing in S-phase but this was compensated by slower fork progression rate (**Fig. 27**) and no effects on cell viability or genetic integrity were observed (**Figs. 29-33**). Next, we aimed at testing the impact of long-term overexpression of Cdc6 *in vivo*.

To this aim, dox was supplied *ad libitum* in the mice diet. The levels of Cdc6 expression after 4 weeks were analyzed by RT-qPCR on total RNA isolated from all major organs (**Fig. 35**). The highest level of Cdc6 overexpression was found in the intestine (>100-

fold), followed by the liver (averaged overexpression ≈ 50 -fold), esophagus and stomach (≈ 30 -fold). 10 to 20-fold increase in Cdc6 expression levels were found in kidney, skin, spleen and thymus and 2 to 5-fold increase in lung, salivary gland and heart. No Cdc6 overexpression was detected in brain or testis, likely due to the inability of dox to cross the blood–brain and blood–testis barriers (Beard et al., 2006).

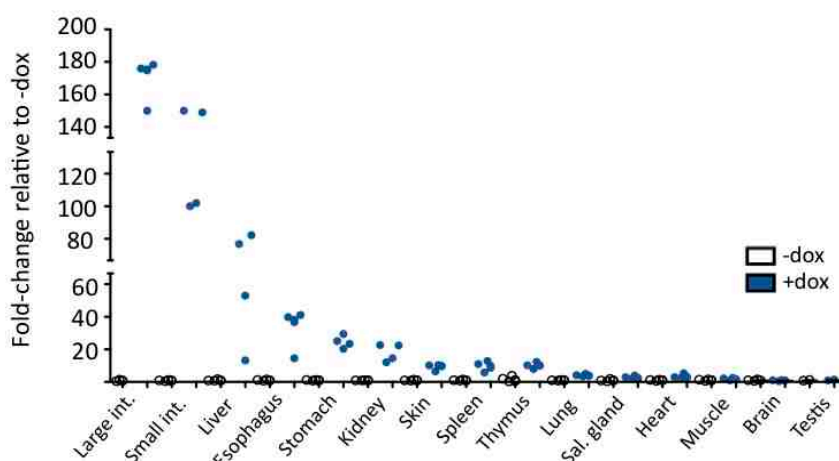


Figure 35. Cdc6 overexpression *in vivo*. Cdc6 expression levels were quantified by RT-qPCR on total RNA isolated from the indicated organs. Cdc6 mRNA levels were normalized to GAPDH gene expression. Fold-change was calculated on the averaged Cdc6 expression levels obtained in the untreated animals (n=4 -dox and 4 +dox animals).

Histopathological analyses of the different organs after 4 weeks of Cdc6 overexpression did not reveal any histological abnormalities (not shown). Higher Mcm6 content was observed in the thymus, skin, intestine and spleen of dox-treated animals (**Fig. 36A**), which are the organs with higher proliferative index (**Fig. 36B**). One striking example is the thymic cortex, in which the Mcm6 enrichment raised by 4-fold (**Fig. 36C**). In any case, cell proliferation in the different organs was not affected by Cdc6 overexpression, as quantified by Ki-67 IHC (**Fig. 36B**).

2.11. Increased tumor susceptibility in Cdc6-overexpressing mice

To study the impact of Cdc6 overexpression in ageing and spontaneous tumorigenesis, two cohorts of mice were established. One group (26 mice) had dox-supplemented diet since weaning and the other (25 mice) was set as control in normal diet. Mice were sacrificed when they showed signs of morbidity, according to the regulation approved by Animal Experimental Ethics Committee of the Instituto de Salud Carlos III and excluded from the study when they could not be histopathologically examined (i.e. upon

death in cage). Although the ageing experiment is not complete yet, the observations to date are suggestive of a shorter lifespan in Cdc6-overexpressing mice (**Fig. 37**). Most of the mice analyzed displayed hematological neoplasias (histiocytic sarcomas and B-cell lymphomas) combined in two cases with pulmonary (untreated) or hepatic adenomas (dox treated), which are benign tumors (**Table 3**).

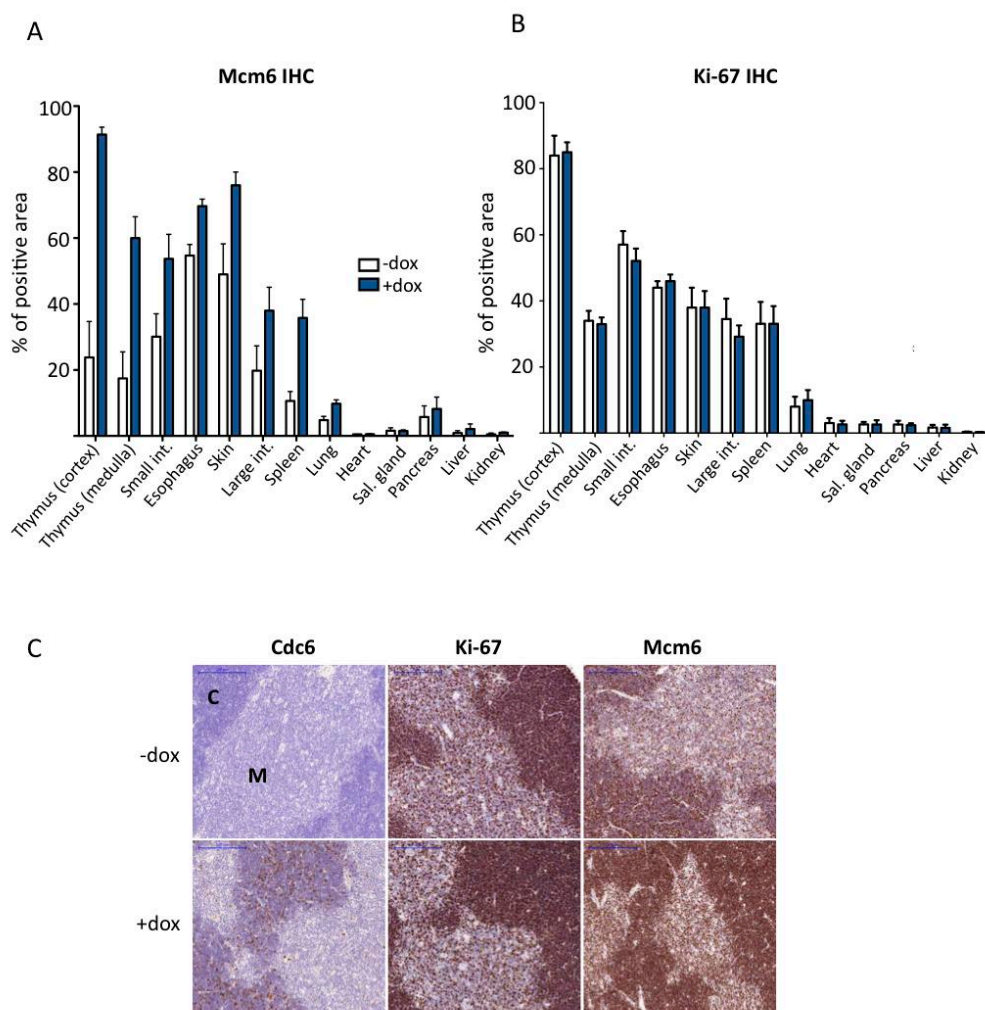


Figure 36. Increased Mcm6 content in proliferative tissues upon Cdc6 overexpression and normal proliferation rate. **A.** Mcm6 positive area was quantified with AxioVision software. The percentage of positive area is calculated over the total area in the indicated tissues (n=4 -dox and 4 +dox mice). Error bars represent SD. **B.** Ki-67 IHC quantification was performed as in A. **C.** Representative pictures of thymus in control and dox-treated animals. IHC for HA-tag (only positive in +dox animals), Ki-67 and Mcm6. Thymic cortex (C); Medulla (M).

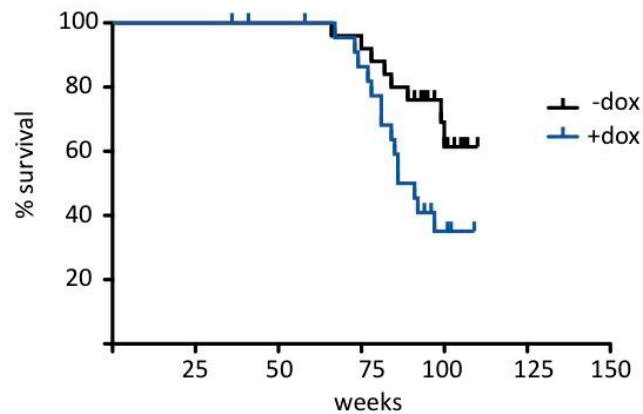


Figure 37. Reduced lifespan after continued Cdc6 overexpression *in vivo*. A. Survival (Kaplan-Meier) curves for dox-treated animals (blue line) and control animals (black line). 25 mice are included in the control group (13 males; 12 females) and 26 mice in the dox-treated group (12 females; 12 males). Breslow statistic test indicates that -/+ dox survival curves are different p value =0.023.

Although the numbers are still low, Cdc6-overexpressing mice seem to have more organs affected with tumors than age-matched untreated ones. If confirmed, this result would indicate that tumors behave more aggressively upon Cdc6 overexpression (**Table 4**). After the observation in K5-CDC6^{tg} mice, it is possible that old dox-treated animals display some ageing-related phenotype in the skin or an effect on the hair growth cycle. However it may be difficult to address this possibility considering their shorter lifespan.

Table 3. Pathologies found after histological examination.

Pathology	-dox	+dox
Hematological neoplasias		
Histiocytic sarcoma	2 (28.6%)	3 (21%)
B-cell lymphoma	3 (43%)	10 (71%)
Histiocytic sarcoma or B-cell lymphoma	2 (28.6)	
Seminal gland hyperplasia (tumor-free)		1
Total analyzed mice	7	14

Table 4. Spreading of B-cell lymphomas in -/+ dox mice.

-dox mice		+dox mice	
Age (weeks)	Organs affected	Age (weeks)	Organs affected
66	Spleen, Int, lymph nodes	67	Spleen, pancreas, kidney, liver lung, intestine, lymph nodes
75	Spleen, lymph nodes	77	Spleen, thymus, lung
82	Spleen, intestine	78	Spleen, lymph nodes, heart, lung
		81	Spleen, lymph nodes
		81	Spleen, pancreas, lung
		85	Spleen
		86	Spleen, stomach, intestine, lung, thymus

Chapter 3. Tet^{ON}-CDC6/CDT1 mouse model

3.1. Cdt1 overexpression by itself does not enhance MCM chromatin association

In order to generate a mouse model for the combined overexpression of Cdc6 and Cdt1, we first generated an inducible mouse for Cdt1 following the same strategy described for Cdc6 (Materials and Methods). In this case, a Flag tag in the C-terminus of Cdt1 was included (**Fig. 38A**). The new mouse strain Tet^{ON}-CDT1 was generated in the CNIO Transgenic Mice Unit. Upon dox addition, Cdt1 is overexpressed by > 10-fold in MEFs (**Fig. 38B**).

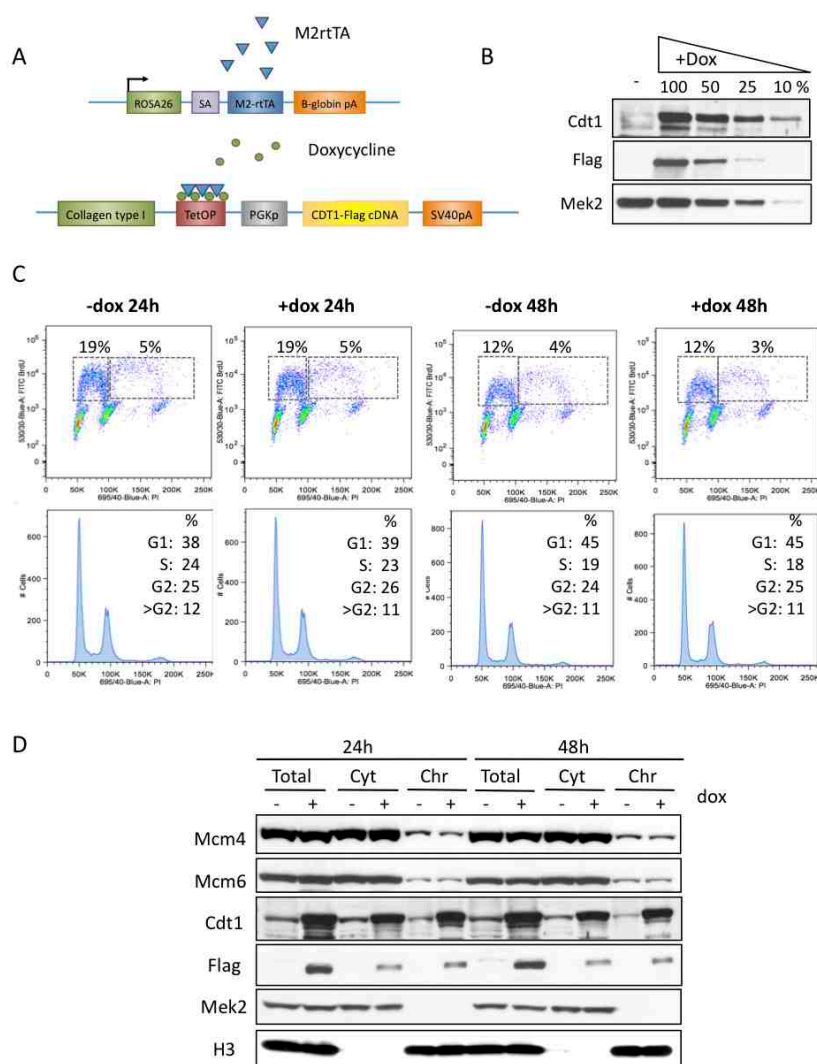


Figure 38. Cdt1 overexpression does not increase MCM chromatin association . A. Schematic representation of the transgenes used to produce inducible mice for Cdt1 overexpression. A Flag tag was included in the C-terminus part of Cdt1. SA, splice acceptor; pA, polyadenylation signal; TetOP, tetracycline/doxycycline responsive operator. **B.** Cdt1 overexpression levels were determined by western blot in MEFs treated for 24 h with dox. Cdt1 is overexpressed by > 10-fold. **C.** BrdU incorporation and cell cycle profiles 24 and 48 h after addition. DNA stained with PI. **D.** Western blot for the indicated proteins after biochemical fractionation of MEFs treated for 24 or 48 h with dox. Total cell extracts, soluble (Cyt) and chromatin-bound (Chr) fractions were analyzed. Mek2 and H3 serve as markers of cytosolic and chromatin-bound proteins, respectively.

The cell cycle profile and BrdU incorporation rate in primary MEFs were not affected by Cdt1 overexpression (**Fig. 38C**). We next analyzed if Cdt1 overexpression affects MCM loading. MEFs treated with dox for 24 and 48 h were subjected to biochemical fractionation. No increased MCM-chromatin association was observed upon Cdt1 overexpression (**Fig. 38D**). Therefore, in contrast to Cdc6, Cdt1 overexpression by itself is not sufficient to increase MCM loading efficiency.

The detailed characterization of the Tet^{ON}-CDT1 strain falls beyond the scope of this work. However, we used it to generate another strain in which both Cdc6 and Cdt1 could be overexpressed simultaneously. To this end, each Tet^{ON}-CDC6 and Tet^{ON}-CDT1 mice were first crossbred to generate homozygous *Col1a1*^{CDC6/CDC6} and *Col1a1*^{CDT1/CDT1} offspring. Subsequently, homozygous mice were crossbred to obtain Tet^{ON}-CDC6/CDT1 descendants. In all the experiments performed with this new mouse strain, the *ROSA26-M2rtTA* allele was kept in heterozygosity (**Fig. 39A**). Mice were obtained at the expected Mendelian ratio. 24 h after dox, Cdc6 and Cdt1 were efficiently overexpressed in primary MEFs(**Fig. 39B**).

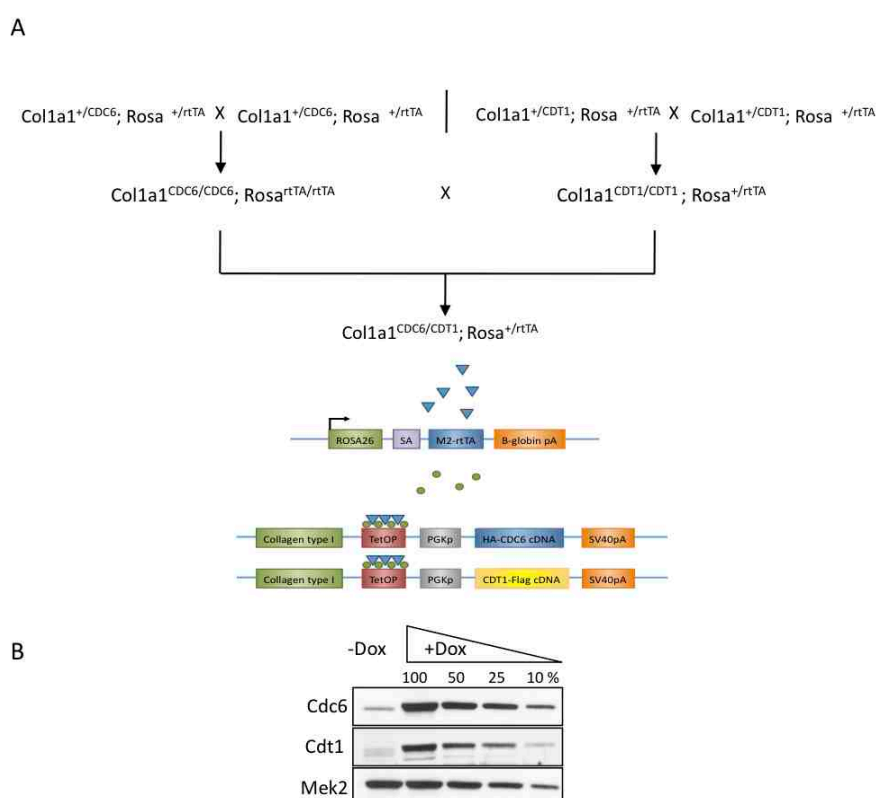


Figure 39. Tet^{ON}-CDC6/CDT1 mouse model. A. Mating strategy for the obtention of Tet^{ON}-CDC6/CDT1 mice. **B.** Cdc6 and Cdt1 overexpression levels were determined by western blot in MEFs treated for 24 h with dox. Both transgenes e overexpressed by > 10-fold.

3.2. Cdc6 and Cdt1 overexpression increases MCM chromatin-association to a similar extent than Cdc6 overexpression alone

Since both Cdc6 and Cdt1 participate in origin licensing, the overexpression of both factors could cooperate to increase MCM-chromatin association. To check this possibility, MEFs from Tet^{ON}-CDC6, Tet^{ON}-CDT1 and Tet^{ON}-CDC6/CDT1 mice were treated for 24 h with dox to compare the levels of MCM subunits in soluble vs chromatin fractions (**Fig. 40A**). First we noted that Cdc6 and Cdt1 bind to chromatin independently of each other. Cdc6 or Cdt1 overexpression did not increase endogenous Cdt1 or Cdc6 chromatin association respectively. As shown before, Cdc6 overexpression, but not Cdt1, increased MCM chromatin loading. Interestingly, simultaneous overexpression of Cdc6 and Cdt1 did not increase MCM association any further, which suggests that Cdc6 is the limiting factor in this assay (**Fig. 40B**).

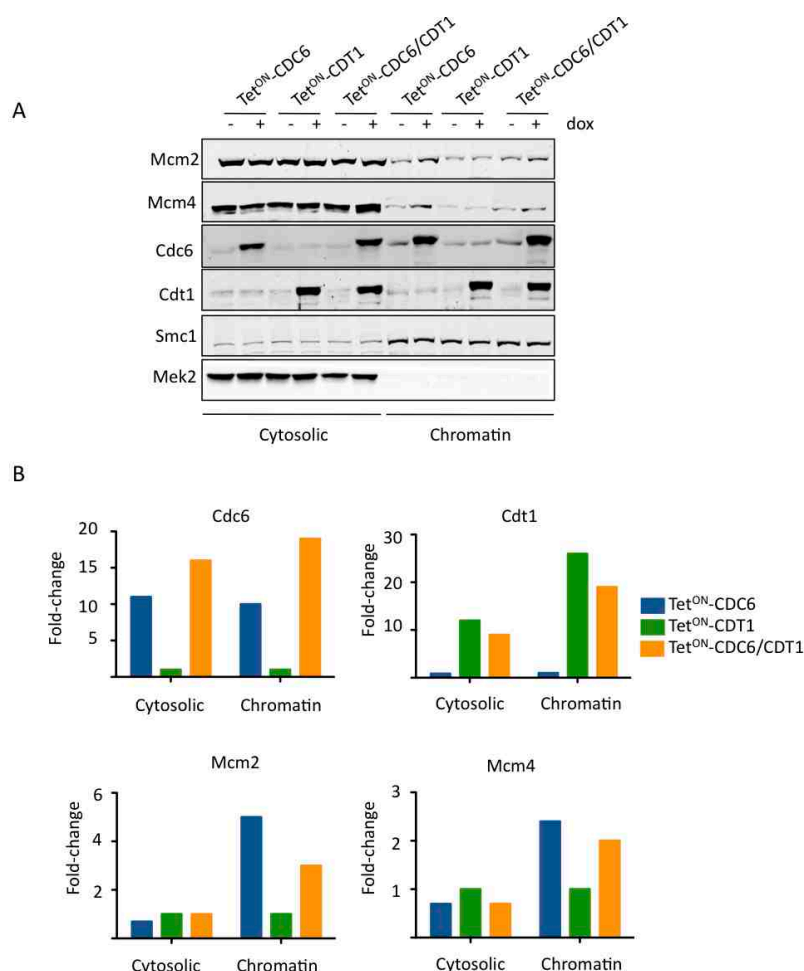


Figure 40. MCM loading upon Cdc6 and Cdt1 overexpression. **A.** Western blot for the indicated proteins after biochemical fractionation of Cdc6-, Cdt1- and Cdc6/Cdt1- overexpressing MEFs +/- dox (24 h). Total cell extracts, soluble and chromatin-bound fractions were analyzed. Mek2 and Smc1 serve as markers of cytosolic and chromatin-bound proteins, respectively. **B.** Chromatin-bound and cytosolic fractions of the indicated proteins in the different cell lines were quantified using LI-COR. Each protein was normalized to its corresponding Smc1 or Mek2 signal. Fold-change was calculated relative to its corresponding untreated control.

3.3. Cdc6 and Cdt1 overexpression leads to a slight increase in cells with >G2 DNA content

The cell cycle profiles of Tet^{ON}-CDC6/CDT1 MEFs revealed a 2-fold increase in cells with > than 2C content upon Cdc6/Cdt1 overexpression (Fig. 41A left panels). This result was clear at 24 h but at later time points (48-72 h) decreased suggesting that these cells are not viable and eliminated from the population. No differences in cells with >2C DNA content were detected upon individual overexpression of Cdc6 or Cdt1 (Fig. 41A middle and right panels). A quantification is shown in figure 41B.

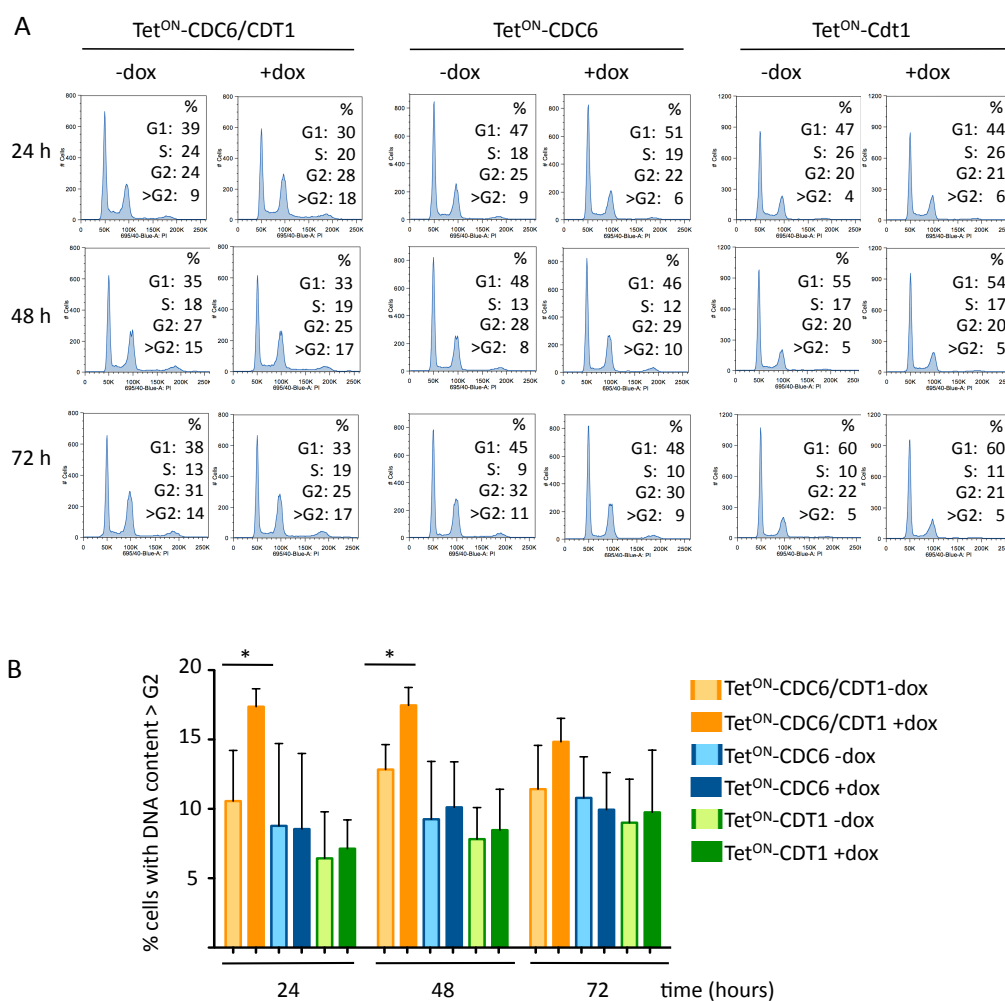


Figure 41. Cdc6/Cdt1 overexpression leads to a slight increase in the number of cells with >G2 DNA content. **A.** Cell cycle profiles obtained in Cdc6/Cdt1- (left), Cdc6- (middle) and Cdt1- (right) overexpressing MEFs treated for 24, 48 and 72 h with dox. DNA stained with PI. **B.** Quantification of >G2 cell population (n= 3 clones per cell line). Error bars represent SD. Statistically significant p-values calculated using Student t-test are indicated with asterisks (*p<0.05).

3.4. Cdc6 and Cdt1 overexpression activates the DNA-damage response

Checkpoint activation through the DDR has been previously shown to occur in cells undergoing re-replication upon geminin inactivation or Cdt1 overexpression and this checkpoint induction, is associated with the appearance of single-stranded DNA and DNA breaks (Mihaylov et al., 2002, Vaziri et al., 2003 Archambault et al., 2005; Green and Li, 2005; Melixetian et al., 2004; Zhu et al., 2004). After 24 h of Cdc6/Cdt1 overexpression, the number of cells containing RPA foci was increased by 5-fold indicating a higher presence of ssDNA stretches (**Fig. 42A**). Accordingly, virtually no control cells but up to 13% of dox-treated cells showed BrdU foci without DNA denaturation. In the presence of HU, this indicator was increased by 2-fold in Cdc6/Cdt1-overexpressing cells (**Fig. 42B**).

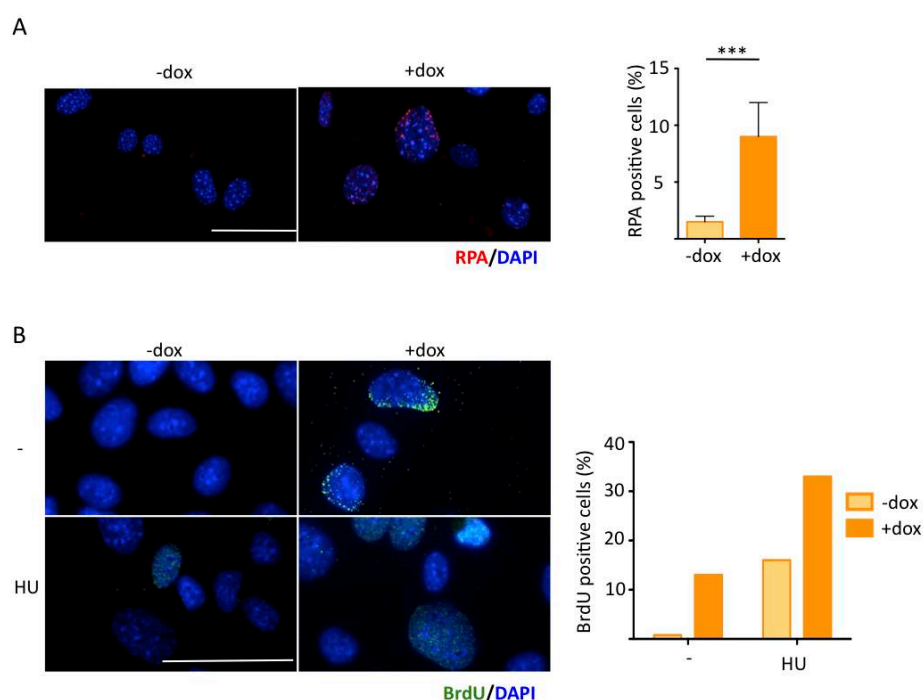


Figure 42. Cdc6/Cdt1 accumulate ssDNA. A. Left, representative images of RPA foci (red). DNA is stained with DAPI (blue). Right, quantification of cells positive for RPA foci. Cells were induced for 24 h with dox (n=5 clones; 500 cells per clone were counted). Scale bar 50 μ m. Statistically significant p-value (Fisher's test) is indicated with asterisks (***) $p < 0.001$. **B.** BrdU IF under native conditions. Cells were induced for 24 h with dox. BrdU was added to the medium for 24 h hours. 1 mM HU was added for 6 h. BrdU is shown in green. Nuclei are stained with DAPI (blue). Scale bar 50 μ m. BrdU-positive cells quantification (500 nuclei per condition were counted).

The appearance of RPA foci in close proximity to 53BP1 foci suggests that DNA replication problems likely results in DSBs (**Fig. 43A and B**). Nuclear intensity and percentage of γ H2AX positive cells were increased in Cdc6/Cdt1-overexpressing cells 24 h after dox and further increased upon HU and aphidicolin treatment (**Fig. 43C and D**). In addition, activation of the DDR was also observed by the levels of γ H2AX and phosphorylation of p53 in Serine 15 (**Fig. 43E**).

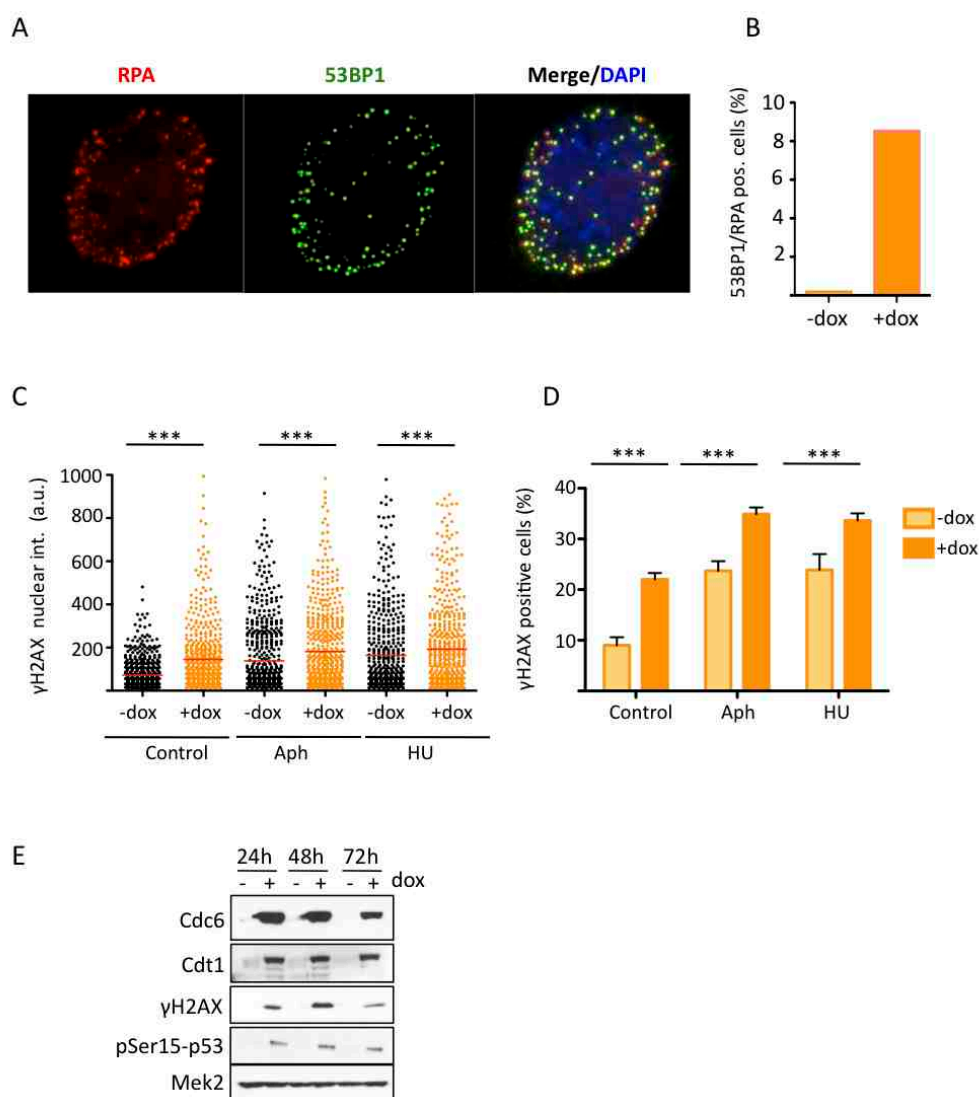


Figure 43. RPA and 53BP1 partial co-localization and DDR activation in Cdc6/Cdt1-overexpressing cells. A. Representative images of RPA (red) and 53BP1 (green) IF. DNA was stained with DAPI (blue). **B.** Quantification of positive cells for RPA and 53BP1 foci after 24 h of dox (500 nuclei per condition). **C.** HTM-mediated quantification of γ H2AX nuclear intensity in normal conditions and upon a 3 h treatment with 5 μ M aphidicolin or 0.5 mM HU. Cdc6/Cdt1 overexpression was induced 24 h before the experiment. Data are representative of results obtained with 3 different clones (600 nuclei per condition). Red bars represent average γ H2AX nuclear intensity. Statistically significant p-values calculated (Mann-Whitney test) are indicated (***= $p < 0.001$). **D.** Quantification of γ H2AX-positive cells under the same experimental conditions (n=3 clones; 600 nuclei per condition). Error bars represent SD. Statistically significant p-values (Fisher's exact test) are indicated (*** $p < 0.001$). **E.** Western blot for the indicated proteins in Cdc6/Cdt1 overexpressing-MEFs treated for 24, 48 and 72 h with dox. Mek2, loading control.

We confirmed the presence of DSB by IF simultaneous visualization of γ H2AX and 53BP1 (**Fig. 44A**). The percentage of cells with γ H2AX and 53BP1 foci increased by 3-fold after 24 h of dox and was further increased upon HU or aphidicolin treatments (**Fig. 44B**). Nevertheless, the number of breaks on metaphase spreads was similar in control and Cdc6/Cdt1 overexpressing-cells, indicating that cells with unrepaired DSB were prevented from entering mitosis by the active checkpoint (data not shown).

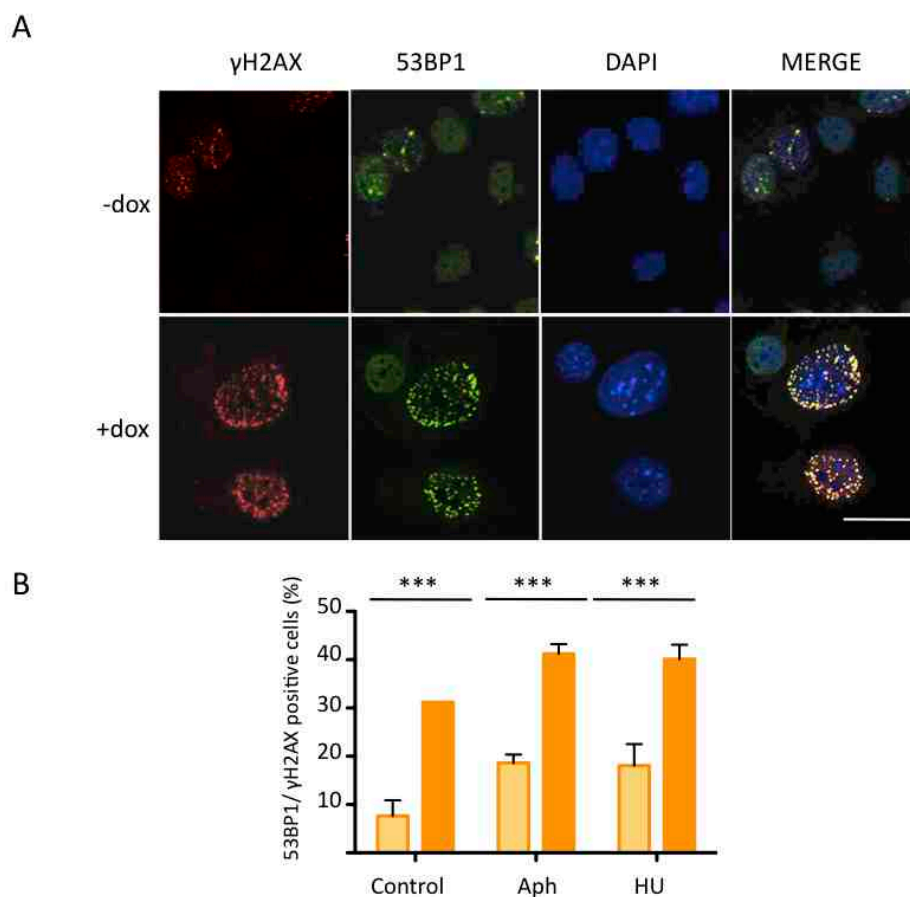


Figure 44. Cdc6/Cdt1-overexpressing cells accumulate DSB. A. Representative images of γ H2AX (red) and 53BP1 (green) IF. Nuclei are stained with DAPI (blue). **B.** Quantification of positive cells for γ H2AX and 53BP1 foci in normal conditions, 0.5 μ M aphidicolin and 0.5 mM HU for 3 h. Cells were considered positive when they presented >2 foci (n=3 clones; > 500 nuclei per clone and condition were counted). Error bars represent SD. Scale bar 25 μ m.

3.5. Cdc6 and Cdt1 overexpression promotes re-replication in primary MEFs.

When the rate of BrdU incorporation was analyzed after 24h of dox, we observed that Cdc6/Cdt1-overexpressing cells accumulated a BrdU-negative population with aberrant DNA content (between 2C and 4C) (**Fig. 45A**, left panels). This observation along with the increase in cells with >2C, suggested that a fraction of cells undergo partial re-replication. This cell population was also detected after 48 and 72 h of Cdc6/Cdt1 overexpression

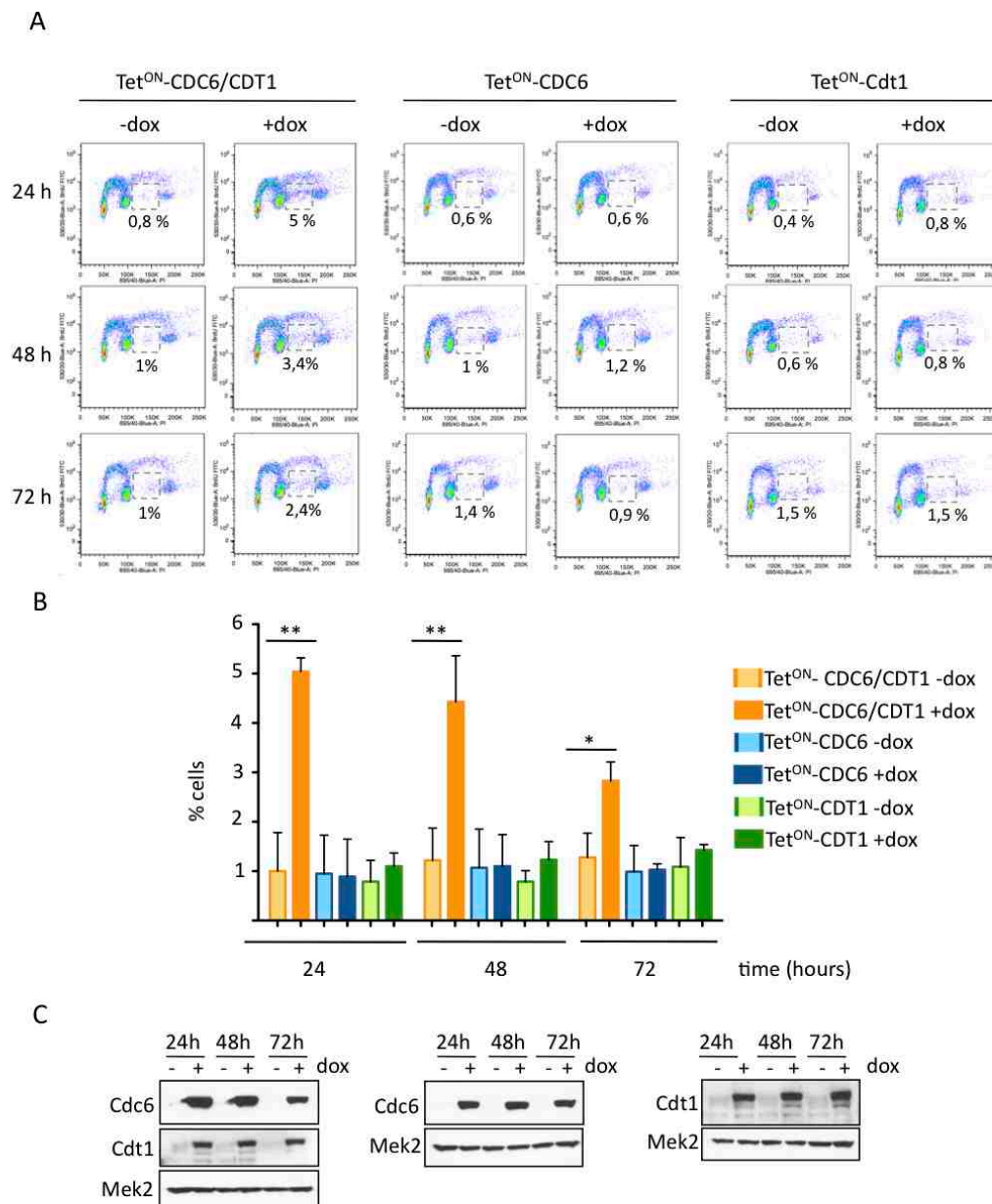


Figure 45. Cdc6/Cdt1-overexpressing cells accumulate aberrant DNA content. **A.** Cdc6/Cdt1 (left), Cdc6 (middle) and Cdt1 (right) overexpressing-MEFs were treated for 24, 48 and 72 h with dox, pulse-labeled for 30 min with BrdU and subjected to flow cytometry. Gates show a BrdU-negative population that accumulates aberrant DNA content (2C-4C). **B.** Quantification of the gated population in A for three independent experiments. Error bars represent SD (n=3 clones per cell line). Statistically significant p-values calculated using Student t-test (**p<0,002; *p<0,05). **C.** Cdc6 and Cdt1 overexpression levels throughout the timecourse. Mek2, loading control.

although it did not accumulate with time, suggesting that these cells are not viable (**Fig. 45A**, left panels). This type of analysis was repeated with three different clones per cell line and the aberrant cell population was consistently detected in Cdc6/Cdt1 overexpressing-cells (**Fig. 45B**) but not upon Cdc6 or Cdt1 individual overexpression (**Fig. 45A** middle and right panels).

The appearance of cells with > 2C DNA content was reproducible but not a very frequent event (5% in most cases). In order to confirm the presence of re-replication events by a different method, we turned to the DNA fiber-spreading assay, previously shown to be more sensitive than flow cytometry in the detection of re-replication events (Dorn et al., 2009). In this case, cells are sequentially pulse-labeled with CldU (first label, visualized in red) and IdU (second label, visualized in green). Ongoing replication forks produce tracks with the first label adjoining the second label (red-green tracks), forks that terminated or stalled during the first incubation contain only the first label (red tracks) and origins that fired during the second incubation contain only the second label (green tracks). However, if an origin that has been fired during the first labeling period were to fire again during the second one, yellow tracks (red+green) would be generated (**Fig. 46A**). Analysis of several hundreds of replication tracks revealed a 2 fold-increase in the number of yellow tracks upon Cdc6 and Cdt1 overexpression (**Fig. 46B**). Some tracks had nearly complete overlap of the red and green signals and others had flanking single-labeled regions. Presumably these differences are related to the timing of the first and second replication events. We tried to determine whether re-replication induced by Cdc6 and Cdt1 overexpression occurred at preferential genomic sites by comparative genomic hybridization (CGH). S-phase cells were sorted based on DNA content from two different Cdc6/Cdt1 clones (-/+ dox for 24 h). DNA from both populations was isolated, differentially labeled with Cy5 and Cy3 fluorophores and hybridized to an array that contained 170,000 oligonucleotides representing the mouse genome. CGH did not show statistically significant DNA gains or losses in any specific region (data not shown).

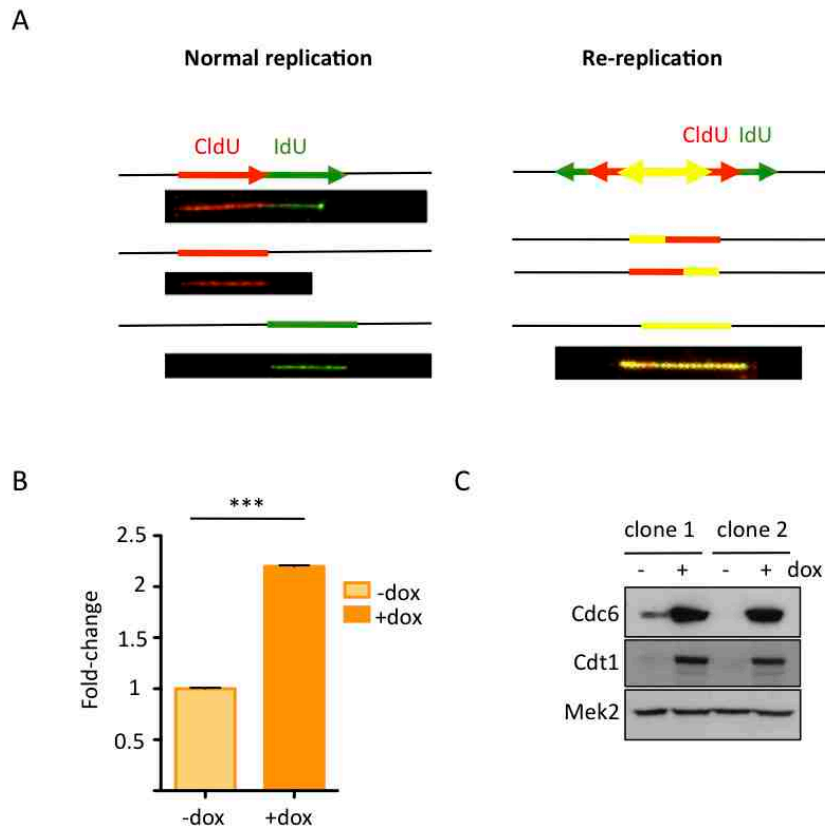


Figure 46. Cdc6 and Cdt1 overexpression increase re-replication events by DNA fiber analysis. **A.** Schematic representation of the replication structures obtained by DNA fiber spreading during normal replication (left) and if re-replication occurs during the second labeling period (right). **B.** Quantification of yellow tracks in $-/+$ dox-treated cells. Percentage of re-replicated tracks (yellow) were calculated over all the second label tracks (green). Fold-change is calculated over the untreated sample, which also present certain degree of yellow tracks ($n=2$ clones; >150 replication tracks per condition were analyzed). Error bars represent SD. Statistically significant p-value (Fisher's exact test) is indicated (***) $p<0,001$. **C.** Cdc6 and Cdt1 overexpression levels in the experiment. Mek2, loading control.

3.6. Cdc6 and Cdt1 overexpressing- cells undergo apoptosis but not senescence

It has been previously shown that re-replicating cells may undergo apoptosis (Melixetian et al., 2004; Zhu et al., 2004). On the other hand, DNA hyperreplication has been associated to persistent activation of DDR and induction of senescence (DiMicco et al., 2006). Given that cells overexpressing Cdc6 and Cdt1 re-replicate and activate the DDR we evaluated whether apoptosis and/or senescence were promoted.

Analysis of TMRE (tetramethylrhodamine ethyl ester) dye retention was used as a readout of apoptosis after Cdc6, Cdt1 and Cdc6/Cdt1 overexpression for 24, 48 and 72 h. Dead cells were also quantified by monitoring cell permeability to DAPI. Increased apoptosis was detected at all time points in Cdc6/Cdt1 overexpressing cells after dox (**Fig. 47A**, left

panels) but not in cells expressing Cdc6 or Cdt1 individually (**Fig. 47A** middle and right panels). Fold-changes in apoptotic and dead cell populations for the different cell lines are shown in **figure 47B**. On the other hand, no differences in senescence-associated β -galactosidase activity (SA- β -gal) were observed for any of the cell lines tested after 7 days of overexpression.

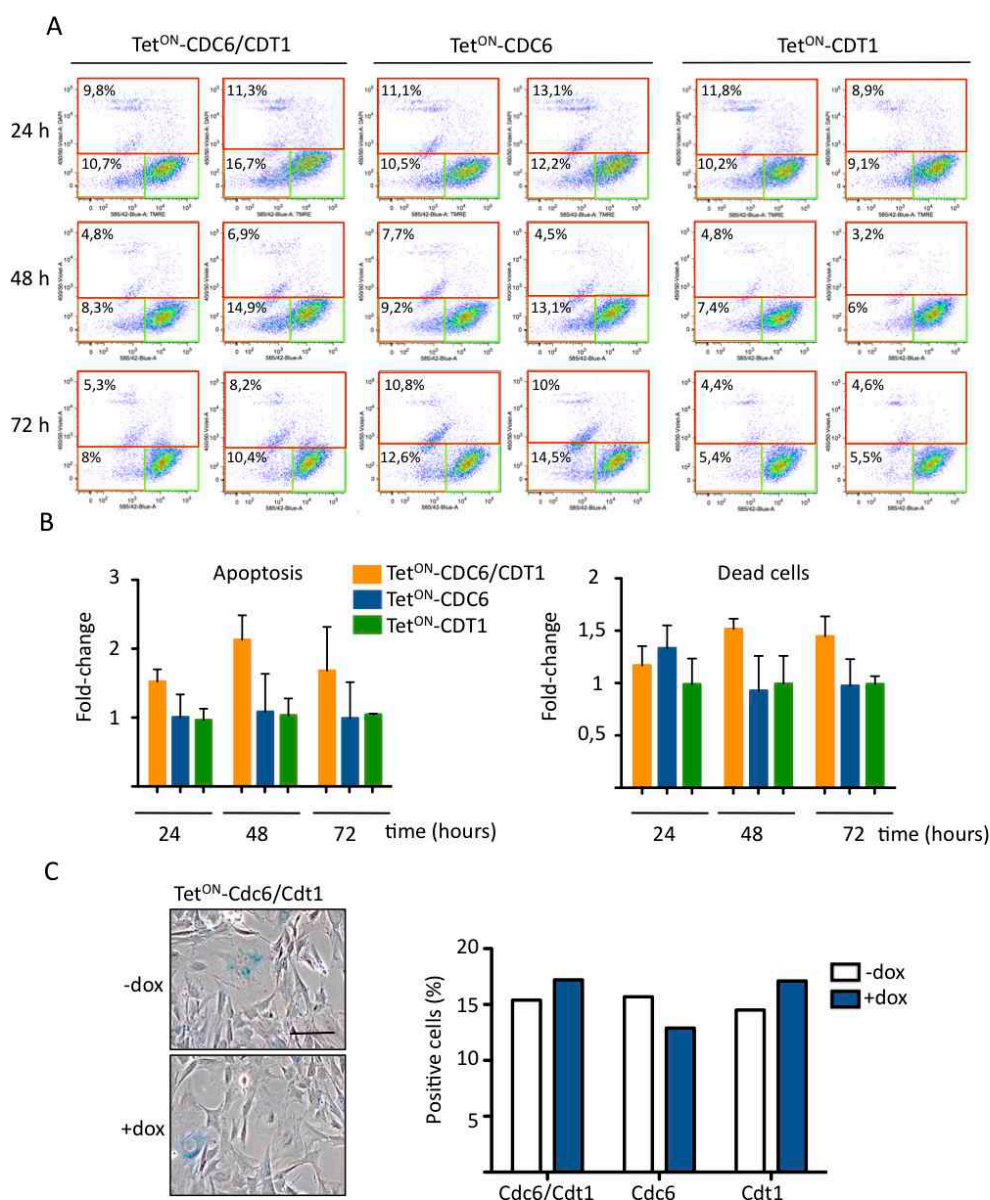


Figure 47. Increased apoptosis in Cdc6/Cdt1 overexpressing-cells. A. Flow cytometry analysis for loss of TMRE retention (bottom left gates, apoptotic cells), DAPI cell permeability (top gates, dead cells) in Cdc6/Cdt1- (left), Cdc6- (middle) and Cdt1- (right) overexpressing MEFs after 24, 48 and 72 h of dox. Green gates (bottom right) contain alive cells. **B.** Quantification of the populations gated in A for apoptotic cells (left) and dead cells (right). Three independent experiments were performed with different clones for each cell line. Error bars represent SD. **C.** Left, representative images after assaying SA- β -gal activity (blue). Right, percentage of positive cells for SA- β -gal activity in Cdc6/Cdt1, Cdc6 and Cdt1 o/e cells after 7 days of dox (300 cells per condition were quantified). Scale bar 100 μ m.

3.7. Overexpression of Cdc6 and Cdt1 is lethal in vivo

Finally, to study the effects of simultaneous Cdc6 and Cdt1 overexpression *in vivo*, dox was supplied *ad libitum* with the Tet^{ON}-CDC6/CDT1 mice diet. Interestingly, dox-treated animals displayed strong signs of morbidity between 7-15 days after the start of treatment and had to be sacrificed due to their severe weight loss (>30%) and lethargic appearance. In these mice, the levels of Cdc6 and Cdt1 overexpression were confirmed by RT-pPCR on total RNA isolated from different organs (**Fig. 48**). The organs with maximal Cdc6 and Cdt1 overexpression were the same that displayed the highest Cdc6 overexpression in Tet^{ON}-CDC6 mice (**Fig. 35**).

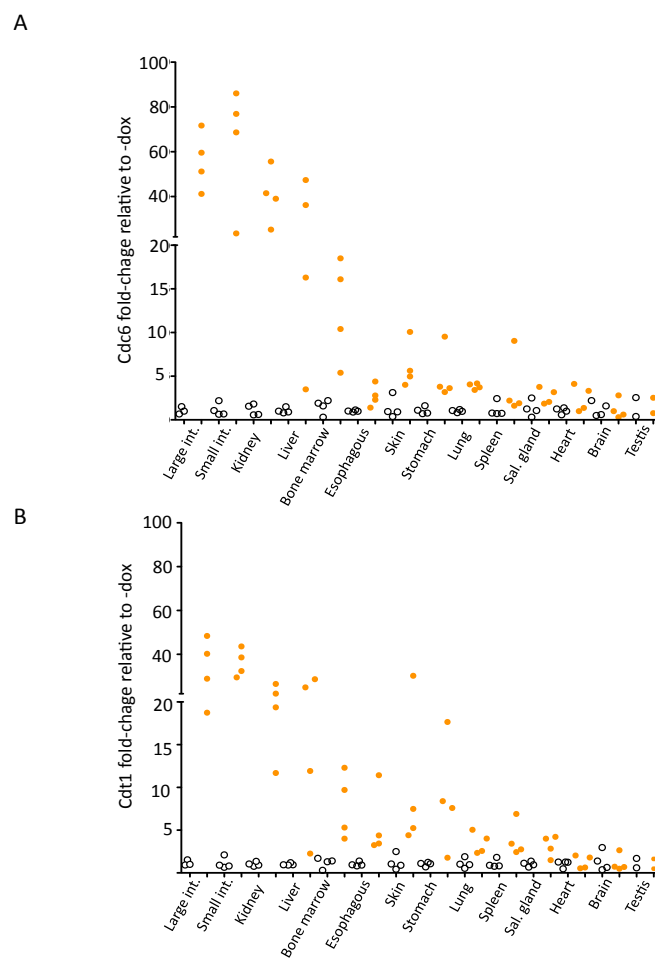


Figure 48. Cdc6 and Cdt1 overexpression levels *in vivo*. Cdc6 (A) and Cdt1 (B) overexpression levels were quantified by RT-qPCR on total RNA isolated from the indicated organs. Cdc6 and Cdt1 mRNA levels were normalized to GAPDH gene expression. Fold-change was calculated on the averaged Cdc6 and Cdt1 expression levels obtained in the untreated animals (n=4 -dox and 4 +dox animals).

Histological analyses of the different organs were carried out to address the cause of morbidity 7 days after dox. It was immediately apparent that several organs with active cell proliferation were affected by Cdc6 and Cdt1 overexpression. For instance, both small and large intestine presented structural and cytological abnormalities with loss of the characteristic parallel arrangement of crypts, irregular lumens, increased cellularity and a marked stromal inflammatory component (**Fig. 49 A and B**). Increased mitotic activity and apoptosis were also observed. Some regions of the intestine presented ulcers due to a complete loss of the intestinal epithelium. These tissue abnormalities impair nutrient absorption, explaining the weight loss and morbidity of dox-treated animals.

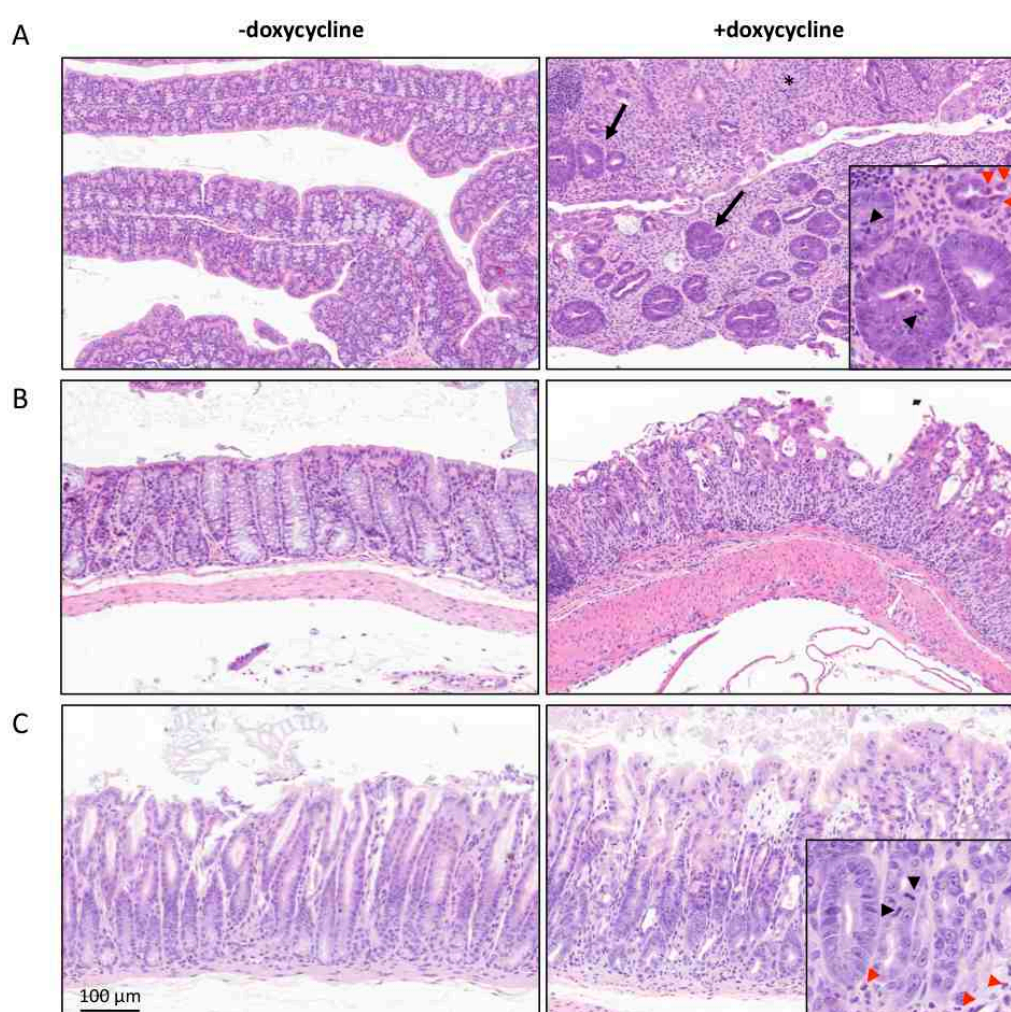


Figure 49. The gastrointestinal tract of dox-treated animals is severely affected by Cdc6 and Cdt1 overexpression. **A.** H-E-stained tissue sections of ileum (small intestine) for control (left) and dox-treated animals (right). Cdc6/Cdt1-overexpressing animals lose intestinal crypts, develop ulcers, present inflammation (asterisks) and crypts with irregular lumens and increased cellularity (arrows). Increased mitotic activity (black arrowheads) and apoptosis (red arrowheads) are also observed (inset). A similar phenotype is found in the colon of Cdc6/Cdt1- overexpressing mice (**B**). **C.** The stomach of dox-treated animals showed dysplasia and increased mitosis (black arrowheads and apoptotic activity (red arrowheads)(insets).

In the stomach, the glandular portion showed dysplasia, increased apoptosis and mitotic activity (**Fig. 49C**). Other tissues such as skin and thymus became atrophic. The skin suffered loss of the subcutaneous adipose layer, thinner epidermis and almost complete loss of sebaceous glands compared to untreated animals (**Fig. 50A**). Thymic atrophy was mostly observed in the medullar region (**Fig. 50B**).

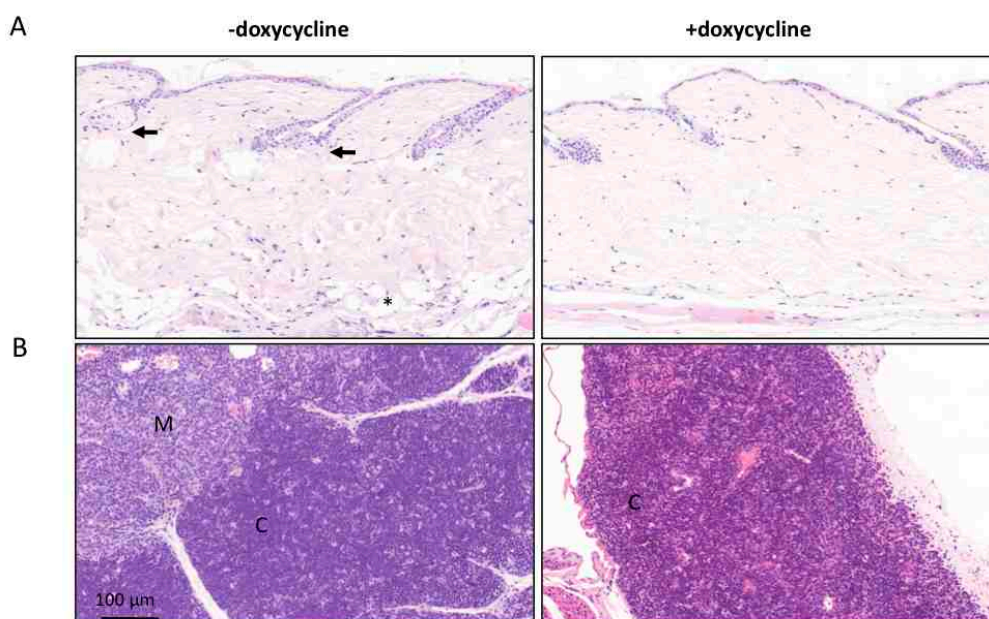


Figure 50. Skin and thymus become atrophic upon Cdc6 and Cdt1 overexpression. **A.** H-E-stained tissue sections of back skin for control (left) and dox-treated animals (right). Epidermis of Cdc6/Cdt1-overexpressing animals is thinner, with almost complete loss of sebaceous glands (indicated with arrows) and subcutaneous fat (indicated with asterisks). **B.** Thymus become atrophic. Upon Cdc6/Cdt1 overexpression the medullar region of the thymus (M) is lost and only cortical thymus remains (C).

Despite the important cytoarchitectural abnormalities in the gastrointestinal tract of dox-treated animals, cells continued to proliferate, as shown by Ki-67 marker. One exception could be the skin, which became atrophic upon dox treatment and presented less Ki-67-positive cells (**Fig. 51**).

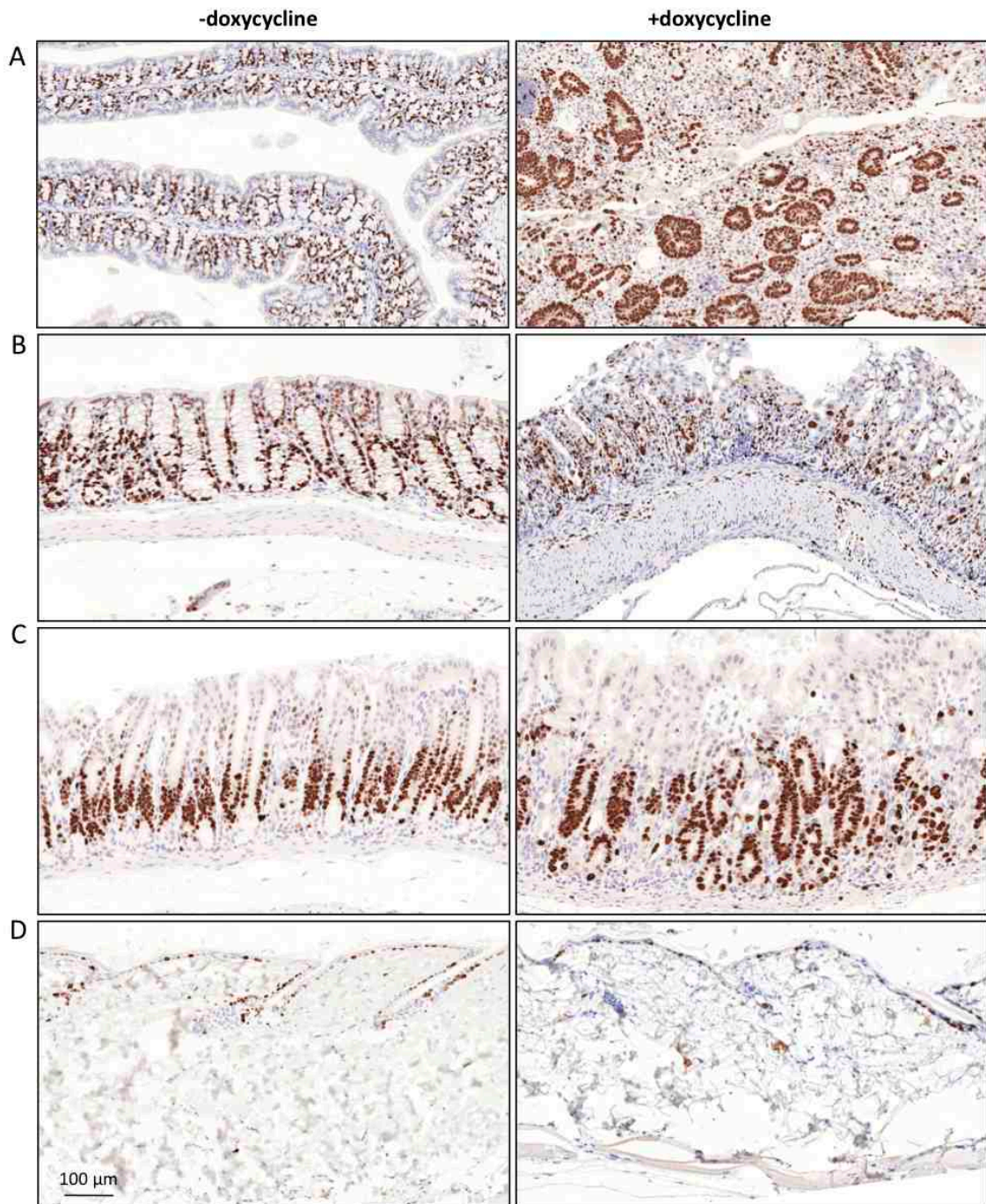


Figure 51. Proliferation in *Cdc6/Cdt1*-overexpressing animals. Ki-67 IHC in tissue sections of ileum (A), colon (B), glandular stomach (C) and skin (D). Tissues of dox-treated animals were proliferating despite the severe cytoarchitectural abnormalities (A to C). D. The skin presented less Ki-67-positive cells.

We also found a striking increase in the number of γ H2AX positive cells in the gastrointestinal tract as well as in the epidermis (**Fig. 52**). Taking into account that in primary tissue culture cells Cdc6 and Cdt1 overexpression led to partial DNA re-replication, activation of the DDR and apoptosis, these phenotypes strongly suggest that these events are also occurring *in vivo* and are sufficient to cause morbidity, due to the loss of correct tissue homeostasis.

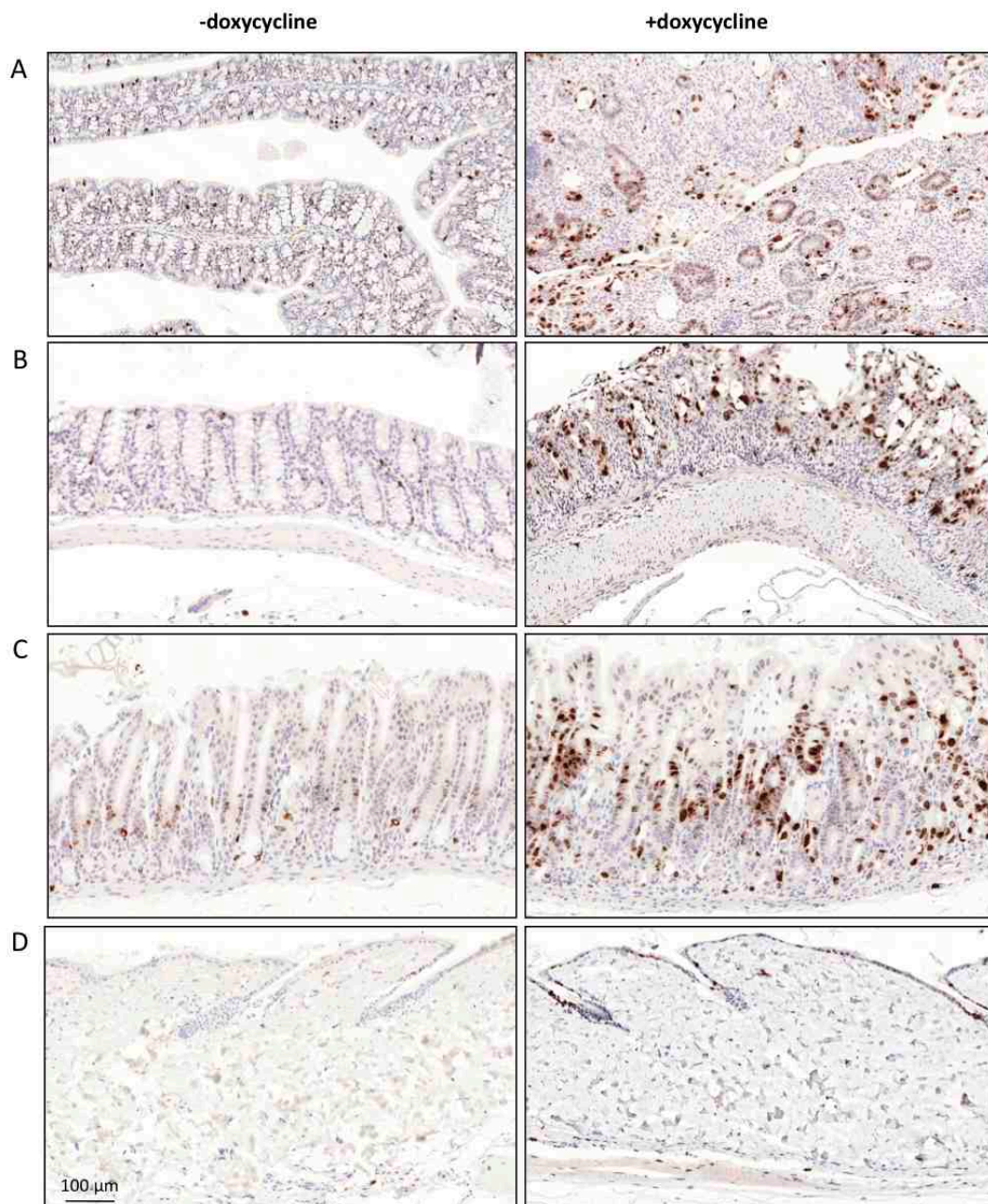


Figure 52. Doxycycline-treated animals accumulate DNA-damage. γ H2AX IHC in tissue sections of ileum (A), colon (B), glandular stomach (C) and back skin (D). Dox-treated animals (left) showed in all cases increased DNA damage compared to control animals.

DISCUSSION

1. Cdc6 increases MCM loading efficiency

We have demonstrated *in vitro* with MEFs and, more importantly, *in vivo* with skin-isolated keratinocytes, that Cdc6 protein levels are rate-limiting for MCM loading onto chromatin. In both cases, an increase in Cdc6 was sufficient to enhance the efficiency of MCM association with chromatin. However, there is a likely limit in the amount of MCM that can be engaged with DNA. When the K5-CDC6^{tg} allele was introduced into a K5-Cre/lox*Cdh1* genetic background, Cdc6 protein levels were markedly increased due to abrogation of the APC/C-Cdh1-mediated Cdc6 proteolysis (Petersen et al., 2000; Mailand and Diffley, 2005; García-Higuera et al., 2008). Nevertheless, no further MCM enrichment on chromatin was observed, suggesting that Cdc6 overexpression levels in the K5-CDC6^{tg} strain already promote maximal MCM chromatin association.

In line with our findings, it was previously shown that Cdc6 expression by adenoviral infection in rat quiescent cells is sufficient to induce MCM chromatin association, but not sufficient to induce initiation of DNA replication (Cook et al., 2002). We performed a similar experiment in MEFs, but overexpressed Cdc6 was efficiently degraded upon serum deprivation most likely by APC/C-Cdh1-mediated proteolysis (Petersen et al., 2000; Mailand and Diffley, 2005). In a cell-free system, where 3T3 nuclei were released from quiescence, overexpression of Cdc6 in G1 nuclei induced premature entry into S-phase (Stoeber et al., 1998). In our own G0 to S experiments, Cdc6 overexpression only started to be detectable 15 h after release from serum-deprivation release, when cells were entering S-phase. Both control and Cdc6-overexpressing cells entered S-phase with similar kinetics.

We also have shown that Cdt1 overexpression did not increase MCM loading in the Tet^{ON} system, and combined Cdc6 and Cdt1 overexpression does not promote a cooperative increase compared to Cdc6 overexpression alone. From these experiments we conclude that, rather than Cdt1, Cdc6 protein levels are limiting for MCM initial chromatin association.

The biochemical roles of Cdc6 and Cdt1 in the licensing process are very different. Cdt1 forms a heptameric complex with MCM2-7 (Tanaka and Diffley, 2002; Kawasaki et al., 2006; Remus et al., 2009) that is only recruited when ORC and Cdc6 are already bound to

replication origins (Speck et al., 2005; Randell et al., 2006; Frijola et al., 2013; Fernández-Cid et al., 2013). Cdc6 is an ATPase that functions coordinately with ORC to engage the MCM complex with the DNA, and Cdt1 likely facilitates the opening and closing of the MCM hexameric ring structure (Randell et al., 2006). Consistent with a 'loading machine' analogy, multiple MCM2-7 hexamers are loaded at each origin (Edwards et al., 2002; Bowers et al., 2004;). It has been shown that after being topologically engaged with the DNA, MCM complexes can slide along dsDNA possibly facilitating the loading of additional hexamers (Remus et al., 2009).

Different possibilities might be envisioned to understand how Cdc6 overexpression increases the efficiency of MCM chromatin association and promotes increased origin activity. First, it is possible that increased Cdc6 levels enhance the ATPase activity of ORC-Cdc6 leading to a faster MCM recruitment, and thus increased density of MCM complexes on chromatin during the licensing period. In support for this notion, an *orc5-1* yeast strain displays initiation defects that can be partially rescued by Cdc6 in a dose-dependent manner (Liang et al., 1995). Another possibility is that increased Cdc6 protein levels may facilitate the licensing of origins that would not be licensed in normal conditions because not all ORC would have access to Cdc6 (**Fig. 53**). To figure out whether Cdc6-overexpressing cells license a higher number of replication origins, a genome-wide analysis of MCM binding sites would be required. Unfortunately, the determination of binding sites for MCM and other pre-RC members in mammalian cells has been extremely difficult and it is possible that pre-RCs are not highly enriched at the same sites in all cells in a population (reviewed by Gilbert, 2010). Alternatively (although not exclusive), MCM loading might be taking place out of schedule. In fact, a Cdc6 yeast mutant has been described that can promote promiscuous MCM chromatin association throughout the cell cycle (Liang and Stillman, 1997). In our study, increased MCM-enrichment was observed in G1 and G2/M upon Cdc6 overexpression but not in the S-phase fraction. The increased MCM chromatin association in G2/M cells could be due to the mitotic cells, since the process of licensing starts in telophase (Méndez and Stillman, 2000).

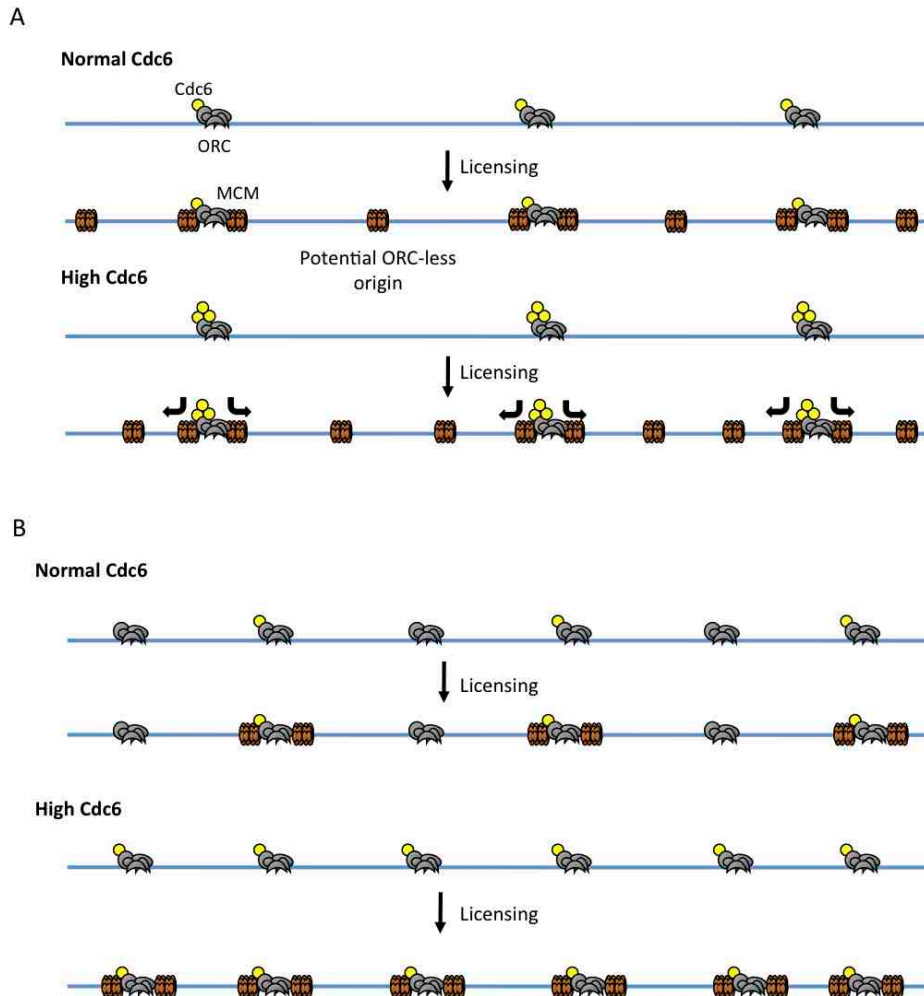


Figure 53. Effect of Cdc6 overexpression at replication origins. **A.** High protein levels of Cdc6 might enhance the efficiency of ORC-CDC6 ‘loading machine’, thus more MCM complexes would be assembled from a given ORC-CDC6 complex in the repetitive loading reaction. **B.** ORC complexes might have a limited access to Cdc6 and only those that are Cdc6-bound, would load the MCM complex in coordination with Cdt1. In the presence of higher Cdc6 protein levels, more ORCs would become functionally active, and thus more potential origins would be assembled.

2. Cdc6 overexpression increases origin firing efficiency

The increase in MCM-chromatin association led us to consider that Cdc6-overexpressing cells might have an increased number of functional replication origins. It has been established that many more MCM complexes are loaded during licensing than activated in a normal S-phase (reviewed by Hyrien et al., 2003). This ‘excess’ of MCM complexes becomes essential for genome stability through back-up origin activation in situations of stress (Woodward et al., 2006; Ge et al., 2007; Ibarra et al., 2008; reviewed by Blow et al., 2011). We first hypothesized that Cdc6 overexpressing-cells might have an

increased pool of back-up origins, and therefore, enhanced resistance to replicative stress. In addition, the delayed ageing skin phenotype found in K5-CDC6^{tg} mice could be related to this, as replicative stress is linked to ageing (Ruzankina et al., 2007; Murga et al., 2009; reviewed by Ruzankina and Brown, 2008; Sperka et al., 2012).

Using DNA fiber spreading, we found that Cdc6-overexpressing cells fired more origins even in normal growth conditions. It was possible that Cdc6 overexpression somehow induced replicative stress, which in turn could be responsible for the activation of back-up origins in the absence of aphidicolin. Nevertheless, no markers of DNA damage (γ H2AX or RPA-foci) were found. A short aphidicolin treatment, which induced a 3-fold increase in origin activation in control cells, only induced a 1.4-fold increase in origin density in Cdc6 overexpressing cells, suggesting a reduced activation of back-up origins. One possible interpretation would be that Cdc6 overexpressing cells could be somehow resistant to agents that induce replicative stress, reducing the need for back-up origin activation. However, upon aphidicolin treatment, the DNA damage response was not attenuated, as indicated by the presence of γ H2AX or RPA-foci in HU-treated cells, suggesting that these cells are equally susceptible to replication stress. After 48 h of Cdc6 overexpression, origin density in Cdc6 overexpressing cells was slightly higher and in this case, aphidicolin treatment did not induce any further origin activation. These results suggest that 48 h of Cdc6 overexpression leads to saturating levels of origin activity that cannot increase upon aphidicolin addition.

It has been shown that increased initiation events induced by Chk1 inhibition may promote DNA breakage and activate the ATR-dependent DNA damage response (Syljuasen et al., 2005; Maya-Mendoza et al., 2007). In this view, increased origin firing could be detrimental. Nevertheless Cdc6-overexpressing cells did not activate the DNA damage response, suggesting that a compensatory mechanism alleviates the effects of increased origin activity. In this regard, replication fork rate was reduced in parallel to the increase in origin density. Origin density and fork rate have been shown to be mutually dependent. On one hand, fork elongation inhibitors such as aphidicolin or HU promote increased origin firing (Anglana et al., 2003; Ge et al., 2007; Courbet et al., 2008; Ibarra et al., 2008) and on the other hand, increased origin firing (e.g. by Chk1 inhibition) slows down fork progression rate (Petermann et al., 2006). Upon Chk1 downregulation, interfering with origin activation by means of CDK2 or Cdc7 abrogation restores normal fork progression rate (Petermann et

al., 2010). Similar results have been recently reported in yeast, where a *ts* mutant strains of Cdc7 or ORC1 with reduced origin firing, display increased fork progression rates (Zhong et al., 2013). One proposed explanation for reduced fork rates upon higher origin density is the availability of limiting replication factors. In this regard, dNTP pools have been shown to be limiting for fork progression because upregulation of ribonucleotide reductase (RNR) activity increases elongation rates (Poli et al., 2012). It will be interesting to test if the slower fork progression rate in Cdc6-overexpressing cells could be corrected by an external dNTP supply. Slower fork progression in Cdc6-overexpressing cells may explain why despite of having a higher number of active origins these cells do not progress faster in S-phase.

Long treatments (> than 6 h) with HU or aphidicolin have been shown to generate DSBs (Saintigny et al., 2001; Hanada et al., 2007). In our study, Cdc6 overexpression did not lead to statistically significant differences in chromatid breaks or HR-mediated DNA damage repair neither under normal growth conditions nor in the presence of aphidicolin or CPT. Cell proliferation was not affected either upon Cdc6 overexpression when Tet^{On}-CDC6 MEFs were challenged with UV-light, MMS or NCS.

3. Cdc6 and origin selection

Replication origins are organized in clusters that give raise to large replication domains, which are activated at different times throughout S-phase following a spatio-temporal program (reviewed by Gilbert 2010). Only a subset of replication origins are used in each cluster and flexibility in the choice of origins is a general feature of both yeast and metazoan replication (reviewed in Méchali et al., 2013). It has been estimated that a replicon is composed of 4-5 potential origins of which only one fires during the S-phase (Cayrou et al., 2011), and the rest remains dormant and may be activated under situations of replicative stress (reviewed by Blow et al., 2011). The mechanism for regulating dormant origins is unclear. A computational simulation has suggested that activation of origins may be stochastic (Blow and Ge, 2009). Most licensed origins are passively replicated by oncoming forks before they have time to initiate. A reduction in fork elongation rate would increase the length of time before inactivation of dormant origins, increasing their probability of firing (Blow and Ge, 2009). Nevertheless, inhibition of ATR, Chk1 and overexpression of Cdc6 in our case, increases origin density even in the absence of stress

(Maya-Mendoza et al., 2005; Petermann et al., 2006; Karnani and Dutta, 2011), which indicates that origin activity is also influenced by specific regulatory mechanisms.

The fact that Cdc6 overexpression induced increased origin firing could indicate that Cdc6 protein is somehow involved in the selection of origins for activation. In human cells Cdc6 is degraded after licensing by APC/C-mediated proteolytic degradation (Petersen et al., 2000; Mailand and Diffley, 2005) although it rapidly re-accumulates and progressively binds to chromatin from S-phase to G2/M (Méndez and Stillman, 2000; Petersen et al., 2000). It has been proposed that Cdc6 coordinates S-phase completion with mitosis (Lau et al., 2006). Interestingly, when origin activity was monitored in S-phase HeLa cells depleted from Cdc6, impaired late origin activation was found (Lau et al., 2006). Interestingly, a direct role for Cdc6 as a chromatin anchor for the cyclin E-CDK2 complex has been proposed in *X.laevis* egg extracts, and this interaction was required for efficient DNA replication (Furstenenthal et al., 2001). These studies, along with our own data suggest that Cdc6 might facilitate DNA replication initiation by promoting the recruitment of replication factors required for efficient origin firing (**Fig. 54**).

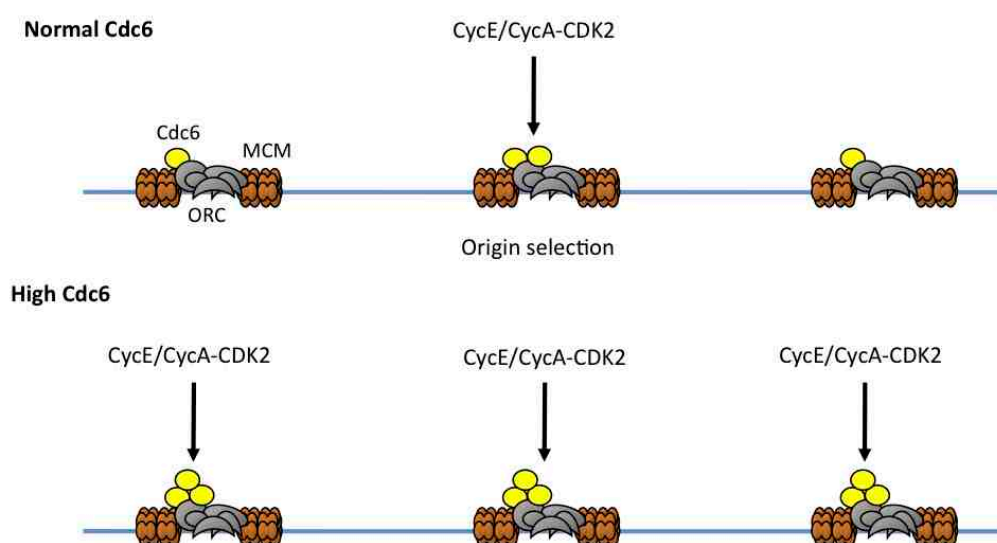


Figure 54. Cdc6 and origin selection. Cdc6 might promote origin activation by serving as a platform for the recruitment of CycE/A-CDK2 (Furstenenthal et al., 2001). Hence, increased Cdc6 levels could recruit the activating kinases to a larger number of origins.

To date, no molecular signature has been reported to define which origins are selected for activation and which are left dormant. We propose that the amount of MCM proteins loaded at each origin could be one of the factors that determine firing probability by promoting the recruitment of origin-activating factors such as GINS or Cdc45 (Aparicio et

al., 2012). In budding yeast, overexpression of replication factors Sld3, Sld7 and Cdc45 leads to genome-wide changes in origin usage (Tanaka et al., 2011). In addition, in fission yeast, the timing of ORC binding in mitosis and pre-RC assembly in G1 correlates with the timing of firing during S and the recruitment of Cdc45. Increasing the length of mitosis leads to a more uniform ORC distribution between early (efficient) and late (inefficient) origins and changes the dynamics of origin firing (Wu and Nurse, 2009). In this view, increasing the amount of MCM on chromatin by Cdc6 overexpression might lead to certain origins with high amount of MCM complexes that would more efficiently recruit other factors needed for origin firing (Fig. 55).

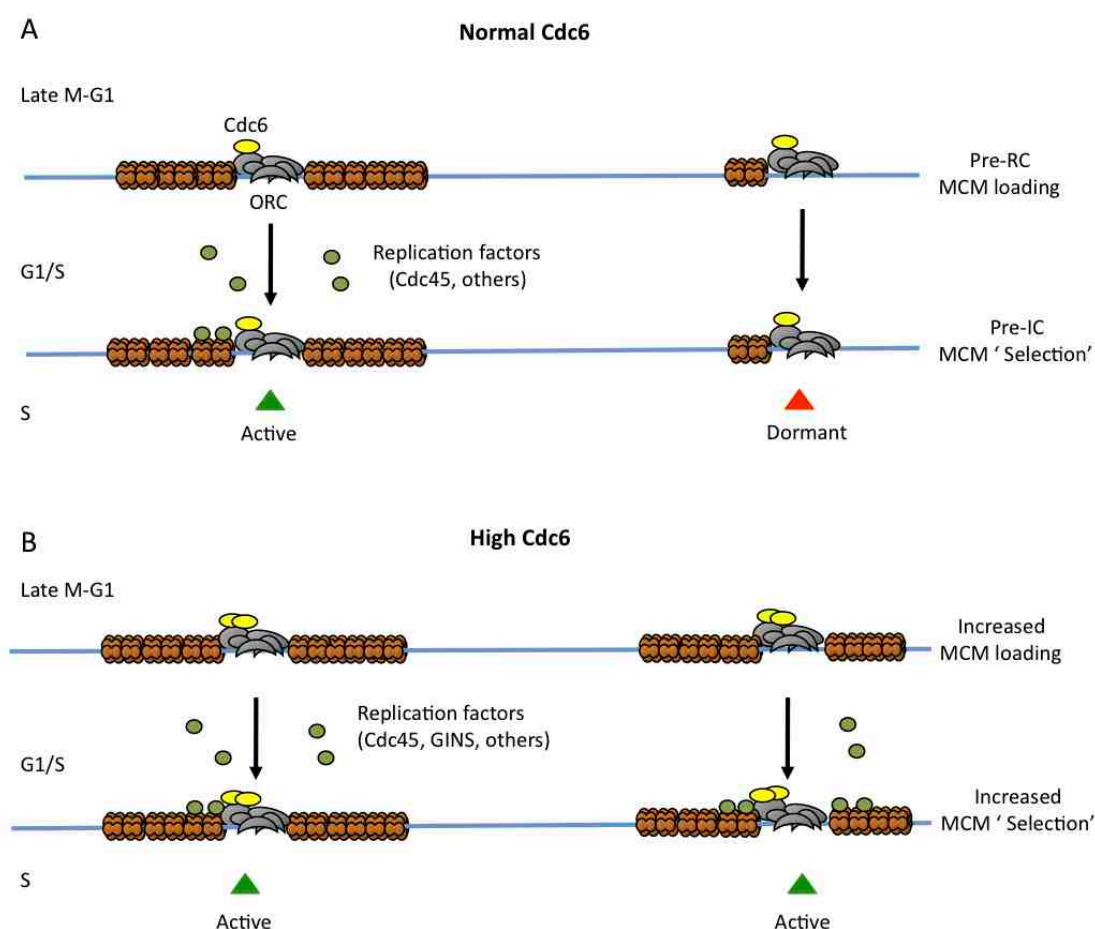


Figure 55. Origin selection and MCM concentration: a model. **A.** Origin selection might result from differential accumulation of MCM complexes on chromatin (Aparicio et. al., 2012). In normal conditions, origins that accumulated more MCM hexamers could recruit activating factors more efficiently, while those with less MCM content might remain dormant. **B.** Upon Cdc6 overexpression, the differential accumulation of MCM complexes at different origins might be attenuated, increasing the firing probability of normally dormant origins.

4. Cdc6 overexpression *in vivo*

We have also studied for the first time the effects of Cdc6 overexpression *in vivo*. We have shown that high levels of Cdc6 lead to increased MCM content in tissues from both K5-CDC6^{tg} and Tet^{ON}-CDC6 mice. In the latter, only the most proliferative tissues displayed increased MCM chromatin content, indicating that MCM recruitment depends on cell proliferation associated to tissue turnover. In spite of the accumulation of CDC6 mRNA in relatively quiescent organs such as liver or kidney, Cdc6 protein is likely targeted for proteolytic degradation by the APC/C complex in quiescent cells (Petersen et al., 2000; Mailand and Diffley, 2005). In fact, HA-Cdc6 was barely detectable by IHC in these tissues (data not shown).

Cdc6 overexpression seems to have different effects depending on the specific tisular context. In general, cell proliferation was not affected in Cdc6 overexpressing tissues. However, Cdc6 overexpression was not innocuous in the long term. First, we observed that Tet^{ON}-CDC6 mice, in which Cdc6 overexpression is induced in most of the tissues, showed increased frequency of hematological neoplasias (histiocytic sarcomas and B-cell lymphomas). Interestingly, Cdc6 has been found to be overexpressed in human mantle cell lymphomas, which is a subtype of B-cell lymphomas (Pinyol et al., 2006). B-lymphocytes may be particularly sensitive to slight alterations in DNA replication because of the specialized processed taking place at the germinal centers during antibody production (class switch recombination, somatic hypermutation) (reviewed by Vitoria and Nussenzweig, 2012).

In contrast to Tet^{ON}-CDC6 mice, the lifespan of K5-CDC6^{tg} animals was similar to wt animals, even in a p53-null background, suggesting that any possible Cdc6 oncogenic activity in the K5-expressing tissues is not restrained by p53 activity. K5-CDC6^{tg} mice showed signs of delayed ageing, as old transgenic animals retained a younger aspect of the hair shaft in terms of density and graying. In collaboration with Cédric Blanpain's lab, it was found that transgenic animals had a slower hair growth cycle, suggesting that they might undergo less hair cycles throughout their lifespan, resulting in better fitness of the hair follicle stem cell compartment. Consistent with delayed ageing of the epidermis, p16 and p19 mRNA levels were decreased in old K5-CDC6^{tg} animals. It has been reported that Cdc6 overexpression promote the transcriptional repression of the *INK4/ARF* locus (Gonzalez et al., 2006), which encode these aging molecular markers. Unfortunately, this effect could not be tested in young mice because the mRNA levels of p16 and p19 are very low and were undetectable by

RT-qPCR. Nevertheless, the repression of p16 and p19 in older mice is not mediated solely through the transcriptional repression of the *INK4/ARF* locus, because old K5-CDC6^{tg} animals that showed an intermediate ageing phenotype showed normal mRNA levels of p16 and p19 despite similar Cdc6 overexpression levels as those detected in the K5-CDC6^{tg} 'fit group'. Further experiments will be needed to characterize this skin-specific anti-ageing phenotype in K5-CDC6^{tg} animals. Ideally, epidermal stem cells should be isolated from old animals to analyze *in vitro* their proliferation potential.

Transcriptional repression of the E-Cadherin locus has been reported after Cdc6 overexpression (Sideridou et al., 2011). In our study, keratinocytes isolated from K5-CDC6^{tg} mice had normal E-Cadherin protein levels by western blot (data not shown). This is in agreement with the fact that no skin architectural distortion has been detected in K5-CDC6^{tg} mice. It should be noted that Sideridou and coworkers found the transcriptional repression of E-Cadherin in a murine cell line derived from a papilloma while we have checked E-Cadherin levels in primary keratinocytes. Interestingly, the authors found a cryptic origin of replication upstream of the E-Cadherin locus that only is activated upon Cdc6 overexpression. This observation further suggests that Cdc6 overexpression influences origin selection.

Cdc6 over-expression has been shown to activate the DDR and promote senescence in tissue culture cells (Bartkova et al., 2006). However, neither keratinocytes in the skin of K5-CDC6^{tg} mice nor Tet^{ON}-CDC6 MEFs show signs of activated DDR, and in the latter case, no sign of senescence was detected after 7 days of Cdc6 overexpression. Actually, Cdc6 overexpression (and higher MCM protein content) seems to cooperate with oncogenic *Ras* *in vivo*, at least in epithelial cells. K5-CDC6^{tg} mice developed more skin papillomas upon DMBA-TPA treatment, which induces a specific *H-Ras* mutation in 90% of the cases (Quintanilla et al., 1986). Increased Cdc6 might confer an initial proliferative advantage that favors clonal outgrowth of *H-Ras* mutated cells, which will form papillomas. Of note, a mouse model that overexpressed MCM7 in the epidermis has been reported to develop more papillomas upon DMBA-TPA treatment than wt counterparts (Honeycutt et al., 2006). No progression towards squamous cell carcinomas (SCC) was observed even in wt mice, but it should also be noted that the C57B/6 background is particularly resistant to transformation from papillomas to SCC skin carcinogenesis protocol (Woodworth et al., 2004).

5. Cdc6 and Cdt1 overexpression induces partial re-replication in primary MEFs

Previous studies have shown that overexpression of Cdt1 or downregulation of Geminin during S-phase and G2 are sufficient to promote re-replication in tumoral and primary tissue culture cells although the extent of re-replication is variable (Vaziri et al., 2003; Melexetian et al., 2004; Zhou et al., 2004; Liu et al., 2007; Klotz-Noack et al., 2012). Substantial re-replication in primary cells after geminin downregulation is only detected by DNA content upon abrogation of the ATR-mediated S-phase checkpoint (Liu et al., 2007). In contrast, here we show that a fraction of the primary MEFs overexpressing Cdc6 and Cdt1 accumulate with >2C DNA, compatible with partial DNA re-replication as soon as 24 h after dox. An increase of this aberrant cell population was not observed upon overexpression of Cdc6 or Cdt1 alone. Interestingly, this effect did not require abrogation of the DDR. The proportion of aberrant cells decreased in latter time points and we believe that this is due to apoptosis activation, but also due to a higher cell confluency, as total BrdU incorporating-cells also decrease with time.

We tried to address whether DNA re-replication occurs at specific genomic locations by detecting copy number variations in S-phase-sorted cells by CGH analysis. No differences in copy number were found between control and Cdc6/Cdt1-overexpressing cells possibly because the small proportion of cells that accumulate significant amounts of re-replicated DNA. In any case, the existence of re-replication events was confirmed by single molecule DNA fiber analysis. This technique has been shown to detect re-replication as soon as after 1h of release into S-phase in HeLa cells overexpressing Cdt1 and in untransformed human fibroblasts depleted from geminin, in which re-replication is undetectable by DNA content but cell cycle checkpoints are activated (Dorn et al., 2009). Events of re-replication occurring early in S-phase would never be detected by DNA flow cytometry because cells would still have a DNA content less than 4C. Apart from detecting re-replicating tracks in Cdc6/Cdt1-overexpressing-cells, a small but quantifiable number of re-replicated tracks was also observed in control cells. The reasons for this re-replication background are not clear, but they may reflect a biological effect rather than an artifact. In fact, the observed accumulation of nascent strands at certain replication origins is suggestive of re-replication events (Gómez and Antequera, 2008). It is possible that individual Cdc6 or Cdt1 overexpression could induce a low level of re-replication, and we are currently exploring this possibility. Future studies with individual Cdc6 and Cdt1 overexpression may address the

influence of re-replication on genomic stability. It has been shown that low levels of re-replication, which do not induce the DDR and cell death, may induce tandem gene amplifications in yeast and a possible mechanism for the gene amplification frequently seen in cancer (Green et al., 2010; Finn and Li, 2013).

6. Re-replication in Cdc6/Cdt1-overexpressing cells induces activation of the DDR

It has been shown that even in the absence of extensive re-replication, primary cells overexpressing Cdt1 or depleted from geminin activate the DDR (Liu et al., 2007; Tatsumi et al., 2006). In our study, Cdc6/Cdt1-overexpressing cells accumulate markers of activated DDR as soon as 24 h after dox induction, likely induced by DSB and ssDNA accumulation (Melixetian et al., 2004; Zhou et al., 2004; Archambault et al., 2005; Green and Li, 2005; Davison et al., 2006; Liu et al., 2007). Indeed, higher amounts of ssDNA as measured by RPA-foci accumulation and BrdU detection under native conditions were found in Cdc6/Cdt1-overexpressing cells. In addition DSB frequency was increased and the physical proximity of 53BP1 and RPA foci, suggested that DSB are caused by collapsed replication forks during the process of re-replication. This is in agreement with a previous study carried out in *X. laevis* egg extracts, in which a head-to-tail fork collision model was proposed to explain the generation of DSBs upon DNA re-replication (Davison et al., 2006). This model suggests that forks 'chase' one another leading to fork collision and DNA fragmentation. The possible mechanisms leading to generation of DNA lesions upon re-replication are depicted in **figure 56**. We propose that simultaneous overexpression of Cdc6 and Cdt1 induces re-licensing of fired origins, increasing the chance of re-replication. In support for this, geminin depletion-induced re-replication is strictly dependent on Cdc6 and Cdt1, as downregulation of any of both factors inhibited it (Melixetian et al., 2004).

Metaphase spreads analysis of Cdc6/Cdt1-overexpressing cells did not reveal increased frequency of chromatid breaks, suggesting that those cells undergoing DNA damage either repair it before mitosis or undergo apoptosis. While persistent activation of the DDR has also been reported to induce senescence (Bartkova et al., 2006; DiMicco et al., 2006), this pathway was not preferentially activated upon Cdc6 and Cdt1 overexpression.

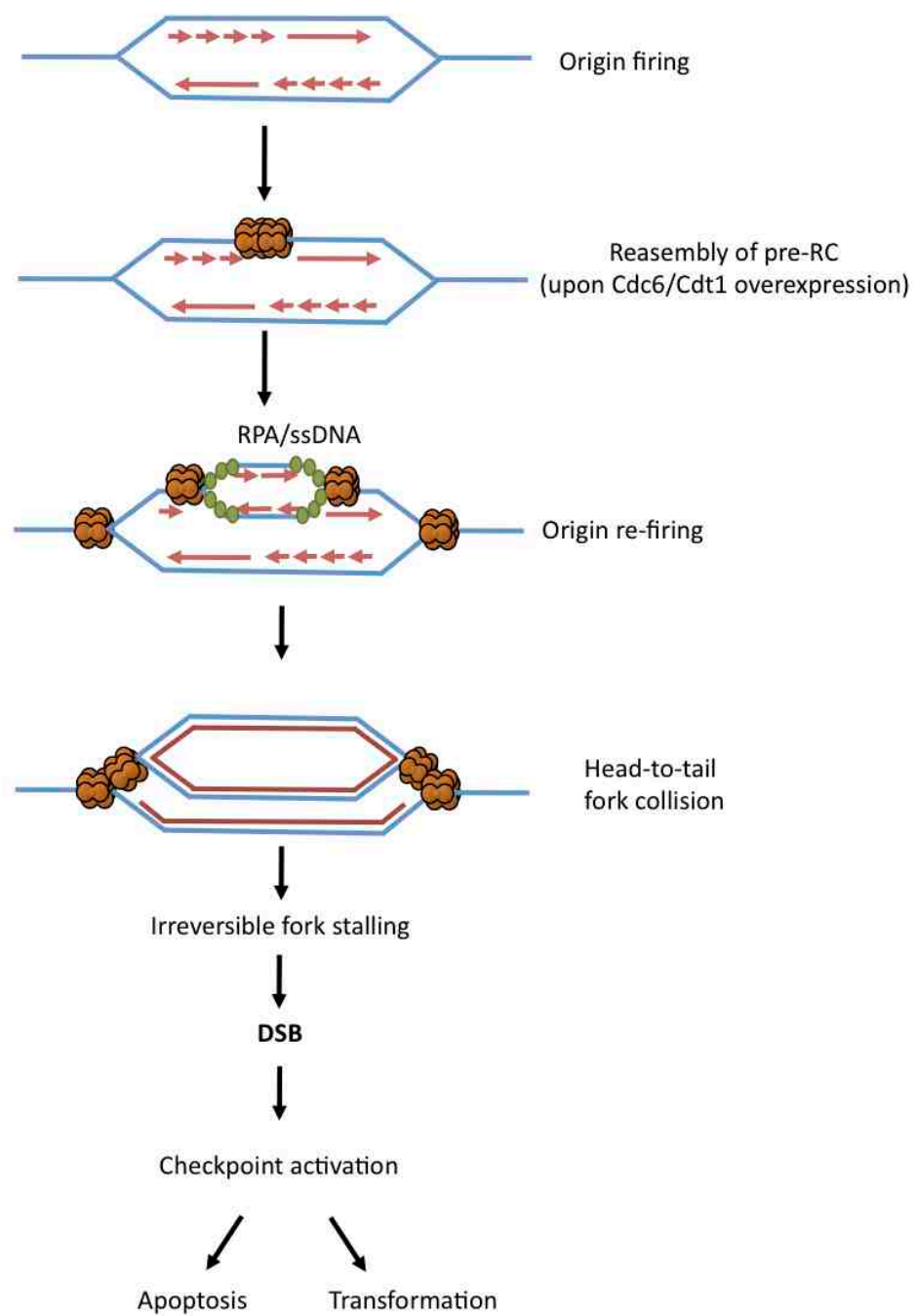


Figure 56. A model for DNA re-replication causing DSB and genetic damage. See text for details (Adapted from Liu et al., 2007; Davison et al., 2006).

7. Cdc6 and Cdt1 overexpression is lethal *in vivo*.

To date, only two *in vivo* studies overexpressing pre-RC components in specific tissues have been reported. Cdt1 overexpression in thymocytes has been shown to cause highly aneuploid lymphoblastic lymphomas only in a p53-null background (Seo et al., 2005). Overexpression of MCM7 in the skin increases the frequency of papillomas and progression towards SCC (Honeycutt et al., 2006). In our case, simultaneous Cdc6 and Cdt1 overexpression had a striking effect *in vivo*. As early as 6 days after the start of the dox treatment, a significant weight loss and overall decline in health was observed bringing the mice to the established humane endpoint. Upon histopathological analysis, it became clear that the most proliferative tissues are severely affected particularly, the intestine, stomach, spleen, skin and thymus. No histological alterations were found in organs with lower proliferation rates such as liver, pancreas, kidney, lung or heart, suggesting that high levels of cell proliferation are required for the toxic effects of Cdc6 and Cdt1 overexpression. In fact, it is possible that proliferation rate influences the stability of at least Cdc6 overexpression as previously commented for the Tet^{ON}-CDC6 mouse strain, in which organs like the liver, presented high CDC6 mRNA levels, but HA-Cdc6 was barely detected by IHC in tissue sections.

We hypothesize that Cdc6 and Cdt1 overexpression *in vivo* induces re-replication in proliferating tissues to an extent sufficient to activate the DDR and induce apoptosis, as a way to eliminate cells that could become genetically unstable. The high rate of apoptosis in tissues such as the intestine prevents proper regeneration of the epithelia, creating ulcers and diminishing functionality in terms of nutrient uptake. Nevertheless tissues are still proliferating, probably in an unsuccessfully attempt to compensate tissue loss due to apoptosis.

In summary, in this study we have generated new mouse models for Cdc6, Cdt1 and combined overexpression of these two replication factors. We found that the effects of Cdc6 overexpression *in vivo* are tissue-dependent and the effects are milder than overexpressing Cdc6 and Cdt1 in combination, which we have proven to be incompatible with life. Both factors deregulate DNA replication at different levels but both Cdc6 and Cdc6/Cdt1 overexpression contribute to genomic instability *in vivo*.

CONCLUSIONS

1. We have generated mouse models for-tissue specific (K5-CDC6^{tg}) and inducible (Tet^{ON}-CDC6; TET^{ON}-CDT1 and Tet^{ON}-CDC6/CDT1) overexpression of Cdc6 and Cdt1.
2. Cdc6, but not Cdt1 overexpression increases the efficiency of MCM loading on chromatin, indicating that Cdc6 is a limiting factor for the origin licensing reaction.
3. K5-CDC6^{tg} mice display a skin-specific delayed-ageing phenotype that correlated with a slow progression of the hair growth cycle.
4. K5-CDC6^{tg} mice had a normal lifespan but are hypersensitive to chemically-induced skin tumorigenesis.
5. Cdc6 overexpression in embryonic fibroblasts increased the efficiency of origin firing and decreased the fork progression rate without activation of the DNA damage response or impairment of cell proliferation *in vitro*.
6. Upon conditions of replicative stress, Cdc6-overexpressing fibroblasts failed to activate dormant origins.
7. Tet^{ON}-CDC6 mice are more susceptible to spontaneous tumorigenesis, with a prevalence of histiocytic sarcomas and B-cell lymphomas.
8. Simultaneous Cdc6 and Cdt1 overexpression induces partial DNA re-replication, activates the DNA-damage response and induces apoptosis.
9. Cdc6 and Cdt1 overexpression is lethal *in vivo*. Activation of the DNA damage response and increased apoptotic activity in proliferative tissues suggest that DNA re-replication is also occurring *in vivo*.

CONCLUSIONES

1. Hemos generado modelos murinos que permiten la sobre-expresión de las proteínas Cdc6 y Cdt1 en tejidos específicos (K5-CDC6^{tg}) y de manera inducible y generalizada en el animal (Tet^{ON}-CDC6; Tet^{ON}-CDT1; Tet^{ON}-CDC6/CDT1).
2. La sobre-expresión de Cdc6, pero no la de Cdt1, incrementa la eficiencia de carga de MCM en cromatina, lo que indica que Cdc6 es un factor limitante en la reacción de “licenciamiento” de orígenes para la replicación.
3. La piel de los ratones K5-CDC6^{tg} muestra signos de envejecimiento atenuado relacionados con la ralentización del ciclo de crecimiento del pelo.
4. Los ratones K5-CDC6^{tg} tienen una esperanza de vida normal y son más susceptibles a la carcinogénesis inducida en la piel.
5. La sobre-expresión de Cdc6 en fibroblastos primarios incrementa la eficiencia de activación de orígenes y disminuye la velocidad de progresión de la horquilla replicativa sin activar la respuesta de daño al ADN ni interferir con la proliferación celular *in vitro*.
6. En presencia de estrés replicativo, las células Tet^{ON}-CDC6 no pueden activar los orígenes latentes que sirven una función de rescate.
7. Los ratones Tet^{ON}-CDC6 son más susceptibles a la aparición espontánea de tumores, con prevalencia de sarcomas histiocíticos y linfomas de tipo B.
8. La sobre-expresión simultánea de Cdc6 y Cdt1 induce re-replicación en fibroblastos primarios, activa la respuesta de daño al ADN e induce apoptosis.
9. La sobre-expresión de Cdc6 y Cdt1 es letal *in vivo*. La activación de la respuesta de daño al ADN y la elevada actividad mitótica detectada en los tejidos proliferativos sugiere que la re-replicación del ADN también ocurre *in vivo*.

BIBLIOGRAPHY

- Aggarwal, P., M.D. Lessie, D.I. Lin, L. Pontano, A.B. Gladden, B. Nuskey, A. Goradia, M.A. Wasik, A.J. Klein-Szanto, A.K. Rustgi, C.H. Bassing, and J.A. Diehl. 2007. Nuclear accumulation of cyclin D1 during S phase inhibits Cul4-dependent Cdt1 proteolysis and triggers p53-dependent DNA rereplication. *Genes Dev.* 21:2908-22.
- Agherbi, H., A. Gaussmann-Wenger, C. Verthuy, L. Chasson, M. Serrano, and M. Djabali. 2009. Polycomb mediated epigenetic silencing and replication timing at the INK4a/ARF locus during senescence. *PLoS One.* 4:e5622.
- Alexandrow, M.G., and J.L. Hamlin. 2004. Cdc6 chromatin affinity is unaffected by serine-54 phosphorylation, S-phase progression, and overexpression of cyclin A. *Mol Cell Biol.* 24:1614-27.
- Alonso, L., and E. Fuchs. 2006. The hair cycle. *J Cell Sci.* 119:391-3.
- Anglana, M., F. Apiou, A. Bensimon, and M. Debatisse. 2003. Dynamics of DNA replication in mammalian somatic cells: nucleotide pool modulates origin choice and interorigin spacing. *Cell.* 114:385-94.
- Aparicio, O.M. 2013. Location, location, location: it's all in the timing for replication origins. *Genes Dev.* 27:117-28.
- Aparicio, T., D. Megias, and J. Mendez. 2012. Visualization of the MCM DNA helicase at replication factories before the onset of DNA synthesis. *Chromosoma.* 121:499-507.
- Archambault, V., A.E. Ikui, B.J. Drapkin, and F.R. Cross. 2005. Disruption of mechanisms that prevent rereplication triggers a DNA damage response. *Mol Cell Biol.* 25:6707-21.
- Arentson, E., P. Faloon, J. Seo, E. Moon, J.M. Studts, D.H. Fremont, and K. Choi. 2002. Oncogenic potential of the DNA replication licensing protein CDT1. *Oncogene.* 21:1150-8.
- Arias, E.E., and J.C. Walter. 2006. PCNA functions as a molecular platform to trigger Cdt1 destruction and prevent re-replication. *Nat Cell Biol.* 8:84-90.
- Arias, E.E., and J.C. Walter. 2007. Strength in numbers: preventing rereplication via multiple mechanisms in eukaryotic cells. *Genes Dev.* 21:497-518.
- Ballabeni, A., M. Melixetian, R. Zamponi, L. Masiero, F. Marinoni, and K. Helin. 2004. Human geminin promotes pre-RC formation and DNA replication by stabilizing CDT1 in mitosis. *EMBO J.* 23:3122-32.
- Balmain, A., M. Ramsden, G.T. Bowden, and J. Smith. 1984. Activation of the mouse cellular Harvey-ras gene in chemically induced benign skin papillomas. *Nature.* 307:658-60.
- Barrandon, Y., and H. Green. 1987. Three clonal types of keratinocyte with different capacities for multiplication. *Proc Natl Acad Sci U S A.* 84:2302-6.
- Barry, E.R., and S.D. Bell. 2006. DNA replication in the archaea. *Microbiol Mol Biol Rev.* 70:876-87.
- Bartek, J., J. Bartkova, and J. Lukas. 2007. DNA damage signalling guards against activated oncogenes and tumour progression. *Oncogene.* 26:7773-9.
- Bartek, J., C. Lukas, and J. Lukas. 2004. Checking on DNA damage in S phase. *Nat Rev Mol Cell Biol.* 5:792-804.
- Bartkova, J., Z. Horejsi, K. Koed, A. Kramer, F. Tort, K. Zieger, P. Guldberg, M. Sehested, J.M. Nesland, C. Lukas, T. Orntoft, J. Lukas, and J. Bartek. 2005. DNA damage response as a candidate anti-cancer barrier in early human tumorigenesis. *Nature.* 434:864-70.

- Bartkova, J., N. Rezaei, M. Lontos, P. Karakaidos, D. Kletsas, N. Issaeva, L.V. Vassiliou, E. Kolettas, K. Niforou, V.C. Zoumpourlis, M. Takaoka, H. Nakagawa, F. Tort, K. Fugger, F. Johansson, M. Sehested, C.L. Andersen, L. Dyrskjot, T. Orntoft, J. Lukas, C. Kittas, T. Helleday, T.D. Halazonetis, J. Bartek, and V.G. Gorgoulis. 2006. Oncogene-induced senescence is part of the tumorigenesis barrier imposed by DNA damage checkpoints. *Nature*. 444:633-7.
- Beard, C., K. Hochedlinger, K. Plath, A. Wutz, and R. Jaenisch. 2006. Efficient method to generate single-copy transgenic mice by site-specific integration in embryonic stem cells. *Genesis*. 44:23-8.
- Bell, S.P., and B. Stillman. 1992. ATP-dependent recognition of eukaryotic origins of DNA replication by a multiprotein complex. *Nature*. 357:128-34.
- Berger, C., A. Strub, C. Staib, M. Lepke, P. Zisimopoulou, K. Hoehn, I. Nanda, M. Schmid, and F. Grummt. 1999. Identification and characterization of a mouse homolog to yeast Cdc6p. *Cytogenet Cell Genet*. 86:307-16.
- Bermejo, R., N. Vilaboa, and C. Cales. 2002. Regulation of CDC6, geminin, and CDT1 in human cells that undergo polyploidization. *Mol Biol Cell*. 13:3989-4000.
- Bicknell, L.S., E.M. Bongers, A. Leitch, S. Brown, J. Schoots, M.E. Harley, S. Aftimos, J.Y. Al-Aama, M. Bober, P.A. Brown, H. van Bokhoven, J. Dean, A.Y. Edrees, M. Feingold, A. Fryer, L.H. Hoefsloot, N. Kau, N.V. Knoers, J. Mackenzie, J.M. Opitz, P. Sarda, A. Ross, I.K. Temple, A. Toutain, C.A. Wise, M. Wright, and A.P. Jackson. 2011. Mutations in the pre-replication complex cause Meier-Gorlin syndrome. *Nat Genet*. 43:356-9.
- Bicknell, L.S., S. Walker, A. Klingseisen, T. Stiff, A. Leitch, C. Kerzendorfer, C.A. Martin, P. Yeyati, N. Al Sanna, M. Bober, D. Johnson, C. Wise, A.P. Jackson, M. O'Driscoll, and P.A. Jeggo. 2011. Mutations in ORC1, encoding the largest subunit of the origin recognition complex, cause microcephalic primordial dwarfism resembling Meier-Gorlin syndrome. *Nat Genet*. 43:350-5.
- Blanpain, C., and E. Fuchs. 2006. Epidermal stem cells of the skin. *Annu Rev Cell Dev Biol*. 22:339-73.
- Blow, J.J., and A. Dutta. 2005. Preventing re-replication of chromosomal DNA. *Nat Rev Mol Cell Biol*. 6:476-86.
- Blow, J.J., and X.Q. Ge. 2009. A model for DNA replication showing how dormant origins safeguard against replication fork failure. *EMBO Rep*. 10:406-12.
- Blow, J.J., X.Q. Ge, and D.A. Jackson. 2011. How dormant origins promote complete genome replication. *Trends Biochem Sci*. 36:405-14.
- Blow, J.J., and P.J. Gillespie. 2008. Replication licensing and cancer--a fatal entanglement? *Nat Rev Cancer*. 8:799-806.
- Boos, D., J. Frigola, and J.F. Diffley. 2012. Activation of the replicative DNA helicase: breaking up is hard to do. *Curr Opin Cell Biol*. 24:423-30.
- Borlado, L.R., and J. Mendez. 2008. CDC6: from DNA replication to cell cycle checkpoints and oncogenesis. *Carcinogenesis*. 29:237-43.
- Bowers, J.L., J.C. Randell, S. Chen, and S.P. Bell. 2004. ATP hydrolysis by ORC catalyzes reiterative Mcm2-7 assembly at a defined origin of replication. *Mol Cell*. 16:967-78.
- Branzei, D. 2011. Ubiquitin family modifications and template switching. *FEBS Lett*. 585:2810-7.
- Bueno, A., and P. Russell. 1992. Dual functions of CDC6: a yeast protein required for DNA replication also inhibits nuclear division. *EMBO J*. 11:2167-76.
- Cayrou, C., P. Coulombe, A. Vigneron, S. Stanojcic, O. Ganier, I. Peiffer, E. Rivals, A. Puy, S. Laurent-Chabaliere, R. Desprat, and M. Mechali. 2011. Genome-scale analysis of metazoan replication

- origins reveals their organization in specific but flexible sites defined by conserved features. *Genome Res.* 21:1438-49.
- Celeste, A., S. Petersen, P.J. Romanienko, O. Fernandez-Capetillo, H.T. Chen, O.A. Sedelnikova, B. Reina-San-Martin, V. Coppola, E. Meffre, M.J. Difilippantonio, C. Redon, D.R. Pilch, A. Oлару, M. Eckhaus, R.D. Camerini-Otero, L. Tessarollo, F. Livak, K. Manova, W.M. Bonner, M.C. Nussenzweig, and A. Nussenzweig. 2002. Genomic instability in mice lacking histone H2AX. *Science.* 296:922-7.
- Chuang, C.H., M.D. Wallace, C. Abratte, T. Southard, and J.C. Schimenti. 2010. Incremental genetic perturbations to MCM2-7 expression and subcellular distribution reveal exquisite sensitivity of mice to DNA replication stress. *PLoS Genet.* 6.
- Chung, J.H., and F. Bunz. 2010. Cdk2 is required for p53-independent G2/M checkpoint control. *PLoS Genet.* 6:e1000863.
- Ciccia, A., and S.J. Elledge. 2010. The DNA damage response: making it safe to play with knives. *Mol Cell.* 40:179-204.
- Cimprich, K.A., and D. Cortez. 2008. ATR: an essential regulator of genome integrity. *Nat Rev Mol Cell Biol.* 9:616-27.
- Clark, R.A.F. 1996. Wound repair: Overview and general considerations. *In* The Molecular and Cellular Biology of Wound Repair. R.A.F. Clark, editor. Plenum, New York. 3–50.
- Clay-Farrace, L., C. Pelizon, D. Santamaria, J. Pines, and R.A. Laskey. 2003. Human replication protein Cdc6 prevents mitosis through a checkpoint mechanism that implicates Chk1. *EMBO J.* 22:704-12.
- Cocker, J.H., S. Piatti, C. Santocanale, K. Nasmyth, and J.F. Diffley. 1996. An essential role for the Cdc6 protein in forming the pre-replicative complexes of budding yeast. *Nature.* 379:180-2.
- Coleman, T.R., P.B. Carpenter, and W.G. Dunphy. 1996. The *Xenopus* Cdc6 protein is essential for the initiation of a single round of DNA replication in cell-free extracts. *Cell.* 87:53-63.
- Collado, M., J. Gil, A. Efeyan, C. Guerra, A.J. Schuhmacher, M. Barradas, A. Benguria, A. Zaballos, J.M. Flores, M. Barbacid, D. Beach, and M. Serrano. 2005. Tumour biology: senescence in premalignant tumours. *Nature.* 436:642.
- Conti, C., B. Sacca, J. Herrick, C. Lalou, Y. Pommier, and A. Bensimon. 2007. Replication fork velocities at adjacent replication origins are coordinately modified during DNA replication in human cells. *Mol Biol Cell.* 18:3059-67.
- Cook, J.G., C.H. Park, T.W. Burke, G. Leone, J. DeGregori, A. Engel, and J.R. Nevins. 2002. Analysis of Cdc6 function in the assembly of mammalian prereplication complexes. *Proc Natl Acad Sci U S A.* 99:1347-52.
- Cotsarelis, G., T.T. Sun, and R.M. Lavker. 1990. Label-retaining cells reside in the bulge area of pilosebaceous unit: implications for follicular stem cells, hair cycle, and skin carcinogenesis. *Cell.* 61:1329-37.
- Courbet, S., S. Gay, N. Arnoult, G. Wronka, M. Anglana, O. Brison, and M. Debatisse. 2008. Replication fork movement sets chromatin loop size and origin choice in mammalian cells. *Nature.* 455:557-60.
- Davidson, I.F., A. Li, and J.J. Blow. 2006. Dereregulated replication licensing causes DNA fragmentation consistent with head-to-tail fork collision. *Mol Cell.* 24:433-43.
- De Marco, V., P.J. Gillespie, A. Li, N. Karantzelis, E. Christodoulou, R. Klompaker, S. van Gerwen, A. Fish, M.V. Petoukhov, M.S. Iliou, Z. Lygerou, R.H. Medema, J.J. Blow, D.I. Svergun, S.

- Taraviras, and A. Perrakis. 2009. Quaternary structure of the human Cdt1-Geminin complex regulates DNA replication licensing. *Proc Natl Acad Sci U S A*. 106:19807-12.
- DePamphilis, M. 2006. DNA Replication and Human Disease Cold Spring Harbor Lab. Press, New York.
- Di Micco, R., M. Fumagalli, A. Cicalese, S. Piccinin, P. Gasparini, C. Luise, C. Schurra, M. Garre, P.G. Nuciforo, A. Bensimon, R. Maestro, P.G. Pelicci, and F. d'Adda di Fagagna. 2006. Oncogene-induced senescence is a DNA damage response triggered by DNA hyper-replication. *Nature*. 444:638-42.
- Diffley, J.F. 2011. Quality control in the initiation of eukaryotic DNA replication. *Philos Trans R Soc Lond B Biol Sci*. 366:3545-53.
- Diffley, J.F., J.H. Cocker, S.J. Dowell, and A. Rowley. 1994. Two steps in the assembly of complexes at yeast replication origins in vivo. *Cell*. 78:303-16.
- DiGiovanni, J. 1992. Multistage carcinogenesis in mouse skin. *Pharmacol Ther*. 54:63-128.
- Dimitrova, D.S., and R. Berezney. 2002. The spatio-temporal organization of DNA replication sites is identical in primary, immortalized and transformed mammalian cells. *J Cell Sci*. 115:4037-51.
- Dominguez, O., and C. Lopez-Larrea. 1994. Gene walking by unpredictably primed PCR. *Nucleic Acids Res*. 22:3247-8.
- Donehower, L.A., M. Harvey, B.L. Slagle, M.J. McArthur, C.A. Montgomery, Jr., J.S. Butel, and A. Bradley. 1992. Mice deficient for p53 are developmentally normal but susceptible to spontaneous tumours. *Nature*. 356:215-21.
- Donovan, S., J. Harwood, L.S. Drury, and J.F. Diffley. 1997. Cdc6p-dependent loading of Mcm proteins onto pre-replicative chromatin in budding yeast. *Proc Natl Acad Sci U S A*. 94:5611-6.
- Dorn, E.S., P.D. Chastain, 2nd, J.R. Hall, and J.G. Cook. 2009. Analysis of re-replication from deregulated origin licensing by DNA fiber spreading. *Nucleic Acids Res*. 37:60-9.
- Duursma, A., and R. Agami. 2005. p53-Dependent regulation of Cdc6 protein stability controls cellular proliferation. *Mol Cell Biol*. 25:6937-47.
- Edwards, M.C., A.V. Tutter, C. Cvetic, C.H. Gilbert, T.A. Prokhorova, and J.C. Walter. 2002. MCM2-7 complexes bind chromatin in a distributed pattern surrounding the origin recognition complex in *Xenopus* egg extracts. *J Biol Chem*. 277:33049-57.
- Ekholm-Reed, S., J. Mendez, D. Tedesco, A. Zetterberg, B. Stillman, and S.I. Reed. 2004. Deregulation of cyclin E in human cells interferes with prereplication complex assembly. *J Cell Biol*. 165:789-800.
- Evrin, C., P. Clarke, J. Zech, R. Lurz, J. Sun, S. Uhle, H. Li, B. Stillman, and C. Speck. 2009. A double-hexameric MCM2-7 complex is loaded onto origin DNA during licensing of eukaryotic DNA replication. *Proc Natl Acad Sci U S A*. 106:20240-5.
- Feng, D., Z. Tu, W. Wu, and C. Liang. 2003. Inhibiting the expression of DNA replication-initiation proteins induces apoptosis in human cancer cells. *Cancer Res*. 63:7356-64.
- Fernandez-Cid, A., A. Riera, S. Tognetti, M.C. Herrera, S. Samel, C. Evrin, C. Winkler, E. Gardenal, S. Uhle, and C. Speck. 2013. An ORC/Cdc6/MCM2-7 Complex Is Formed in a Multistep Reaction to Serve as a Platform for MCM Double-Hexamer Assembly. *Mol Cell*. 50:577-88.
- Finn, K.J., and J.J. Li. 2013. Single-stranded annealing induced by re-initiation of replication origins provides a novel and efficient mechanism for generating copy number expansion via non-allelic homologous recombination. *PLoS Genet*. 9:e1003192.

- Flores, I., M.L. Cayuela, and M.A. Blasco. 2005. Effects of telomerase and telomere length on epidermal stem cell behavior. *Science*. 309:1253-6.
- Frank, S., and H. Kämpfer. 2003. Excisional Wound Healing *In* T Wound Healing. Vol. 78. 3-15.
- Frigola, J., D. Remus, A. Mehanna, and J.F. Diffley. 2013. ATPase-dependent quality control of DNA replication origin licensing. *Nature*. 495:339-43.
- Fuchs, E., and S. Raghavan. 2002. Getting under the skin of epidermal morphogenesis. *Nat Rev Genet*. 3:199-209.
- Fujita, M. 2006. Cdt1 revisited: complex and tight regulation during the cell cycle and consequences of deregulation in mammalian cells. *Cell Div*. 1:22.
- Furstenthal, L., B.K. Kaiser, C. Swanson, and P.K. Jackson. 2001. Cyclin E uses Cdc6 as a chromatin-associated receptor required for DNA replication. *J Cell Biol*. 152:1267-78.
- Gannon, H.S., L.A. Donehower, S. Lyle, and S.N. Jones. 2011. Mdm2-p53 signaling regulates epidermal stem cell senescence and premature aging phenotypes in mouse skin. *Dev Biol*. 353:1-9.
- Garcia-Higuera, I., E. Manchado, P. Dubus, M. Canamero, J. Mendez, S. Moreno, and M. Malumbres. 2008. Genomic stability and tumour suppression by the APC/C cofactor Cdh1. *Nat Cell Biol*. 10:802-11.
- Ge, X.Q., D.A. Jackson, and J.J. Blow. 2007. Dormant origins licensed by excess Mcm2-7 are required for human cells to survive replicative stress. *Genes Dev*. 21:3331-41.
- Gilbert, D.M. 2010. Evaluating genome-scale approaches to eukaryotic DNA replication. *Nat Rev Genet*. 11:673-84.
- Gomez, M., and F. Antequera. 2008. Overreplication of short DNA regions during S phase in human cells. *Genes Dev*. 22:375-85.
- Gonzalez, M.A., K.E. Tachibana, R.A. Laskey, and N. Coleman. 2005. Control of DNA replication and its potential clinical exploitation. *Nat Rev Cancer*. 5:135-41.
- Gonzalez, S., P. Klatt, S. Delgado, E. Conde, F. Lopez-Rios, M. Sanchez-Cespedes, J. Mendez, F. Antequera, and M. Serrano. 2006. Oncogenic activity of Cdc6 through repression of the INK4/ARF locus. *Nature*. 440:702-6.
- Gorgoulis, V.G., L.V. Vassiliou, P. Karakaidos, P. Zacharatos, A. Kotsinas, T. Liloglou, M. Venere, R.A. Dittullo, Jr., N.G. Kastrinakis, B. Levy, D. Kletsas, A. Yoneta, M. Herlyn, C. Kittas, and T.D. Halazonetis. 2005. Activation of the DNA damage checkpoint and genomic instability in human precancerous lesions. *Nature*. 434:907-13.
- Gossen, M., and H. Bujard. 1992. Tight control of gene expression in mammalian cells by tetracycline-responsive promoters. *Proc Natl Acad Sci U S A*. 89:5547-51.
- Green, B.M., K.J. Finn, and J.J. Li. 2010. Loss of DNA replication control is a potent inducer of gene amplification. *Science*. 329:943-6.
- Guernsey, D.L., M. Matsuoka, H. Jiang, S. Evans, C. Macgillivray, M. Nightingale, S. Perry, M. Ferguson, M. LeBlanc, J. Paquette, L. Patry, A.L. Rideout, A. Thomas, A. Orr, C.R. McMaster, J.L. Michaud, C. Deal, S. Langlois, D.W. Superneau, S. Parkash, M. Ludman, D.L. Skidmore, and M.E. Samuels. 2011. Mutations in origin recognition complex gene ORC4 cause Meier-Gorlin syndrome. *Nat Genet*. 43:360-4.
- Hall, J.R., E. Kow, K.R. Nevis, C.K. Lu, K.S. Luce, Q. Zhong, and J.G. Cook. 2007. Cdc6 stability is regulated by the Huwe1 ubiquitin ligase after DNA damage. *Mol Biol Cell*. 18:3340-50.

- Hall, J.R., H.O. Lee, B.D. Bunker, E.S. Dorn, G.C. Rogers, R.J. Duronio, and J.G. Cook. 2008. Cdt1 and Cdc6 are destabilized by rereplication-induced DNA damage. *J Biol Chem.* 283:25356-63.
- Hanada, K., M. Budzowska, S.L. Davies, E. van Drunen, H. Onizawa, H.B. Beverloo, A. Maas, J. Essers, I.D. Hickson, and R. Kanaar. 2007. The structure-specific endonuclease Mus81 contributes to replication restart by generating double-strand DNA breaks. *Nat Struct Mol Biol.* 14:1096-104.
- Harlow, L., and D. Lane. 1999. Using antibodies: A Laboratory Manual. CSHL Press, New York.
- Hartwell, L.H. 1976. Sequential function of gene products relative to DNA synthesis in the yeast cell cycle. *J Mol Biol.* 104:803-17.
- Harvey, D.M., and A.J. Levine. 1991. p53 alteration is a common event in the spontaneous immortalization of primary BALB/c murine embryo fibroblasts. *Genes Dev.* 5:2375-85.
- Hateboer, G., A. Wobst, B.O. Petersen, L. Le Cam, E. Vigo, C. Sardet, and K. Helin. 1998. Cell cycle-regulated expression of mammalian CDC6 is dependent on E2F. *Mol Cell Biol.* 18:6679-97.
- Hermans, D., and P. Nurse. 2007. Cdc18 enforces long-term maintenance of the S phase checkpoint by anchoring the Rad3-Rad26 complex to chromatin. *Mol Cell.* 26:553-63.
- Higa, L.A., I.S. Mihaylov, D.P. Banks, J. Zheng, and H. Zhang. 2003. Radiation-mediated proteolysis of CDT1 by CUL4-ROC1 and CSN complexes constitutes a new checkpoint. *Nat Cell Biol.* 5:1008-15.
- Hofmann, J.F., and D. Beach. 1994. cdt1 is an essential target of the Cdc10/Sct1 transcription factor: requirement for DNA replication and inhibition of mitosis. *EMBO J.* 13:425-34.
- Honeycutt, K.A., Z. Chen, M.I. Koster, M. Miers, J. Nuchtern, J. Hicks, D.R. Roop, and J.M. Shohet. 2006. Deregulated minichromosomal maintenance protein MCM7 contributes to oncogene driven tumorigenesis. *Oncogene.* 25:4027-32.
- Hu, D., and J.C. Cross. 2009. Development and function of trophoblast giant cells in the rodent placenta. *Int J Dev Biol.* 54:341-54.
- Hyrien, O., K. Marheineke, and A. Goldar. 2003. Paradoxes of eukaryotic DNA replication: MCM proteins and the random completion problem. *Bioessays.* 25:116-25.
- Ibarra, A., E. Schwob, and J. Mendez. 2008. Excess MCM proteins protect human cells from replicative stress by licensing backup origins of replication. *Proc Natl Acad Sci U S A.* 105:8956-61.
- Ito, M., Y. Liu, Z. Yang, J. Nguyen, F. Liang, R.J. Morris, and G. Cotsarelis. 2005. Stem cells in the hair follicle bulge contribute to wound repair but not to homeostasis of the epidermis. *Nat Med.* 11:1351-4.
- Jallepalli, P.V., G.W. Brown, M. Muzi-Falconi, D. Tien, and T.J. Kelly. 1997. Regulation of the replication initiator protein p65cdc18 by CDK phosphorylation. *Genes Dev.* 11:2767-79.
- Jenkins, G. 2002. Molecular mechanisms of skin ageing. *Mech Ageing Dev.* 123:801-10.
- Jensen, K.B., C.A. Collins, E. Nascimento, D.W. Tan, M. Frye, S. Itami, and F.M. Watt. 2009. Lrig1 expression defines a distinct multipotent stem cell population in mammalian epidermis. *Cell Stem Cell.* 4:427-39.
- Karakaidos, P., S. Taraviras, L.V. Vassiliou, P. Zacharatos, N.G. Kastrinakis, D. Kougiou, M. Kouloukoussa, H. Nishitani, A.G. Papavassiliou, Z. Lygerou, and V.G. Gorgoulis. 2004. Overexpression of the replication licensing regulators hCdt1 and hCdc6 characterizes a subset of non-small-cell lung carcinomas: synergistic effect with mutant p53 on tumor growth and chromosomal instability--evidence of E2F-1 transcriptional control over hCdt1.

- Am J Pathol.* 165:1351-65.
- Karnani, N., and A. Dutta. 2011. The effect of the intra-S-phase checkpoint on origins of replication in human cells. *Genes Dev.* 25:621-33.
- Kawabata, T., S.W. Luebben, S. Yamaguchi, I. Ilves, I. Matise, T. Buske, M.R. Botchan, and N. Shima. 2011. Stalled fork rescue via dormant replication origins in unchallenged S phase promotes proper chromosome segregation and tumor suppression. *Mol Cell.* 41:543-53.
- Kawasaki, Y., H.D. Kim, A. Kojima, T. Seki, and A. Sugino. 2006. Reconstitution of *Saccharomyces cerevisiae* prereplicative complex assembly in vitro. *Genes Cells.* 11:745-56.
- Kelly, T.J., G.S. Martin, S.L. Forsburg, R.J. Stephen, A. Russo, and P. Nurse. 1993. The fission yeast *cdc18+* gene product couples S phase to START and mitosis. *Cell.* 74:371-82.
- Kim, W.Y., and N.E. Sharpless. 2006. The regulation of INK4/ARF in cancer and aging. *Cell.* 127:265-75.
- Kim, Y., and E.T. Kipreos. 2007. Cdt1 degradation to prevent DNA re-replication: conserved and non-conserved pathways. *Cell Div.* 2:18.
- Klotz-Noack, K., D. McIntosh, N. Schurch, N. Pratt, and J.J. Blow. 2012. Re-replication induced by geminin depletion occurs from G2 and is enhanced by checkpoint activation. *J Cell Sci.* 125:2436-45.
- Kondo, T., M. Kobayashi, J. Tanaka, A. Yokoyama, S. Suzuki, N. Kato, M. Onozawa, K. Chiba, S. Hashino, M. Imamura, Y. Minami, N. Minamino, and M. Asaka. 2004. Rapid degradation of Cdt1 upon UV-induced DNA damage is mediated by SCFSkp2 complex. *J Biol Chem.* 279:27315-9.
- Krishnamurthy, J., C. Torrice, M.R. Ramsey, G.I. Kovalev, K. Al-Regaiey, L. Su, and N.E. Sharpless. 2004. Ink4a/Arf expression is a biomarker of aging. *J Clin Invest.* 114:1299-307.
- Kunnev, D., M.E. Rusiniak, A. Kudla, A. Freeland, G.K. Cady, and S.C. Pruitt. 2010. DNA damage response and tumorigenesis in Mcm2-deficient mice. *Oncogene.* 29:3630-8.
- Lau, E., G.G. Chiang, R.T. Abraham, and W. Jiang. 2009. Divergent S phase checkpoint activation arising from prereplicative complex deficiency controls cell survival. *Mol Biol Cell.* 20:3953-64.
- Lau, E., C. Zhu, R.T. Abraham, and W. Jiang. 2006. The functional role of Cdc6 in S-G2/M in mammalian cells. *EMBO Rep.* 7:425-30.
- Lee, C., B. Hong, J.M. Choi, Y. Kim, S. Watanabe, Y. Ishimi, T. Enomoto, S. Tada, and Y. Cho. 2004. Structural basis for inhibition of the replication licensing factor Cdt1 by geminin. *Nature.* 430:913-7.
- Levy, V., C. Lindon, Y. Zheng, B.D. Harfe, and B.A. Morgan. 2007. Epidermal stem cells arise from the hair follicle after wounding. *FASEB J.* 21:1358-66.
- Li, A., and J.J. Blow. 2004. Non-proteolytic inactivation of geminin requires CDK-dependent ubiquitination. *Nat Cell Biol.* 6:260-7.
- Li, A., and J.J. Blow. 2005. Cdt1 downregulation by proteolysis and geminin inhibition prevents DNA re-replication in *Xenopus*. *EMBO J.* 24:395-404.
- Liang, C., and B. Stillman. 1997. Persistent initiation of DNA replication and chromatin-bound MCM proteins during the cell cycle in *cdc6* mutants. *Genes Dev.* 11:3375-86.
- Liang, C., M. Weinreich, and B. Stillman. 1995. ORC and Cdc6p interact and determine the frequency of initiation of DNA replication in the genome. *Cell.* 81:667-76.

- Lin, J.J., M.A. Milhollen, P.G. Smith, U. Narayanan, and A. Dutta. 2010. NEDD8-targeting drug MLN4924 elicits DNA rereplication by stabilizing Cdt1 in S phase, triggering checkpoint activation, apoptosis, and senescence in cancer cells. *Cancer Res.* 70:10310-20.
- Liontos, M., M. Koutsami, M. Sideridou, K. Evangelou, D. Kletsas, B. Levy, A. Kotsinas, O. Nahum, V. Zoumpourlis, M. Kouloukoussa, Z. Lygerou, S. Taraviras, C. Kittas, J. Bartkova, A.G. Papavassiliou, J. Bartek, T.D. Halazonetis, and V.G. Gorgoulis. 2007. Deregulated overexpression of hCdt1 and hCdc6 promotes malignant behavior. *Cancer Res.* 67:10899-909.
- Liu, E., A.Y. Lee, T. Chiba, E. Olson, P. Sun, and X. Wu. 2007. The ATR-mediated S phase checkpoint prevents rereplication in mammalian cells when licensing control is disrupted. *J Cell Biol.* 179:643-57.
- Liu, J., C.L. Smith, D. DeRyckere, K. DeAngelis, G.S. Martin, and J.M. Berger. 2000. Structure and function of Cdc6/Cdc18: implications for origin recognition and checkpoint control. *Mol Cell.* 6:637-48.
- Lundin, C., K. Erixon, C. Arnaudeau, N. Schultz, D. Jenssen, M. Meuth, and T. Helleday. 2002. Different roles for nonhomologous end joining and homologous recombination following replication arrest in mammalian cells. *Mol Cell Biol.* 22:5869-78.
- Mailand, N., and J.F. Diffley. 2005. CDKs promote DNA replication origin licensing in human cells by protecting Cdc6 from APC/C-dependent proteolysis. *Cell.* 122:915-26.
- Maiorano, D., J. Moreau, and M. Mechali. 2000. XCDT1 is required for the assembly of pre-replicative complexes in *Xenopus laevis*. *Nature.* 404:622-5.
- Malumbres, M., R. Manges, N. Ferrer, S. Lu, and A. Pellicer. 1997. Isolation of high molecular weight DNA for reliable genotyping of transgenic mice. *Biotechniques.* 22:1114-9.
- Manchado, E., M. Eguren, and M. Malumbres. 2010. The anaphase-promoting complex/cyclosome (APC/C): cell-cycle-dependent and -independent functions. *Biochem Soc Trans.* 38:65-71.
- Mantiero, D., A. Mackenzie, A. Donaldson, and P. Zegerman. 2011. Limiting replication initiation factors execute the temporal programme of origin firing in budding yeast. *EMBO J.* 30:4805-14.
- Martin, P. 1997. Wound healing--aiming for perfect skin regeneration. *Science.* 276:75-81.
- Mascre, G., S. Dekoninck, B. Drogat, K.K. Youssef, S. Brohee, P.A. Sotiropoulou, B.D. Simons, and C. Blanpain. 2012. Distinct contribution of stem and progenitor cells to epidermal maintenance. *Nature.* 489:257-62.
- Maya-Mendoza, A., E. Petermann, D.A. Gillespie, K.W. Caldecott, and D.A. Jackson. 2007. Chk1 regulates the density of active replication origins during the vertebrate S phase. *EMBO J.* 26:2719-31.
- McGarry, T.J., and M.W. Kirschner. 1998. Geminin, an inhibitor of DNA replication, is degraded during mitosis. *Cell.* 93:1043-53.
- Mechali, M. 2010. Eukaryotic DNA replication origins: many choices for appropriate answers. *Nat Rev Mol Cell Biol.* 11:728-38.
- Mechali, M., K. Yoshida, P. Coulombe, and P. Pasero. 2013. Genetic and epigenetic determinants of DNA replication origins, position and activation. *Curr Opin Genet Dev.* 23:124-31.
- Melixetian, M., A. Ballabeni, L. Masiero, P. Gasparini, R. Zamponi, J. Bartek, J. Lukas, and K. Helin. 2004. Loss of Geminin induces rereplication in the presence of functional p53. *J Cell Biol.* 165:473-82.

- Mendez, J., and B. Stillman. 2000. Chromatin association of human origin recognition complex, cdc6, and minichromosome maintenance proteins during the cell cycle: assembly of prereplication complexes in late mitosis. *Mol Cell Biol.* 20:8602-12.
- Mendez, J., and B. Stillman. 2003. Perpetuating the double helix: molecular machines at eukaryotic DNA replication origins. *Bioessays.* 25:1158-67.
- Mendez, J., X.H. Zou-Yang, S.Y. Kim, M. Hidaka, W.P. Tansey, and B. Stillman. 2002. Human origin recognition complex large subunit is degraded by ubiquitin-mediated proteolysis after initiation of DNA replication. *Mol Cell.* 9:481-91.
- Mihaylov, I.S., T. Kondo, L. Jones, S. Ryzhikov, J. Tanaka, J. Zheng, L.A. Higa, N. Minamino, L. Cooley, and H. Zhang. 2002. Control of DNA replication and chromosome ploidy by geminin and cyclin A. *Mol Cell Biol.* 22:1868-80.
- Milhollen, M.A., U. Narayanan, T.A. Soucy, P.O. Veiby, P.G. Smith, and B. Amidon. 2011. Inhibition of NEDD8-activating enzyme induces rereplication and apoptosis in human tumor cells consistent with deregulating CDT1 turnover. *Cancer Res.* 71:3042-51.
- Mizushima, T., N. Takahashi, and B. Stillman. 2000. Cdc6p modulates the structure and DNA binding activity of the origin recognition complex in vitro. *Genes Dev.* 14:1631-41.
- Moll, R., D. Dhouailly, and T.T. Sun. 1989. Expression of keratin 5 as a distinctive feature of epithelial and biphasic mesotheliomas. An immunohistochemical study using monoclonal antibody AE14. *Virchows Arch B Cell Pathol Incl Mol Pathol.* 58:129-45.
- Muller-Rover, S., B. Handjiski, C. van der Veen, S. Eichmuller, K. Foitzik, I.A. McKay, K.S. Stenn, and R. Paus. 2001. A comprehensive guide for the accurate classification of murine hair follicles in distinct hair cycle stages. *J Invest Dermatol.* 117:3-15.
- Murga, M., S. Bunting, M.F. Montana, R. Soria, F. Mulero, M. Canamero, Y. Lee, P.J. McKinnon, A. Nussenzweig, and O. Fernandez-Capetillo. 2009. A mouse model of ATR-Seckel shows embryonic replicative stress and accelerated aging. *Nat Genet.* 41:891-8.
- Murillas, R., F. Larcher, C.J. Conti, M. Santos, A. Ullrich, and J.L. Jorcano. 1995. Expression of a dominant negative mutant of epidermal growth factor receptor in the epidermis of transgenic mice elicits striking alterations in hair follicle development and skin structure. *EMBO J.* 14:5216-23.
- Neuwald, A.F., L. Aravind, J.L. Spouge, and E.V. Koonin. 1999. AAA+: A class of chaperone-like ATPases associated with the assembly, operation, and disassembly of protein complexes. *Genome Res.* 9:27-43.
- Nguyen, V.Q., C. Co, and J.J. Li. 2001. Cyclin-dependent kinases prevent DNA re-replication through multiple mechanisms. *Nature.* 411:1068-73.
- Nijhof, J.G., K.M. Braun, A. Giangreco, C. van Pelt, H. Kawamoto, R.L. Boyd, R. Willemze, L.H. Mullenders, F.M. Watt, F.R. de Gruijl, and W. van Ewijk. 2006. The cell-surface marker MTS24 identifies a novel population of follicular keratinocytes with characteristics of progenitor cells. *Development.* 133:3027-37.
- Nishitani, H., Z. Lygerou, T. Nishimoto, and P. Nurse. 2000. The Cdt1 protein is required to license DNA for replication in fission yeast. *Nature.* 404:625-8.
- Nishitani, H., and P. Nurse. 1995. p65cdc18 plays a major role controlling the initiation of DNA replication in fission yeast. *Cell.* 83:397-405.
- Nowak, J.A., and E. Fuchs. 2009. Isolation and culture of epithelial stem cells. *Methods Mol Biol.* 482:215-32.

- Oehlmann, M., A.J. Score, and J.J. Blow. 2004. The role of Cdc6 in ensuring complete genome licensing and S phase checkpoint activation. *J Cell Biol.* 165:181-90.
- Ohta, S., M. Koide, T. Tokuyama, N. Yokota, S. Nishizawa, and H. Namba. 2001. Cdc6 expression as a marker of proliferative activity in brain tumors. *Oncol Rep.* 8:1063-6.
- Ohtani, K., A. Tsujimoto, M. Ikeda, and M. Nakamura. 1998. Regulation of cell growth-dependent expression of mammalian CDC6 gene by the cell cycle transcription factor E2F. *Oncogene.* 17:1777-85.
- Ohtsuka, M., H. Miura, M. Sato, M. Kimura, H. Inoko, and C.B. Gurumurthy. 2012. PITT: pronuclear injection-based targeted transgenesis, a reliable transgene expression method in mice. *Exp Anim.* 61:489-502.
- Paolinelli, R., R. Mendoza-Maldonado, A. Cereseto, and M. Giacca. 2009. Acetylation by GCN5 regulates CDC6 phosphorylation in the S phase of the cell cycle. *Nat Struct Mol Biol.* 16:412-20.
- Paus, R., and G. Cotsarelis. 1999. The biology of hair follicles. *N Engl J Med.* 341:491-7.
- Pelizon, C., M.A. Madine, P. Romanowski, and R.A. Laskey. 2000. Unphosphorylatable mutants of Cdc6 disrupt its nuclear export but still support DNA replication once per cell cycle. *Genes Dev.* 14:2526-33.
- Petermann, E., and T. Helleday. 2010. Pathways of mammalian replication fork restart. *Nat Rev Mol Cell Biol.* 11:683-7.
- Petermann, E., A. Maya-Mendoza, G. Zachos, D.A. Gillespie, D.A. Jackson, and K.W. Caldecott. 2006. Chk1 requirement for high global rates of replication fork progression during normal vertebrate S phase. *Mol Cell Biol.* 26:3319-26.
- Petermann, E., M. Woodcock, and T. Helleday. 2010. Chk1 promotes replication fork progression by controlling replication initiation. *Proc Natl Acad Sci U S A.* 107:16090-5.
- Petersen, B.O., J. Lukas, C.S. Sorensen, J. Bartek, and K. Helin. 1999. Phosphorylation of mammalian CDC6 by cyclin A/CDK2 regulates its subcellular localization. *EMBO J.* 18:396-410.
- Petersen, B.O., C. Wagener, F. Marinoni, E.R. Kramer, M. Melixetian, E. Lazzerini Denchi, C. Gieffers, C. Matteucci, J.M. Peters, and K. Helin. 2000. Cell cycle- and cell growth-regulated proteolysis of mammalian CDC6 is dependent on APC-CDH1. *Genes Dev.* 14:2330-43.
- Piatti, S., C. Lengauer, and K. Nasmyth. 1995. Cdc6 is an unstable protein whose de novo synthesis in G1 is important for the onset of S phase and for preventing a 'reductional' anaphase in the budding yeast *Saccharomyces cerevisiae*. *EMBO J.* 14:3788-99.
- Pinyol, M., I. Salaverria, S. Bea, V. Fernandez, L. Colomo, E. Campo, and P. Jares. 2006. Unbalanced expression of licensing DNA replication factors occurs in a subset of mantle cell lymphomas with genomic instability. *Int J Cancer.* 119:2768-74.
- Poli, J., O. Tsaponina, L. Crabbe, A. Keszthelyi, V. Pantesco, A. Chabes, A. Lengronne, and P. Pasero. 2012. dNTP pools determine fork progression and origin usage under replication stress. *EMBO J.* 31:883-94.
- Pruitt, S.C., K.J. Bailey, and A. Freeland. 2007. Reduced Mcm2 expression results in severe stem/progenitor cell deficiency and cancer. *Stem Cells.* 25:3121-32.
- Quintanilla, M., K. Brown, M. Ramsden, and A. Balmain. 1986. Carcinogen-specific mutation and amplification of Ha-ras during mouse skin carcinogenesis. *Nature.* 322:78-80.
- Ramirez, A., A. Bravo, J.L. Jorcano, and M. Vidal. 1994. Sequences 5' of the bovine keratin 5 gene direct tissue- and cell-type-specific expression of a lacZ gene in the adult and during

- development. *Differentiation*. 58:53-64.
- Randell, J.C., J.L. Bowers, H.K. Rodriguez, and S.P. Bell. 2006. Sequential ATP hydrolysis by Cdc6 and ORC directs loading of the Mcm2-7 helicase. *Mol Cell*. 21:29-39.
- Remeseiro, S., A. Cuadrado, M. Carretero, P. Martinez, W.C. Drosopoulos, M. Canamero, C.L. Schildkraut, M.A. Blasco, and A. Losada. Cohesin-SA1 deficiency drives aneuploidy and tumourigenesis in mice due to impaired replication of telomeres. *EMBO J*. 31:2076-89.
- Remus, D., F. Beuron, G. Tolun, J.D. Griffith, E.P. Morris, and J.F. Diffley. 2009. Concerted loading of Mcm2-7 double hexamers around DNA during DNA replication origin licensing. *Cell*. 139:719-30.
- Remus, D., and J.F. Diffley. 2009. Eukaryotic DNA replication control: lock and load, then fire. *Curr Opin Cell Biol*. 21:771-7.
- Rialland, M., F. Sola, and C. Santocanale. 2002. Essential role of human CDT1 in DNA replication and chromatin licensing. *J Cell Sci*. 115:1435-40.
- Rodier, F., J. Campisi, and D. Bhaumik. 2007. Two faces of p53: aging and tumor suppression. *Nucleic Acids Res*. 35:7475-84.
- Ruzankina, Y., A. Asare, and E.J. Brown. 2008. Replicative stress, stem cells and aging. *Mech Ageing Dev*. 129:460-6.
- Ruzankina, Y., C. Pinzon-Guzman, A. Asare, T. Ong, L. Pontano, G. Cotsarelis, V.P. Zediak, M. Velez, A. Bhandoola, and E.J. Brown. 2007. Deletion of the developmentally essential gene ATR in adult mice leads to age-related phenotypes and stem cell loss. *Cell Stem Cell*. 1:113-26.
- Saha, P., J. Chen, K.C. Thome, S.J. Lawlis, Z.H. Hou, M. Hendricks, J.D. Parvin, and A. Dutta. 1998. Human CDC6/Cdc18 associates with Orc1 and cyclin-cdk and is selectively eliminated from the nucleus at the onset of S phase. *Mol Cell Biol*. 18:2758-67.
- Saintigny, Y., F. Delacote, G. Vares, F. Petitot, S. Lambert, D. Averbek, and B.S. Lopez. 2001. Characterization of homologous recombination induced by replication inhibition in mammalian cells. *EMBO J*. 20:3861-70.
- Schultz, L.B., N.H. Chehab, A. Malikzay, and T.D. Halazonetis. 2000. p53 binding protein 1 (53BP1) is an early participant in the cellular response to DNA double-strand breaks. *J Cell Biol*. 151:1381-90.
- Sclafani, R.A., and T.M. Holzen. 2007. Cell cycle regulation of DNA replication. *Annu Rev Genet*. 41:237-80.
- Seo, J., Y.S. Chung, G.G. Sharma, E. Moon, W.R. Burack, T.K. Pandita, and K. Choi. 2005. Cdt1 transgenic mice develop lymphoblastic lymphoma in the absence of p53. *Oncogene*. 24:8176-86.
- Shima, N., A. Alcaraz, I. Liachko, T.R. Buske, C.A. Andrews, R.J. Munroe, S.A. Hartford, B.K. Tye, and J.C. Schimenti. 2007. A viable allele of Mcm4 causes chromosome instability and mammary adenocarcinomas in mice. *Nat Genet*. 39:93-8.
- Sideridou, M., R. Zakopoulou, K. Evangelou, M. Lontos, A. Kotsinas, E. Rampakakis, S. Gagos, K. Kahata, K. Grabusic, K. Gkouskou, I.P. Trougakos, E. Kolettas, A.G. Georgakilas, S. Volarevic, A.G. Eliopoulos, M. Zannis-Hadjopoulos, A. Moustakas, and V.G. Gorgoulis. 2011. Cdc6 expression represses E-cadherin transcription and activates adjacent replication origins. *J Cell Biol*. 195:1123-40.
- Slominski, A., and R. Paus. 1993. Melanogenesis is coupled to murine anagen: toward new concepts for the role of melanocytes and the regulation of melanogenesis in hair growth. *J Invest*

Dermatol. 101:90S-97S.

- Sonoda, E., M.S. Sasaki, C. Morrison, Y. Yamaguchi-Iwai, M. Takata, and S. Takeda. 1999. Sister chromatid exchanges are mediated by homologous recombination in vertebrate cells. *Mol Cell Biol.* 19:5166-9.
- Sotiropoulou, P.A., A.E. Karambelas, M. Debaugnies, A. Candi, P. Bouwman, V. Moers, T. Revenco, A.S. Rocha, K. Sekiguchi, J. Jonkers, and C. Blanpain. 2013. BRCA1 deficiency in skin epidermis leads to selective loss of hair follicle stem cells and their progeny. *Genes Dev.* 27:39-51.
- Speck, C., Z. Chen, H. Li, and B. Stillman. 2005. ATPase-dependent cooperative binding of ORC and Cdc6 to origin DNA. *Nat Struct Mol Biol.* 12:965-71.
- Sperka, T., J. Wang, and K.L. Rudolph. 2012. DNA damage checkpoints in stem cells, ageing and cancer. *Nat Rev Mol Cell Biol.* 13:579-90.
- Stenn, K.S., and R. Paus. 2001. Controls of hair follicle cycling. *Physiol Rev.* 81:449-494.
- Stiff, T., M. Alagoz, D. Alcantara, E. Outwin, H.G. Brunner, E.M. Bongers, M. O'Driscoll, and P.A. Jeggo. 2013. Deficiency in origin licensing proteins impairs cilia formation: implications for the aetiology of Meier-Gorlin syndrome. *PLoS Genet.* 9:e1003360.
- Stoeber, K., A.D. Mills, Y. Kubota, T. Krude, P. Romanowski, K. Marheineke, R.A. Laskey, and G.H. Williams. 1998. Cdc6 protein causes premature entry into S phase in a mammalian cell-free system. *EMBO J.* 17:7219-29.
- Syljuasen, R.G., C.S. Sorensen, L.T. Hansen, K. Fugger, C. Lundin, F. Johansson, T. Helleday, M. Sehested, J. Lukas, and J. Bartek. 2005. Inhibition of human Chk1 causes increased initiation of DNA replication, phosphorylation of ATR targets, and DNA breakage. *Mol Cell Biol.* 25:3553-62.
- Tada, S., A. Li, D. Maiorano, M. Mechali, and J.J. Blow. 2001. Repression of origin assembly in metaphase depends on inhibition of RLF-B/Cdt1 by geminin. *Nat Cell Biol.* 3:107-13.
- Takeda, D.Y., Y. Shibata, J.D. Parvin, and A. Dutta. 2005. Recruitment of ORC or CDC6 to DNA is sufficient to create an artificial origin of replication in mammalian cells. *Genes Dev.* 19:2827-36.
- Tanaka, S., and J.F. Diffley. 2002. Interdependent nuclear accumulation of budding yeast Cdt1 and Mcm2-7 during G1 phase. *Nat Cell Biol.* 4:198-207.
- Tanaka, S., R. Nakato, Y. Katou, K. Shirahige, and H. Araki. 2011. Origin association of Sld3, Sld7, and Cdc45 proteins is a key step for determination of origin-firing timing. *Curr Biol.* 21:2055-63.
- Tanaka, T., D. Knapp, and K. Nasmyth. 1997. Loading of an Mcm protein onto DNA replication origins is regulated by Cdc6p and CDKs. *Cell.* 90:649-60.
- Tatsumi, Y., S. Ohta, H. Kimura, T. Tsurimoto, and C. Obuse. 2003. The ORC1 cycle in human cells: I. cell cycle-regulated oscillation of human ORC1. *J Biol Chem.* 278:41528-34.
- Tatsumi, Y., N. Sugimoto, T. Yugawa, M. Narisawa-Saito, T. Kiyono, and M. Fujita. 2006. Deregulation of Cdt1 induces chromosomal damage without rereplication and leads to chromosomal instability. *J Cell Sci.* 119:3128-40.
- Terret, M.E., R. Sherwood, S. Rahman, J. Qin, and P.V. Jallepalli. 2009. Cohesin acetylation speeds the replication fork. *Nature.* 462:231-4.
- Tuduri, S., H. Tourriere, and P. Pasero. 2010. Defining replication origin efficiency using DNA fiber assays. *Chromosome Res.* 18:91-102.

- Varma, D., S. Chandrasekaran, L.J. Sundin, K.T. Reidy, X. Wan, D.A. Chasse, K.R. Nevis, J.G. DeLuca, E.D. Salmon, and J.G. Cook. 2012. Recruitment of the human Cdt1 replication licensing protein by the loop domain of Hec1 is required for stable kinetochore-microtubule attachment. *Nat Cell Biol.* 14:593-603.
- Vaziri, C., S. Saxena, Y. Jeon, C. Lee, K. Murata, Y. Machida, N. Wagle, D.S. Hwang, and A. Dutta. 2003. A p53-dependent checkpoint pathway prevents rereplication. *Mol Cell.* 11:997-1008.
- Victoria, G.D., and M.C. Nussenzweig. 2012. Germinal centers. *Annu Rev Immunol.* 30:429-57.
- Ward, I.M., and J. Chen. 2001. Histone H2AX is phosphorylated in an ATR-dependent manner in response to replicational stress. *J Biol Chem.* 276:47759-62.
- Weinreich, M., C. Liang, H.H. Chen, and B. Stillman. 2001. Binding of cyclin-dependent kinases to ORC and Cdc6p regulates the chromosome replication cycle. *Proc Natl Acad Sci U S A.* 98:11211-7.
- Weinreich, M., C. Liang, and B. Stillman. 1999. The Cdc6p nucleotide-binding motif is required for loading mcm proteins onto chromatin. *Proc Natl Acad Sci U S A.* 96:441-6.
- Whittaker, A.J., I. Royzman, and T.L. Orr-Weaver. 2000. Drosophila double parked: a conserved, essential replication protein that colocalizes with the origin recognition complex and links DNA replication with mitosis and the down-regulation of S phase transcripts. *Genes Dev.* 14:1765-76.
- Wigler, M., S. Silverstein, L.S. Lee, A. Pellicer, Y. Cheng, and R. Axel. 1977. Transfer of purified herpes virus thymidine kinase gene to cultured mouse cells. *Cell.* 11:223-32.
- Williams, G.H., and K. Stoeber. 2007. Cell cycle markers in clinical oncology. *Curr Opin Cell Biol.* 19:672-9.
- Williams, R.S., R.V. Shohet, and B. Stillman. 1997. A human protein related to yeast Cdc6p. *Proc Natl Acad Sci U S A.* 94:142-7.
- Wohlschlegel, J.A., B.T. Dwyer, S.K. Dhar, C. Cvetic, J.C. Walter, and A. Dutta. 2000. Inhibition of eukaryotic DNA replication by geminin binding to Cdt1. *Science.* 290:2309-12.
- Woodward, A.M., T. Gohler, M.G. Luciani, M. Oehlmann, X. Ge, A. Gartner, D.A. Jackson, and J.J. Blow. 2006. Excess Mcm2-7 license dormant origins of replication that can be used under conditions of replicative stress. *J Cell Biol.* 173:673-83.
- Woodworth, C.D., E. Michael, L. Smith, K. Vijayachandra, A. Glick, H. Hennings, and S.H. Yuspa. 2004. Strain-dependent differences in malignant conversion of mouse skin tumors is an inherent property of the epidermal keratinocyte. *Carcinogenesis.* 25:1771-8.
- Wu, P.Y., and P. Nurse. 2009. Establishing the program of origin firing during S phase in fission Yeast. *Cell.* 136:852-64.
- Yan, Z., J. DeGregori, R. Shohet, G. Leone, B. Stillman, J.R. Nevins, and R.S. Williams. 1998. Cdc6 is regulated by E2F and is essential for DNA replication in mammalian cells. *Proc Natl Acad Sci U S A.* 95:3603-8.
- Yanagi, K., T. Mizuno, Z. You, and F. Hanaoka. 2002. Mouse geminin inhibits not only Cdt1-MCM6 interactions but also a novel intrinsic Cdt1 DNA binding activity. *J Biol Chem.* 277:40871-80.
- Yoshida, K., N. Sugimoto, S. Iwahori, T. Yugawa, M. Narisawa-Saito, T. Kiyono, and M. Fujita. 2010. CDC6 interaction with ATR regulates activation of a replication checkpoint in higher eukaryotic cells. *J Cell Sci.* 123:225-35.
- Zhong, W., H. Feng, F.E. Santiago, and E.T. Kipreos. 2003. CUL-4 ubiquitin ligase maintains genome stability by restraining DNA-replication licensing. *Nature.* 423:885-9.

- Zhong, Y., T. Nellimoottil, J.M. Peace, S.R. Knott, S.K. Villwock, J.M. Yee, J.M. Jancuska, S. Rege, M. Tecklenburg, R.A. Sclafani, S. Tavaré, and O.M. Aparicio. 2013. The level of origin firing inversely affects the rate of replication fork progression. *J Cell Biol.* 201:373-83.
- Zhou, C., S.H. Huang, and A.Y. Jong. 1989. Molecular cloning of *Saccharomyces cerevisiae* CDC6 gene. Isolation, identification, and sequence analysis. *J Biol Chem.* 264:9022-9.
- Zhu, W., Y. Chen, and A. Dutta. 2004. Rereplication by depletion of geminin is seen regardless of p53 status and activates a G2/M checkpoint. *Mol Cell Biol.* 24:7140-50.
- Zindy, F., D.E. Quelle, M.F. Roussel, and C.J. Sherr. 1997. Expression of the p16INK4a tumor suppressor versus other INK4 family members during mouse development and aging. *Oncogene.* 15:203-11.
- Zou, L., and S.J. Elledge. 2003. Sensing DNA damage through ATRIP recognition of RPA-ssDNA complexes. *Science.* 300:1542-8.